

# ENEA

Italian National Agency for New Technologies,  
Energy and Sustainable Economic Development

# 2012 ACTIVITY REPORT

TECHNICAL UNIT

DEVELOPMENT and APPLICATIONS

of RADIATION



Italian National Agency for New Technologies, Energy  
and Sustainable Economic Development



# ACTIVITY REPORT 2012

## UTAPRAD TECHNICAL UNIT

### UTAPRAD DIRECTOR

Roberta Fantoni

*[roberta.fantoni@enea.it](mailto:roberta.fantoni@enea.it)*

This report was prepared by the Scientific and technical staff of ENEA's Technical Unit Development and Application of Radiation - UTAPRAD

### SCIENTIFIC EDITORS

Roberta Fantoni

Antonio Palucci

Rosa Maria Montereali

Giuseppe Dattoli

Gian Piero Gallerano

### DESIGN AND COMPOSITION

Flavio Miglietta

### EXTERNAL RELATIONS

Monica Cimino

LABORATORY WEBSITE : <http://www.frascati.enea.it/utaprad>

# CONTENTS

<b>1</b>	<b>DIAGNOSTIC AND METROLOGY LABORATORY</b>	<b>7</b>
1.1	MISSION AND INFRASTRUCTURES	7
1.2	DIAGNOSTICS FOR SECURITY	8
1.3	DIAGNOSTICS FOR SAFETY	17
1.4	ENVIRONMENTAL DIAGNOSTIC RELATED TO CLIMATE CHANGES	19
1.5	DIAGNOSTICS FOR CULTURAL HERITAGE PRESERVATION AND FRUITION	25
1.6	TECHNOLOGIES FOR ENERGY	32
1.7	TECHNOLOGIES FOR INDUSTRY SUPPORT	38
1.8	EDUCATION AND KNOWLEDGE DISSEMINATIONS	38
<b>2</b>	<b>PHOTONICS MICRO AND NANO-STRUCTURES LABORATORY</b>	<b>39</b>
2.1	MISSION AND INFRASTRUCTURES	39
2.2	NANOSTRUCTURES AND NANOTECHNOLOGIES FOR ENERGY EFFICIENCY	40
2.3	LIGHT SOURCES, OPTICAL SENSORS AND TECHNOLOGIES FOR PHOTONICS	46
2.4	SPECTROSCOPIC CHARACTERIZATION AND PHOTO-DEGRADATION OF LIGHT-EMITTING ORGANIC FILMS	53
2.5	OPTICAL FIBRE SENSORS	54
2.6	ACTIVITIES IN ENVIRONMENTAL AND SEISMIC SECTORS	57
2.7	EDUCATION AND KNOWLEDGE DISSEMINATION ACTIVITIES	58
<b>3</b>	<b>MATHEMATICAL MODELING LABORATORY</b>	<b>59</b>
3.1	MISSION AND INFRASTRUCTURES	59
3.2	FREE ELECTRON LASER ACTIVITY	59
3.3	DESIGN OF ELECTRON AND CARM SOURCE	63
3.4	THEORETICAL PHYSICS	66
3.5	APPLIED MATHEMATICS	70
<b>4</b>	<b>RADIATION SOURCES LABORATORY</b>	<b>71</b>
4.1	MISSION AND INFRASTRUCTURES	71
4.2	SHORT-WAVELENGTH SOURCES AND APPLICATIONS	72
4.3	TERAHERTZ SOURCES AND APPLICATIONS IN THE BIOLOGICAL FIELD	78
4.5	“OLOCONTROLLO EMULATIVO” TECHNOLOGY	83
4.6	CONTRIBUTIONS TO OTHER PROJECTS	86
<b>5</b>	<b>LIST OF PERSONNEL</b>	<b>88</b>
<b>6</b>	<b>RESEARCH PRODUCTS</b>	<b>90</b>
6.1	PATENTS	90
6.2	PEER REVIEW PAPERS	90
6.3	CONFERENCE PROCEEDINGS	94
6.4	CONFERENCE LECTURES	96
6.5	TECHNICAL REPORTS	102

**PUBLISHED BY :**

ENEA Frascati  
Via Enrico Fermi, 45  
00044 Frascati, Rome, Italy

## PREFACE

Almost three years after the formation of UTAPRAD in ENEA, it is proper to make some considerations about its mission and strategy, especially taking into account the evolving international scenario and the economical crisis.

UTAPRAD is a technical unit dedicated to the development of physical technologies, specifically to the application of radiations. Technologies, and relevant methodologies, concern ionizing and non-ionizing (e.g. lasers and long wavelengths emissions) radiations, particle accelerators (electrons, protons), micro and nano-devices (emitters, detectors), the respective physical modeling relevant to radiation transport and radiation-matter interaction. The broad application fields, ranging from industry (opto-electronics, photonics, energetics), environment (marine and atmospheric monitoring, cultural heritage diagnostics), health (imaging diagnostics and radio-therapy), security (NBCR-E threats) and safety (food, seismic), required since the beginning a multidisciplinary expertise that increased with the recent recruitment policy. At Dec. 31, 2012 the graduated personnel distribution was the following (Figure 1).

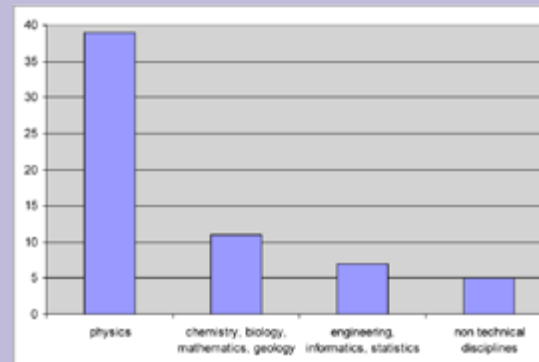


Fig. 1 – Graduated personnel distribution at UTAPRAD on Dec. 31, 2012

The staff member composition was completed with 28 specialized technicians and 5 administrative employees.



Our expertise gathers in three main clusters relevant to:

1. Laser systems for diagnostics and processing,
2. Particle accelerators and free electron lasers,
3. Micro- and nano-structures, photonics.

In 2012 funds for all researches carried out came from international and national projects, with the prevailing of European projects for Security, both Italian and European contributions to environment and cultural heritage, the prevailing Italian support on other topics (Industrial and fundamental researches from MIUR, Industria 2015 and programme agreements on energetic from MiSE), researches directly funded by industries are present as well.

As in the past, a significant part of the research activities are conducted in cooperation with different ENEA UTs, some of them upon the leadership of UTAPRAD or with shared responsibility (e.g. with UTICT for Cultural

Heritage), some on charge of other UTs better complying with the respective mission (e.g. UTFUS for diagnostics inside fusionistic vessels).

The activity is conducted at ENEA Frascati research center, where a more than 60 years old background on relevant technologies is located (Figure 2).

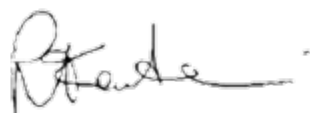
Major results obtained in 2012 are shown here according to our four laboratory scheme:

- Diagnostics and Metrology – DIM
- Mathematical Modeling – MAT
- Micro and Nanostructures, photonics – MNF
- Radiation Sources – SOR

However joint groups from the different laboratories, together with the senior staff at the UT direction, participate to different research projects as far as they can be involved for specific knowledge and available facilities.

A growing and growing attention to the dissemination and exploitation of scientific results was paid during 2012, outstanding initiatives are mentioned where relevant.

Have a nice reading!



Dr. Roberta Fantoni  
UTAPRAD Director



Fig. 2 - Frascati Sinchrotron old building at ENEA, currently hosting electrons and protons accelerators.

## 1 DIAGNOSTIC AND METROLOGY LABORATORY

### 1.1 MISSION AND INFRASTRUCTURES

The Diagnostic and Metrology Laboratory, included in the ENEA Frascati Research Centre, is mainly focused in the development of laser sensors for environmental monitoring applications in devoted outdoor campaigns. The implemented laser technologies are dedicated to find the state of the art in the electro-optical spectroscopic tools that are better tailored in terms of discrimination and sensitivity in diagnostic and metrology field of applications. More in details the allocated roles to the Laboratory are:

- the development of spectroscopic and optic systems for in-situ or remote (lidar systems) in sensing and metrological applications (environmental, Cultural heritage, Security and health);
- the development of compact and miniaturized sensors to be operated in hostile environments and space explorations;
- the development of imaging sensors for in-situ applications in different fields of interest supporting also data analysis and images release;
- the support to data merging from different active and passive optical sensors.

The competences available in the Laboratory are originated from the expertise in different scientific disciplines as laser spectroscopy, optics, active and passive sensors, terrestrial and marine biology, analytical chemistry, biology and data analysis. This know-how is fruitfully devoted to the development of sensors for scientific and industrial applications. In details the tasks assigned are summarized as follows:

- the design, implementation and tests of compact optical systems for environmental active and passive remote sensing including

harsh environments, Cultural heritage and Security.

- the execution of monitoring campaigns with own instruments installed in dedicated payloads to be connected with terrestrial and/or marine autonomous robots or rovers, merging data from other sensors;
- the design, implementation and tests compact and/or imaging spectroscopic sensors for real time analysis of hazardous materials scattered in different matrices, for health applications and for the goods characterization;
- the development of optical tools for in-situ and remote sensing on demand of other UTs;
- the maintenance and hardware upgrading of its own mobile laboratories for environmental monitoring;
- the participation to research activities in national and international joint ventures.

List of facilities and sensors available at UTAPRAD-DIM during present activity are here summarized:

- Satellite oceanographic data analysis and merging laboratory
- Plant biology laboratory
- Environmental analytic laboratory
- Laser scanning flow cytometry laboratory
- LIBS and XRF laboratory
- Bio-electro-magnetism laboratory
- Atmospheric mobile lidar laboratory
- Molecular spectroscopy laboratory
- Non linear spectroscopy laboratory
- Artificial vision laboratory with 3D laser scanners
- Lidar fluorosensor and LIF scanning sensor

## Fundings and projects

The research activities of the UTAPRAD-DIM Laboratory are mainly funded in the frame of the EC Framework Programmes FP7 SECURITY as coordinator of BONAS project (Bomb factory detection by Networks of Advanced Sensors), partner of CUSTOM project (Drugs And Precursors Sensing By Complementing Low Cost Multiple Techniques), coordinator of the RADEX project (Radar Detection of Explosives) and joining the BCT project (Big City Trial) both in the frame of the NATO Science for Peace special project STANDEX. In FP7 Environment the laboratory participate to PERSEUS project (Policy-orientated marine Environmental Research for the Southern European Seas) and MYOCEAN (Ocean Monitoring And Forecasting).

Two European projects were funded by the European Research Council, CO2VOLC (Quantifying the global volcanic CO2 cycle) and BRIDGE (Bridging the gap between gas emissions and geophysical observations at active volcanoes).

International projects are also established through the Italian Foreign Office, CLIMAT "Utilisation complémentaire du lidar afin de valider les données bio-optiques obtenues par mesures satellitaires dans l'estuaire du Saint-Laurent" with Canada and UNELAS (Underwater network of laser sensors for water monitoring) with Israel.

Furthermore at national level, the Laboratory holds research projects in the frame of MIUR PON: IT@CHA finalized to boost the technological innovation in maritime archaeology. (coordinated by CETMA Consortium, TRAMP (TRASporto in Sicurezza di Merci Pericolose) coordinated by TRAIN Consortium, within Industria 2015 from MISE we participate to SAL@CQO (Sviluppo di un Apparato Laser per misure di spettroscopia molecolare per la Conservazione e il controllo di valori afferenti le Qualità Organolettiche dei prodotti alimentari con tecniche non invasive contro adulterazioni naturali e/o fraudolente),

MUSS (Mobilità Urbana ed Infraurbana Sostenibile e Sicura). Incomes are also originated from other national institutions e.g. the project Incamp (Interazione del Campo Magnetico a frequenza di ionorisonanza con enzimi e Proteine) from INAIL.

The UTAPRAD DIM laboratory has strengthened its commitment for a constructive networking with Large Industries and SMEs both at national and European level. Personnels are members of European lobby activities as in IMG-S (Industrial and Research Stakeholders Group for Security), participate to international networks like NDE (Network for Detection of Explosives) and ENRCIP-DEMON (European Network on Critical Infrastructures - Detection of Explosive for non Aviation) and to in the Italian technological platform for Security (SERIT) and Photonics at national level. The collaboration in existing partnerships has been upgraded while, at the same time, laying the basis for new ones. This action aims at ensuring a high level of cross-fertilization to fully exploit the possibilities arising from European and national funding schemes as well to enable market channels for the laboratory scientific achievements.

## 1.2 DIAGNOSTICS FOR SECURITY

### Detection of drugs and precursors



The EC FP7 Security project Drugs And Precursors Sensing By Complementing Low Cost Multiple Techniques (CUSTOM), now entered in its third year of activity, is aimed to develop a portable device capable of detecting traces of precursor chemicals used in the manufacture of the most dangerous drugs on the international market. Selex S.I. is the coordinator. The sensor is based on an air sampler, feeding two analytical sensor respectively based on Laser Photoacoustic (LPAS) and LED Induced Fluorescence technique (LFLUO). DIM Laboratory is responsible for the sampler and the master control board (MCB) development.

The vessel containing all the sub-assemblies of the CUSTOM sensor has been designed by using CAD software to produce an advanced technological demonstrator at laboratory level. The final structure occupies a total volume of 25ℓ with more than enough room for allocating the CUSTOM sensor sub-assemblies, namely LPAS and FLUO modules the hydraulic circuit, the air sampler, the pre-concentrator and the electronic of the Master Control Board, while keeping in mind the requirements posed by the electrical connections, hydraulic connections, and finally the heat production and pathways for heat dissipation).

Extensive laboratory tests have been performed with the MCB prototype board prepared and manufactured in previous years; from the outcomes of the experimental measurements it has been possible to get relevant suggestions to optimize the overall system performances. A new design and a final version (revision 3.0) of printed circuit board for the MCB has been produced (Figure 1); the heart of the MCB is an ARM cortex-M3 microcontroller for control and data acquisition of the prototype board. An purposely developed firmware is burned into the processor ROM flash and a real-time operating system runs, allowing for data acquisition from the LPAS and FLUO

sensors under the User control.

New features added in hardware and implemented in the developed firmware are now giving support for:

- GPS device integrated at the MCB hardware level;
- direct powering of additional external devices (pressure gauge, laser power meter, etc.);
- double buffering for external device to increase both communication speed and the noise immunity (LPAS);
- additional RAM memory to support large capacity buffer for I/O operations

To provide the CUSTOM project Partners with devices to make laboratory experiments two test beds have been developed and populated with appropriate hardware; the first one was developed for testing the Pre-concentrator polystyrene beads developed by Università di Salerno as active medium of the molecular concentrator (see Figure 2 left), while the second test bed was designed to test the thermal management of the Quantum Cascade Laser (QCL) as active light source (see Figure 2 right). The systems were built and delivered as units ready to use, including the

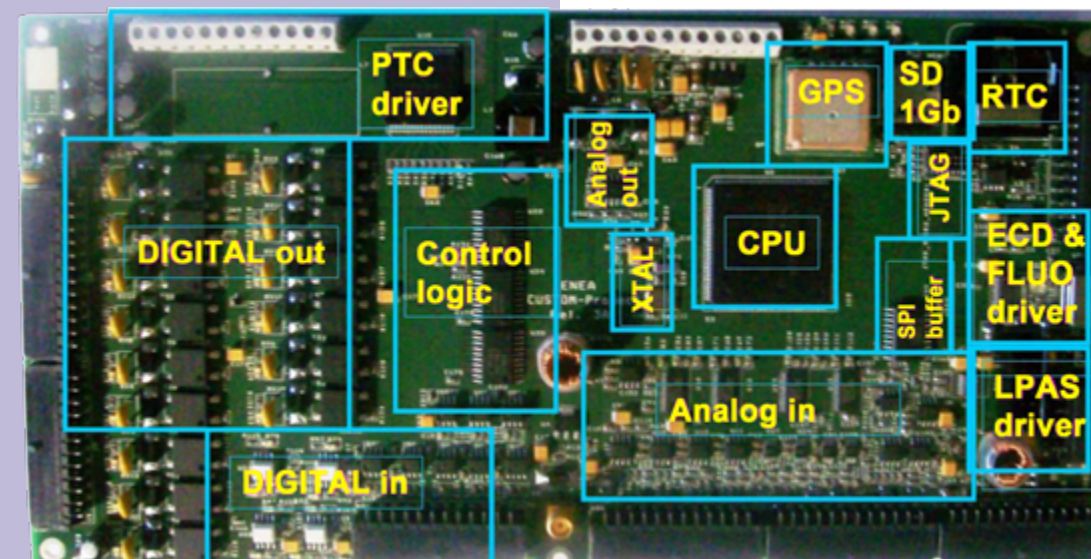


Fig. 1 - The final prototype of MCB release 3.0.

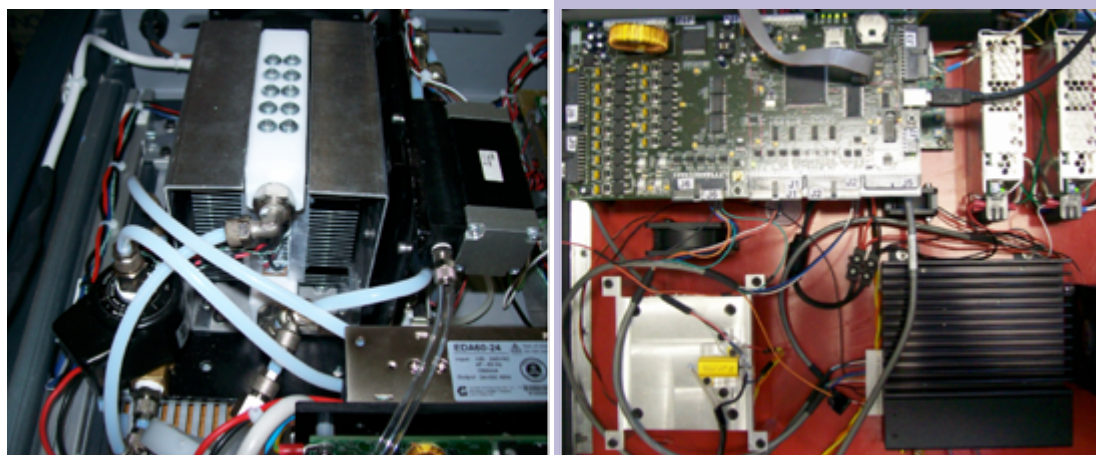


Fig. 2 - The second Test bed including the molecular concentrator (left) and the thermal management of the QCL as active light source and the MCB (right).

control software burned into the flash memory and running in the MCB processor.

As the Pre-concentrator unit is concerned, software support gives the opportunity to control the chamber thermal cycle, also actuating the air pump to provide sampling in the same condition of the final device. All parameters like the cycle duration, lower an upper temperature limits, etc. can be changed by the User, thus allowing the optimization of the concentration process. As the QCL is concerned the following controls have been designed in implemented as hardware devices: crystal temperature control and External Cavity Driver (ECD) position to control the emitted wavenumber by mean of an external mirror.

#### Detection of explosive precursors BONAS (BOmb factory detection by Networks of Advanced Sensors)



ENEA is coordinating the European project BONAS (BOmb factory detection by Networks of Advanced Sensors) for Security Call. The main aim of this project is to design, develop and test an innovative sensor wireless network.

BONAS is designed in order to increase

citizen protection and homeland security from terrorist attacks, especially against the threat posed by improvised explosive devices (IEDs). ENEA is in charge to support the development of two sensors, for volatile and particulate substances emitted or released in the surrounding environment.

The first sensor is a lidar/DIAL remote sensor based on spectroscopic techniques. In 2012 the laboratory Lidar/DIAL apparatus was installed for calibration purpose (Figure 3 left). The high resolution spectroscopic database by PNNL (Pacific Northwest National Laboratory) has been compared to our measurements in the optimal spectral bands for the lidar/DIAL detection of IEDs.

Figure 3 right is an example of acetone spectrum, showing the good agreement between our measurements and the database. These results demonstrate that the OPO (optical parametric oscillator) that is the hearth of our experimental system is adequate for the realization of a Lidar/DIAL remote sensor.

At the end of this study, relevant spectroscopic data were distributed to the project partners, while the actual choice of the ON and OFF wavelengths has been reported only in a confidential annex.

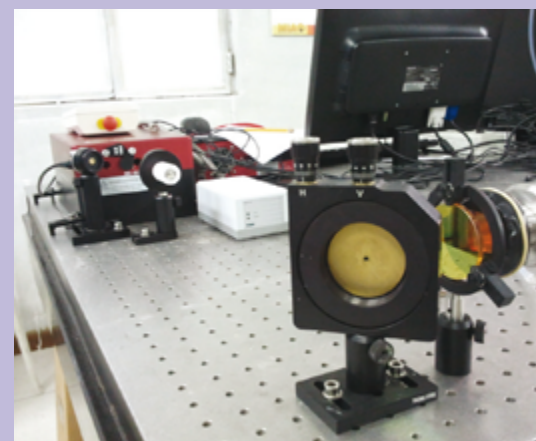
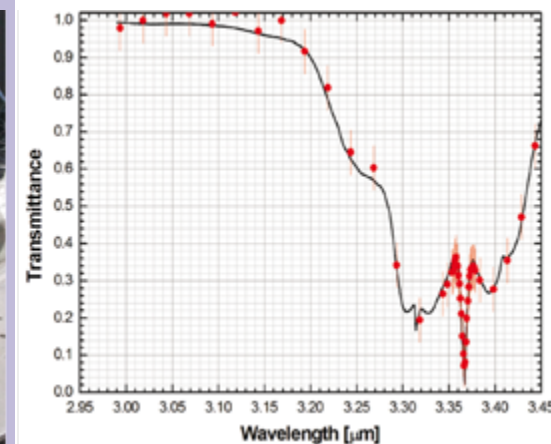


Fig. 3 - Picture of the experimental system (left). In the background the OPO source, in the foreground the gold-coated mirror reflecting the laser beam into the spectroscopic cell. Experimental measurement (red dots) and PNNL data (black line) of acetone (right).



#### The Surface Enhanced Raman Spectroscopy: evaluation of substrate amplification factor on explosive compounds for BONAS

The second sensor for BONAS is mainly based on the Raman spectroscopy (RS) due to the possibility to extract spectral fingerprints related to chemical bonding in compounds to be identified. However, the major drawback of RS is the low cross-section of the spontaneous Raman scattering, which affects the detection of substances at trace level. The Raman scattering signal can be greatly enhanced when the scatterer is placed on a roughened noble-metal substrate, a process that nowadays is known as Surface-Enhanced Raman-Scattering (SERS).

In BONAS, ENEA is in charge to support the project's Swedish partner Serstech in developing a small and compact sensor selecting the appropriate substrates commercially available and ad-hoc realized by two other partners as the University of Belfast and the King College of London. With the collaboration of UTAPRAD-MNF sets of SERS measurements on some common military explosives (ethylene glycol dinitrate, EGDN, pentaerythritol tetranitrate, PETN, trinitrotoluene, TNT and 1,3,5-trinitroperhydro-1,3,5-triazine, RDX) were acquired with a table-top micro-Raman system integrated with the minispectrometer prototype (Figure 4).

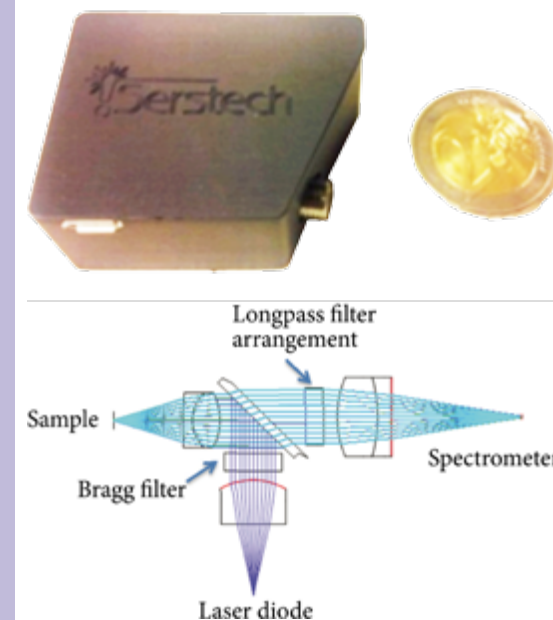


Fig. 4 - Compact spectrometer designed for BONAS project by Serstech (top) and the optical lay-out to be implemented in the next period (bottom).

This set of substances was chosen because they are nitro-based explosives that contains the nitro ( $\text{NO}_2$ ) group and can be classified on the basis of their chemical structure, being representative of those that currently represents the greatest threat to security. Three major classes of nitro-containing explosives can be identified: those based on aliphatic

nitrate ester (R-O-NO<sub>2</sub>), the nitro-aromatic (Ar-NO<sub>2</sub>), and the cycloaliphatic nitramine (>N-NO<sub>2</sub>) groups. Among them EGDN and PETN are representative of the first class (Nitrate ester), TNT is representative of the second class (Nitro-aromatic) and RDX is representative of the third (Nitramine).

Samples of explosives were prepared depositing 0.1 µl drops of 1 mg/ml solutions onto commercial SERS substrates. The solvents evaporate in about one minute, after which it is possible to carry out the Raman measurements (Figure 5).

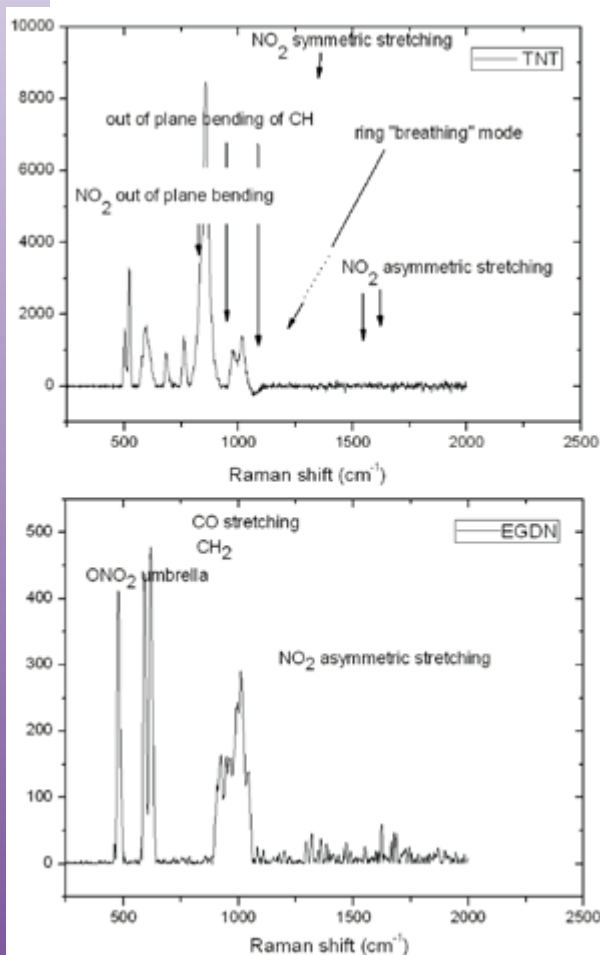


Fig. 5 - Surface-enhanced Raman spectra of TNT and EGDN. The mass probed by laser is about 200 µg for each substance. The acquisition time is 10 s. The laser power is 150 mW.

### FORLAB Project (FORensic LABoratory for in-situ evidence analysis in a post blast scenario)

**forlab** Post blast forensic laboratory. The FORLAB Project (FORensic LABoratory for in-situ evidence analysis in a post blast scenario) has been approved by the EC and funded under 7th FWP. Its final goal is to optimize the evidence collection in a post blast scene after an IED (Improvised Explosive Device) attack and to reduce the time and resources in the laboratory, while preserving the chain of custody so as to minimize the time required to identify the responsible for the attack.

ENEA is leader of the work package "focussed development of screening tools". The main objective of this work package is to develop portable sensors that are necessary for fast screening of post-blast evidences, reducing the number of evidences sent to the reference forensic laboratory and increasing the information provided by the evidences left by the explosion during the investigations.

The sensors must be fast and reliable to select/identify those evidences that can lead to a fast identification of the terrorist group or even the bomb maker.

In this frame, the development of an innovative sensor based on the Laser Induced Fluorescence (LIF) is in progress in UTAPRAD-DIM laboratory for the detection of plastic debris coming from IEDs components, such as containers, adhesive tapes and electronic boards.

To this aim, preliminary measurements have been done by the LIF scanning instrument already realized at DIM able to collect fluorescence images on large areas, in order to test the system performance in forensic context. The system arrangement allows for a hyperspectral analysis of large targets thanks to a line by line scanning and for the remote operation up to some tens of meters.

The instrument has the capability to give

information on substances having specific spectral signatures. Information on analytical composition and qualitative presence of different materials can be obtained by fluorescence band analysis. Data are collected both as 2D monochromatic images and LIF spectra. In particular, some plastic materials of interest have been analyzed and the resulting fluorescence emission spectra are shown in Figure 6.

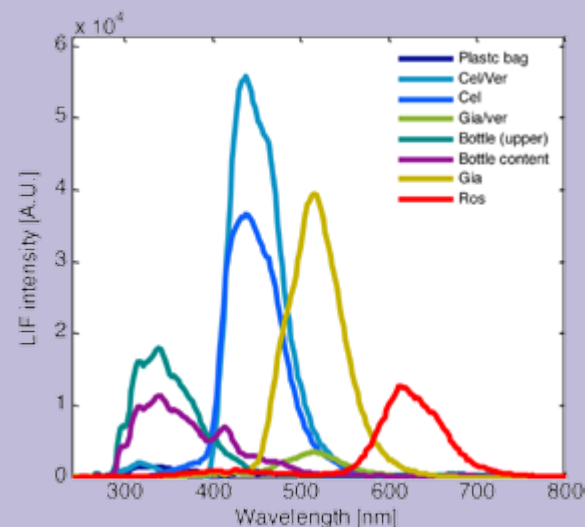


Fig. 6 - LIF emission spectra of plastic material

Distinct bands depending on the target material at 320 nm, 420 nm, 530 nm and 610 nm have been identified allowing the detection of substances having characterized by spectral signatures.

Fluorescence images can be reconstructed in false color by using the three most intense detected bands, corresponding to the main features, as red, green and blue channels (RGB) permitting to detect and localize characteristics invisible to the naked eye. The RGB false-color reconstruction of the acquired fluorescence image of some plastic samples on the floor is reported, as example, in Figure 7. The traditional related picture is shown for comparison.

The main components of the new sensor to be realized within the FORLAB are: a laser source, a laser beam delivery optics, a fluorescence

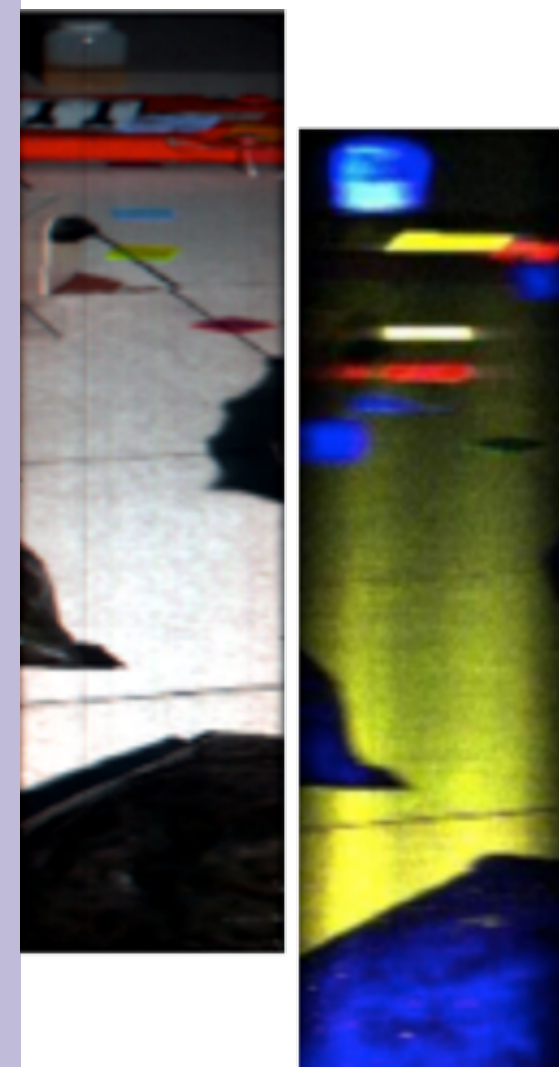


Fig. 7 - False-color fluorescence image of some plastic samples on the floor (right) compared to the related traditional picture (left).

collecting optics, a spectral discriminating system, a UV-VIS sensitive CCD camera, a mechanical system for scene scanning, a computer-based system for process control, data acquisition and data integration with other sensors response.



## RADEX (RAman Detection of EXplosives) project



In the wake of several terroristic attacks in various cities during the last years, there is a need to develop reliable and effective instrumentations able to detect explosives and precursors at trace levels for homeland security applications. Among the detection technologies available, Raman-based spectroscopy has recently gained consents as potential tool for the detection of explosives at a certain distance due to technical improvements. In the context of the STANDEX (STANdoff Detection of Explosives) program, under the Science for Peace STANDEX programme (SfP-984 1966), defined to develop an explosive warning system that includes fusion of explosives detection sensors designed to work in an existing mass transit infrastructure, a new instrumentation has been developed at DIM for the proximal detection of explosives (target at a distance between 10 cm and 200 m). The RADEX (RAman Detection of EXplosives) system under development is a Raman-based technology to detect trace explosives on fabrics. The STANDEX program also includes an adaptation and a validation phase of the different technologies under development, in real conditions of use in a public mass transit facility (the Big City Trials project). During the BCT project, the RADEX system will be validated, together with the other instrumentations, during a demonstration where the association and coordination of the different technologies will be tested for the detection of suicide bombers.

Military explosives typically contain only the atoms of carbon (C), hydrogen (H), oxygen, (O), and nitrogen (N), having oxygen carried by  $\text{NO}_2$ . That functionality may be attached to oxygen (O- $\text{NO}_2$ ) as in the nitrate esters (NC, NG, or PETN), to carbon (C- $\text{NO}_2$ ) as in the nitroarenes (TNT, picric acid, or tetryl), or to nitrogen (N- $\text{NO}_2$ ) as in the nitramines

(RDX, HMX, or CL-20). There are also many oxidizer salts that potentially might be used to make composite explosives when mixed with suitable fuels. Raman spectra of nitro-containing explosives like TNT are usually identified through the symmetric ( $\sim 1250$ - $1375 \text{ cm}^{-1}$ ) and antisymmetric ( $1487$ - $1630 \text{ cm}^{-1}$ )  $\text{NO}_2$  stretching bands. The strongest  $1356 \text{ cm}^{-1}$  band derives from  $\text{NO}_2$  symmetric stretching coupled.

The operational principle of the RADEX system, for the proximal detection of explosives with UV Raman spectroscopy, is the following: an eye-safe laser beam is focused on the target and the Raman scattered radiation, emitted from the laser illuminated surface, is collected by a telescope and imaged onto the entrance of a Raman spectrometer. The radiation is then analyzed giving a spectrum suitable for the explosive detection and identification. The receiver is based on a telescope and a fiber bundle. Its acceptance can be optimized at different ranges (changing telescope diameter and focal length as well as fiber bundle diameter). Geometrical optics and ray tracing show that a 1-mirror telescope has the best efficiency. Moreover, it is easier to align because it is directly focused to the fiber bundle. With the values of the experimental layout we expect in the test site (Paris subway) a telescope of diameter 0.3 m and focal length 1 m is the best choice: with a bundle diameter  $d_f = 0.2 \text{ mm}$  the telescope is optimized at  $5\div 7 \text{ m}$ .

Preliminary tests were performed with samples of ammonium nitrate deposited on an aluminium substrate at different surface densities in the range of the target defined by the project. The samples, with an homogeneous deposition on the surface of the substrate, were analysed with the RADEX apparatus and the Raman signals from the ammonium nitrate were acquired also at the target surface density of  $0.1 \text{ mg/cm}^2$ . Then, samples of ammonium nitrate on a synthetic fabric as polyethylene (simulant of bags, k-ways, etc) were prepared and tested. Measurements were performed

with the samples at a distance of around 7 m from the telescope and the Raman spectrum is reported in Figure 8. The spectra of the fabric without ammonium nitrate was also acquired. The observed peaks at  $1044 \text{ cm}^{-1}$  is assigned to the totally symmetric vibration of  $\text{NO}_3$  ions. The Raman spectrum of ammonium nitrate is in agreement with previously reported spectra in literature. First measurements clearly indicates the ability of the instrument in the proximal detection of trace amounts on ammonium nitrate.

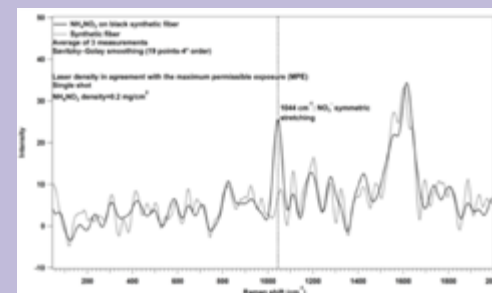


Fig. 8 - Raman spectra of ammonium nitrate on synthetic fiber from proximal measurements.

## BCT (Big City Trials) project

The BCT demonstration will be hosted in the "Bibliothèque François Mitterrand" metro station in Paris. After a visit to the metro station it was possible to figure out the way the instrument can be deployed during the demonstration. Several possibilities have been taken into account but at the end the most reasonable configuration is that one with the instrument located on the floor and protected by barriers pointing in the direction of the public mass transit area (Figure 9).

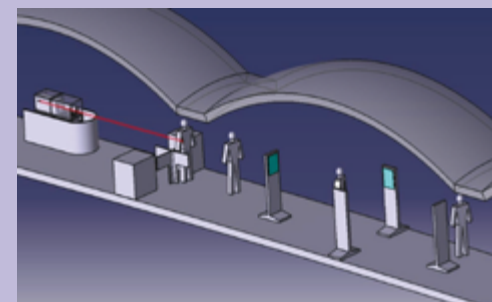


Fig. 9 - Schematic representation of the instrument deployment during the Demonstration in the metro station in Paris.

To test the RADEX prototype with samples of different explosives deposited on fabrics with different surface densities, a measurement campaign was performed at the Fraunhofer Institute for Chemical Technology ICT (Pfinzta, Germany). The main purpose of this campaign was the evaluation of the detection limits of a certain number of explosives in order to provide information about which compounds can be better detected and at which surface density. This campaign was also the first opportunity to test the RADEX apparatus with samples homogeneously deposited on fabrics. The samples were prepared with a piezoelectric Nano-Plotter™ developed by ICT. The piezoelectric Nano-Plotter™ can deliver a precise number of droplets on a well define surface thus, this method is less subject to human errors and provides more uniform target surface coverage (Figure 10).

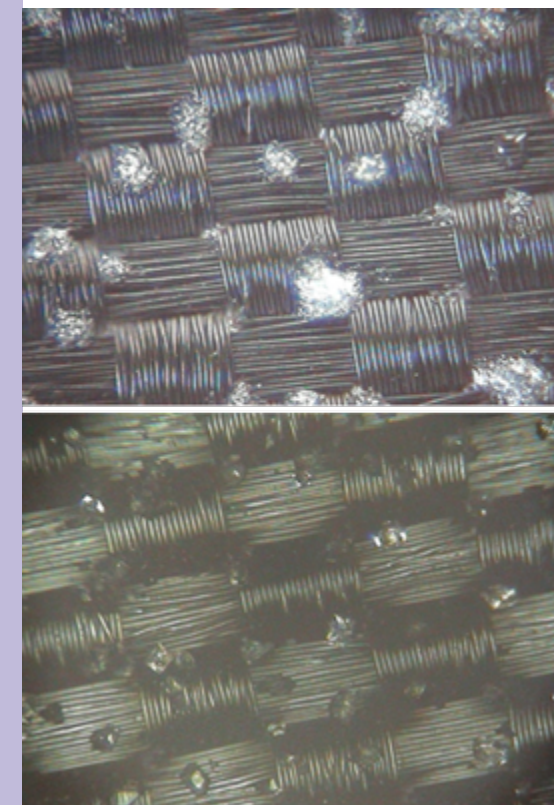


Fig. 10 - Ammonium nitrate (top,  $400 \mu\text{g/cm}^2$ ) and ammonium perchlorate (bottom,  $400 \mu\text{g/cm}^2$ ) deposited on synthetic fabrics with the piezoelectric Nano-Plotter™.

The proximal detections were performed with different energetic materials (PETN, TNT, ammonium nitrate, ecc) deposited on different types of fabrics (denim, leather, polyamide, polyester) and with the target at three different distances (6.4 m, 7 m, 10 m). The response of the instrument in presence of TNT at trace levels (same amount for each sample) on different fabrics is shown in Figure 11. The Raman band at around  $1361\text{ cm}^{-1}$  from TNT deposited on leather and polyamide derives from  $\text{NO}_2$  symmetric stretching coupled to CN stretching.

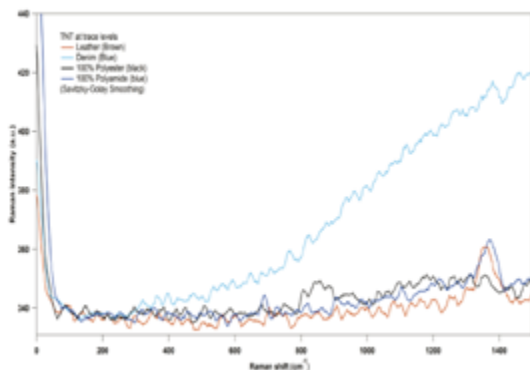


Fig. 11 - Raman spectra of TNT at trace levels on fabrics from proximal measurements.

#### Development of mathematical methods for artificial intelligence applied to diagnostics

The General Plan for Transport and Logistics (2003-2005) included, among its main strategic objectives, “increasing transport safety”, with the following main actions:

- regulate the movement of dangerous goods in the area, preserving the residential areas, places to naturalistic and infrastructure;
- know promptly the occurrence of spills of substances in the environment-polluting;
- know the dangerous substances involved in an accident about what territories happened shedding.

In this context TRAMP Project is focused onto the innovative use of machine learning

techniques, in this case to evaluate possible risks for goods and the immediate environment during transport. In order to have a continue monitoring of the payload (and of the related vector) the Artificial Neural Networks (ANN) are used in TRAMP Project with the task to predict the neighbor trend of the signals coming from heterogeneous sensors (VICON MX infrared camera, accelerometers, breaks temperature).

Therefore a particular class of ANN, named autoencoder (obtained from the contraction of Auto-Associative Artificial Neural Network Encoder) has been chosen. An ANN autoencoder class (in our case with a standard structure feed forward and fully connected) is trained to reproduce the exact output vector of values received as input. This model can be used for many purposes, from the compression of information to the reconstruction of missing signals to prediction in time series. Autoencoder does learn implicitly some properties underlying the data with which they are trained, or it can learn the inherent characteristics of the space of the input data without any a priori knowledge.

Given a time series it is common practice to use a sliding window to process data sequentially. To train a neural network able to predict the behavior of payload in a future time interval, two sliding windows: one containing the temporal sequence of  $m$  future assumed events ( $S$  future) and another with the sequence of the last  $n$  observed events ( $S$  history) have been used for each instance of training. A downstream Data Fusion step does gather the verdict of the single ANNs, each trained and tested on basis of characteristics of the sensors, providing in real-time a global measure of the risk. Project TRAMP ended in March 2012.

### 1.3 DIAGNOSTICS FOR SAFETY

#### Agro-alimentary diagnostics to protect the “made in Italy” products



Pioneering studies aimed to detect adulterants in food products and beverages was performed with the ENEA Laser Photoacoustic Spectroscopy (LPAS) test

facility operating at Watt power level in the 9-11  $\mu\text{m}$  spectral region. The feasibility studies were designed in the frame of the National Project MI01\_00182 - SAL@CQO (“Sviluppo di un Apparato Laser per misure di spettroscopia molecolare per la Conservazione e il controllo di valori afferenti le Qualità Organolettiche dei prodotti alimentari con tecniche non invasive contro adulterazioni naturali e/o fraudolente”) whose general purpose is to certify the quality of ‘Made-in-Italy’ labelled agro-alimentary products by mean of fast non invasive optical methods based on high resolution spectroscopy.

The SAL@CQO Project aims at developing and apply an innovative easy-to-use product-instrument that could be employed both by Scientific research laboratories (to analyse and check the presence in the molecules of remarkable markers showing the presence of toxic substances), and by industry supply chain and for production chains where food processing requires the continuous monitoring of quality and preservation of food included in the process.

The deliverable is a laser equipment able to perform measurements based on molecular spectroscopy in the infrared to detect parameters showing adulteration, if any, and performing a control to check the overall preservation of organoleptic and taste qualities of food and beverages. Such controls shall be performed using timely and non-invasive techniques to detect the presence of adulterating elements, that are often identified as specific molecules. Particular attention was devoted by the project to volatile adulterating

substances, and among them to methanol.

Methanol, also known as wood alcohol, is produced as natural by-product during the wine fermentation process in very low concentration, where the very main alcoholic content is due to ethanol. Differently from ethanol, methanol has a strong specific toxicity for the human body.

The high toxicity of methanol in humans is realized by two mechanisms. At the trace concentration found in wine, it is tolerated by the body, but accidental intake of the compound at higher concentration will result in severe intoxication due to accumulation of highly toxic metabolites. The minimal lethal dose of methanol in adults is believed to be 1mg/kg of body weight.

Nonetheless, a number of illegal adulteration of alcoholic beverages with methanol were detected, and some damage to people happened. This adulterating practice is due its to lower cost of methanol with respect to ethanol. The presence of methanol in beverages is not evident. Because of its similarities in both appearance and odour to ethanol, it is difficult to differentiate between the two alcohols. The alcoholic composition is stated by chemical analysis.

An innovative contribution to fast detection of methanol may be given by the high resolution IR spectroscopy. LPAS is a high resolution spectroscopy, which is characterized by absence of any requirement for chemical reagent purchase/disposal or sample pre-treatment and ease-of-use after initial method development. In principle, LPAS has the capability to record in detail the spectral fingerprint of methanol.

We applied the LPAS technique to the analysis of alcoholic mixtures in view to give a novel and improved contribution to the optical detection of methanol in alcoholic beverages. Spectra of both alcohols were analyzed by the LPAS facility equipped with a cuvette holding the aqueous alcoholic mixtures (Figure 12).

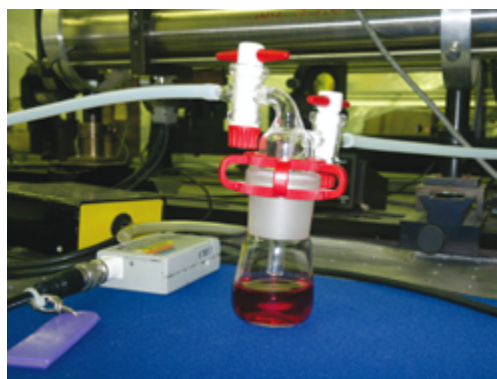


Fig. 12 - The cuvette holding alcohol-water solutions, connected to the PA cell for the analysis.

Mixtures were analyzed at low alcohol concentration, down to 10 ppmv in water. Comparing the two spectral profiles, significant wavelength dependent differences are observable in term of relative absorption intensity, as expected. The differences existing among the recorded spectra stressed the Principal Component Analysis (PCA) method operated on the experimental records and shown in the Figure 13 which represents a 2D view of the mentioned statistical analysis.

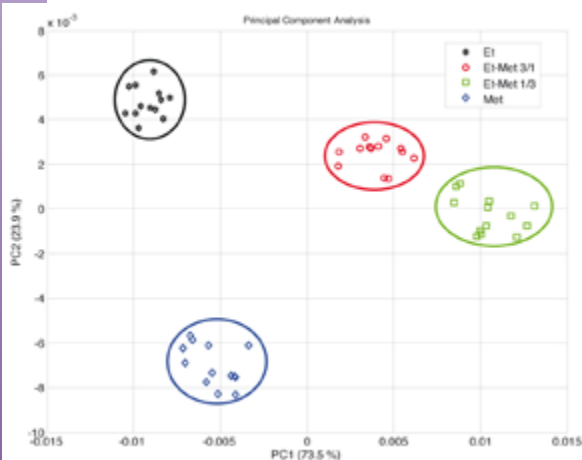


Fig. 13 - 2D view of the PCA operated on ethanol/methanol mixtures in water, at different relative concentration.

### Extremely Low Frequency (ELF) weak electromagnetic fields as diagnostic tool for livings

In 2012, the activities of the InCamp project (Interaction of the magnetic field at a frequency of ion resonance with enzymes and proteins) funded by INAIL (ex Ispesl), was successfully fulfilled. The main task of this research was the IR spectroscopy testing as a viable tool in the investigation of the interactions between low intensity-low frequency electromagnetic fields and the proteins and enzymes structures. Results have shown that this techniques is able to evidence long lasting modifications in the structure of Glutamic acid under exposure at magnetic field (Figure 14).

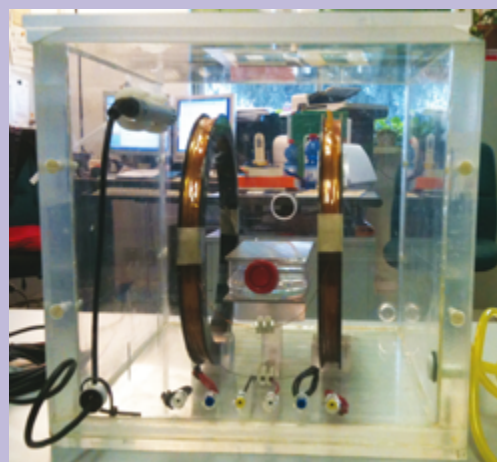


Fig. 14 - Cell culture incubator for exposition to electromagnetic fields developed in the laboratory of bio-electromagnetism.

However, it is not clear yet whether such modifications have an effect on the capability of Glutamic acid to participate to biochemical reactions, i.e. if they have a real impact on biological mechanisms.

### Development of techniques for tissue engineering.

In 2012 UTAPRAD-DIM Laboratory in collaboration with Tor Vergata University concentrated the attention on the host reaction after scaffold implantation. In fact, although

the isogenic orthotopical transplantation led to the formation of new myofibers in the acellular scaffold, a severe inflammatory response reduced myogenesis and led to a too early absorption of the scaffold (Figure 15). Our research was focused on the functionalization of the acellular scaffold before transplantation in order to modulate the intensity of the inflammation. We decellularized Tibialis Anterior (TA) muscle of murine cadaveric origin. The decellularization process was achieved by a method developed by us. The acellular scaffold was then functionalized with: i) polyethylene glycol (PEG), ii) murine serum or iii) pre-seeded with different progenitor cells. To replace homologous muscles, we orthotopically transplanted decellularized scaffolds, by suturing them to the host tendon extremities following TA removal. Scaffolds pre-treated with PEG or mice serum gave rise to an inflammatory response similar or more severe than the control. Pre-seeded scaffold with C2C12 led to a lower inflammation. We are currently assessing whether transplanted C2C12 are directly responsible for myogenesis or indirectly promote it by diminishing inflammation.

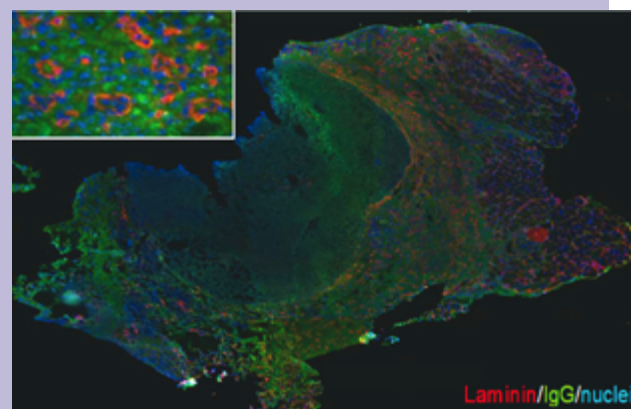


Fig. 15 - Immunofluorescence staining of laminin (red), immunoglobuline G (green).

### 1.4 ENVIRONMENTAL DIAGNOSTIC RELATED TO CLIMATE CHANGES

DIM Laboratory develops remote and in-situ instrumentation for marine campaign. The activity includes the intercalibration and analysis of satellite ocean color data collector on larger time scale.

#### PERSEUS



Ocean color activities have been performed in the framework

of PERSEUS (Policy-oriented marine Environmental Research for the Southern European Seas) project that started the 1st January 2012 and will continue until the end of 2015. UTAPRAD-DIM is involved in WP4 of PERSEUS that have the objective of evaluate the Southern European Seas environmental status with existing and upgraded remotely operated monitoring and modeling capabilities. In particular UTAPRAD-DIM will contribute to two tasks devoted to the estimate of the spatial and temporal variability of primary productivity and phytoplankton size classes.

In particular this WP use modeling and remote sensing techniques on a time scale encompassing the first two decades of the 21<sup>st</sup> century to:

- Provide synthetic indexes that can indicate the “status” of the environment
- Provide an integrated analysis of ecosystem attributes that will contribute to the criteria for good environmental status relevant to the MFS descriptors as indicated in the EU directive on “Good Environmental Status”.

Within this Work Package ENEA conducts a research activity for the Remotely sensed identification of the pelagic Phytoplankton Size Classes (PSC).

Algorithms based on absorption models that relate PSC to phytoplankton absorption spectra  $aph(\lambda)$  and bio-optical algorithms that relate particle size distribution to the

backscattering coefficient spectrum  $bbp(\lambda)$  provided by ocean colour satellite data have been implemented for the Mediterranean Sea. The goal is to distinguish, at least, three size classes from satellite: picoplankton ( $0 < 2 \mu\text{m}$ ), nanoplankton ( $2-20 \mu\text{m}$ ) and microplankton ( $>20 \mu\text{m}$ ). The opportunity to use different size classes will be investigated while developing the PSC Mediterranean and Black Sea procedure. In situ observations (e.g. Coulter counter, flow cytometry, etc.) eventually available from other WPs of this project will be used to test the satellite methods. Satellite PSC time series will be produced starting from SeaWiFS data available since 1998. The analysis of the entire SeaWiFS mission (1998 to 2010) will be delivered by the end of February 2013. Preliminary results, based on the Brewin et al. (2011) model, suggest that this size analysis is a promising tool to investigate the European Seas environmental status on the basis of remote sensing data. Figure 16 is an example of the phytoplankton size classes spatial distribution for typical Summer conditions.

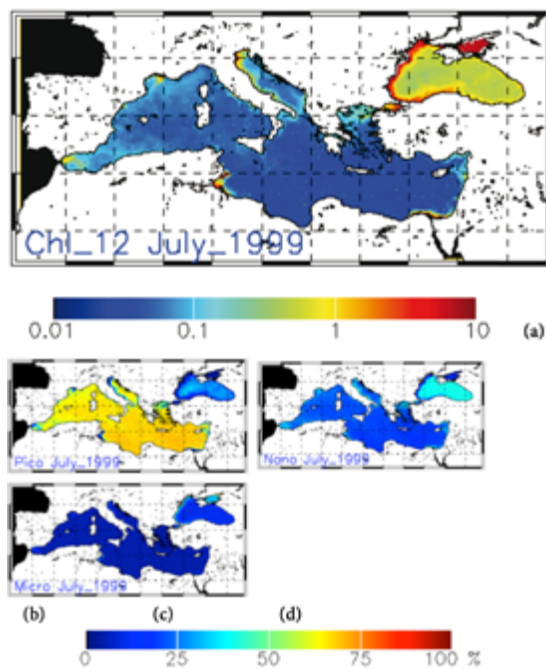


Fig. 16 - Phytoplankton Size Classes on July 1999. (a) Chlorophyll a concentration ( $\text{mg}/\text{m}^3$ ), (b) percent of Pico, (c) percent of nano, (d) percent of micro.

### Measurement of Mediterranean pigment composition by HPLC: WMED BIOOPT 2012 marine campaign

Field experiment activity included the analysis of the data acquired during the BIOOPT2012 cruise in March-April 2012 and the preparation of the 2013 experiment that will take place in April.

Pigment analysis have been done in the framework of PERSEUS (Policy-oriented marine Environmental Research for the Southern European Seas). Water samples (about 200 ml of water fixed using formaldehyde) were acquired for flow cytometer analysis of phytoplankton functional types. The analysis of the samples will start soon.

The development of our HPLC (high performance liquid chromatography) method combined with the use of other diagnostic methods (in-situ and satellite methods) was applied during the WMED BIOOPT 2012 campaign with the aim to contribute to the comprehension of the carbon biogeochemical cycles in the Mediterranean Sea and estimate spatial and temporal variability of its phytoplankton population.

The campaign took place in the period 22/03/2012-10/04/2012 and was organized by the Istituto di Scienze dell'Atmosfera e del Clima of the Italian National Council of Research (ISAC CNR), on board of the ship Urania.

The WMED BIOOPT 2012 campaign main objective is the characterization of Tyrrhenian and Sardinian Sea bio-optical and hydrological properties during the spring phytoplankton bloom phase through in situ measurements and further evaluation and comparison with satellite data. Station map of the investigated area is shown in Figure 17.

Recent methods used to estimate the distribution of phytoplankton groups are based on the measurement of pigment composition through HPLC. Pigment composition may be related to algal group composition through some Diagnostic Pigment Indicators, DPIs.

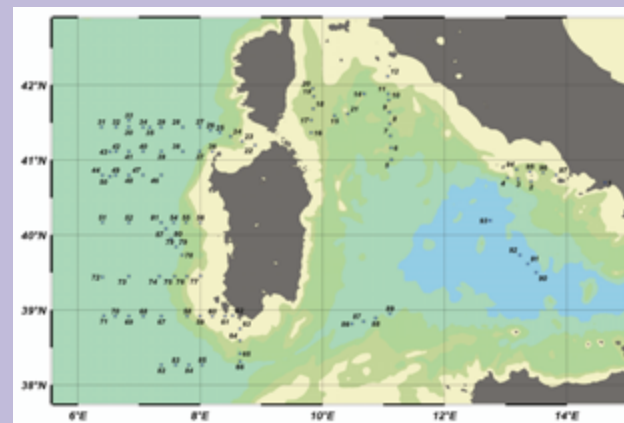


Fig. 17 - Map of the BIOOPT2012 campaign study area reporting the 97 investigated stations.

Samples collected during the WMED-BIOOPT 2012 campaign were analyzed by HPLC in order to detect 8 pigments usually used as DPIs.

Water samples were collected at different depths (surface, 10 and 25 m) and filtered. Filters were immediately frozen in liquid nitrogen for subsequent HPLC analysis. Pigment extraction was performed in 2 ml of 100% acetone. Samples were then sonicated for 10 min and finally left to extract for 24 h at  $+4^\circ\text{C}$ .

The set of the 1156 available data will be used for the following applications:

- data calibration of Sea Tech fluorometer [Chl a] data and subsequent validation of ocean colour satellite data;
- development of a primary production model in the Mediterranean;
- determination of phytoplankton group and size class distribution through diagnostic pigment analysis;
- calibration of lidar and CASPER [Chl a] dataset.

### MyOcean OCEAN MONITORING and FORECASTING: new products for Sea Water Surface Temperature



In the frame of MyOcean project we developed an advanced method for new high temporal resolution Sea Water Surface Temperature (SST).

This research activity started in 2011, continued in 2012 and was concluded by submitting the paper describing the results of the research to Remote Sensing of the Environment in November 2012. We evaluated the capability of SEVIRI to resolve the diurnal SST variability in the Mediterranean Sea in presence of clouds or other limiting environmental factors and to understand the role of air-sea heat and momentum exchanges in modulate its variability and we produced a new algorithm to reconstruct the hourly SST field over the Mediterranean Sea. This work is done in collaboration with colleagues working at CMS (Centre de Météorologie Spatial) MeteoFrance.

Having former demonstrated that in situ measurements and satellite data both contain a diurnal signal, the next question to answer is whether drifter, model, SEVIRI and DOISST SST data describe the same diurnal cycle. A first answer can be obtained by comparing the mean diurnal cycle by binning all the data at hourly intervals (local time) over the matched-up points (Figure 18). shows the result of this exercise.

All the three SSTs peak between 15:00 and 16:00 LST. The amplitude of the SEVIRI and drifter SST diurnal cycles are approximately the same ( $\sim 1.2^\circ\text{C}$ ) with a nearly constant bias of  $0.15^\circ\text{C}$ . This agreement is a confirmation of former findings over the entire SEVIRI disk. The model cycle, on the contrary, shows a reduced amplitude ( $\sim 1^\circ\text{C}$ ) with a positive bias of about  $0.2^\circ\text{C}$  before 10:00 and after 17:00 LST.

Next step was the evaluation of the capability of model and satellite OI reconstructed SST

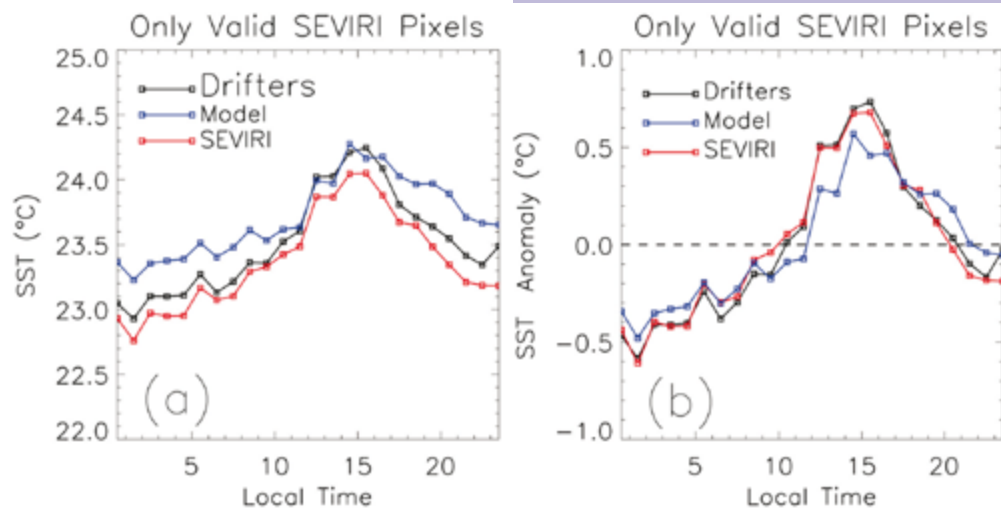


Fig. 18 - Comparison between the mean diurnal cycle observed by satellite, model and drifters. Mean hourly SST values from SEVIRI valid data (red), model (blue) and drifters (black) computed using all the satellite-in situ match-up points (a). Mean SST anomalies obtained from the three curves in figure 18a after removal the mean daily value (b).

estimate to capture diurnal warming (DW) events over the Mediterranean Sea. The diurnal warming is defined as the difference between the surface temperature at a given location minus the foundation SST, the latter being defined as the temperature of the water column just below the diurnal warming layer, free of diurnal temperature variability or equivalently the temperature at the first instants of the day when the heat gain from the solar radiation absorption exceeds the heat loss at the sea surface (see GHRSSST definition at <https://www.ghrsst.org/ghrsst-science/sst-definitions/>).

Our evaluation has been operated by analyzing the DW signal observed by drifters, by SEVIRI original data and by DOISST and model fields. From a satellite point of view, which experiences the presence of data voids due to cloud cover, DW can be equivalently defined as the hourly SST measured during daytime minus the mean of the previous night-time SST.

The latter temperature can be defined as the mean of all the valid SST measurements between midnight and the time when the solar

zenith angle becomes less than 90°. Within this study we applied this definition to our SEVIRI dataset and to the corresponding DOISST and model temperatures and we compared these DW estimates with corresponding DW observed in the drifters.

#### RITMARE Project



The Italian Flagship Project RITMARE (La Ricerca Italiana per il Mare) is one of

the National Research Programmes funded by the Italian Ministry of University and Research. The project officially started in January 2012 and will last until 2016. Our laboratory is involved in the subproject Observation Systems WP2 Observation systems based on remote sensing data, action 4 development of a marine lidar system.

During 2012 we started the design activity of the lidar fluorosensor apparatus to be operated on different carries in order to perform continuous measurements of environmental sea parameters.

#### RIMA



RIMA (Rete Integrata Mediterranea e Accesso a dati e prodotti) project has been proposed and approved in the framework of the “Sviluppo di servizi di Accesso a Dati e Prodotti in supporto alla Gestione dell’Ambiente Marino e Costiero mediante l’utilizzo di un Sistema Previsionale” of the Italian Ligurian Region and active since October 2012. The DIM activity is devoted to the development of a lidar sensor in collaboration with a private company that will exploit the future commercialization and installation on board of ship opportunities. Moreover the Laboratory is involved in the development of new software products for marine environment at regional and coastal scale.

#### Spectrofluorometric characterization of natural waters

Laser sensing can be very effective in significant measurements of the bio-optical parameters in natural waters. Our CASPER (Compact and Advanced laser SPECTrometer for Riade) completely realized and patented is based on double filtration (30  $\mu\text{m}$  and 0.22  $\mu\text{m}$ ) and double excitation (frequency quadrupled Nd:YAG laser emitting at 266 nm and diode laser emitting at 405 nm) in order to detect both dissolved and particulate components of waters coming from aquifers, rivers and lakes.

In 2011, CASPER has been deployed in the St. Lawrence Estuary (SLE), near Rimouski (Quebec, Canada), in the frame of the project CLIMAT “Utilisation complémentaire du lidar afin de valider les données bio-optiques obtenues par mesures satellitaires dans l’estuaire du Saint-Laurent”, in collaboration with ISMER-UQAR “Institut des Sciences de la Mer de Rimouski, Université du Québec à Rimouski”. The data collected in 2011 have been used to construct relationships between chlorophyll concentration and fluorescence, based on CASPER fluorescence line height measurements and ocean satellite sensors.

Phytoplankton abundance as estimated from the spectrofluorometer was relatively high NE of the maximum turbidity zone (upper Estuary), and areas influenced by fronts or freshwater plumes derived from secondary rivers (lower Estuary - Figure 19).

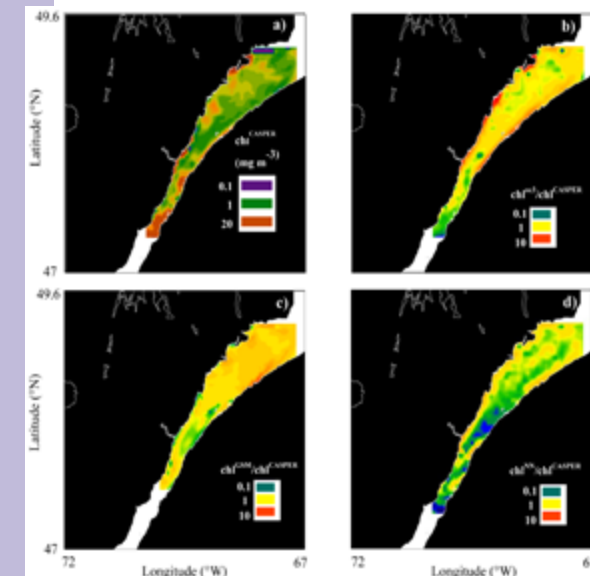
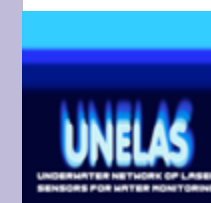


Fig. 19 - Spatial distribution of bias between global ocean color products and CASPER-related proxy of chl. a) CASPER-derived chl, b) ratio between oc3 and CASPER models, c) idem as (b) but for the Garver-Siegel-Maritorena model and d) idem as (b) but for the neural network model. No data (white pixels), land (black pixels), plots are in log<sub>10</sub> scale.

#### UNELAS Project



In the framework of the Scientific, Industrial and Technological Cooperation between Italy and Israel, the Israeli Ministry of Science and Technology and the Italian Ministry of Foreign Affairs

approved the project UNELAS – Underwater network of laser sensors for water monitoring. The partners are the Satellite and Wireless Communication Laboratory of the Ben Gurion University of the Negev (BGU), Israel and our laboratory. Building on the complementary experiences on underwater optical wireless communication (Israel) and bio-optical

characterization of natural waters by light-induced fluorescence (Italy), UNELAS aims to demonstrate the deployment of an underwater sensor network for coastal zones monitoring. The Israeli group is developing an underwater optical communication device, based on its wireless technology to transfer the information from the submersible sensor to the processing center above the sea surface. The Italian group is developing SOMBRERO, an underwater spectrofluorometer, based on its experience on CASPER, a patented instrument for the bio-optical characterization of natural waters by laser-induced fluorescence. The breakthrough of SOMBRERO is the use of UV and blue LEDs instead of lasers, thus reducing size, weight and cost.

The laboratory test of SOMBRERO (Figure 20) has been carried out obtaining the results shown in Figure 21.

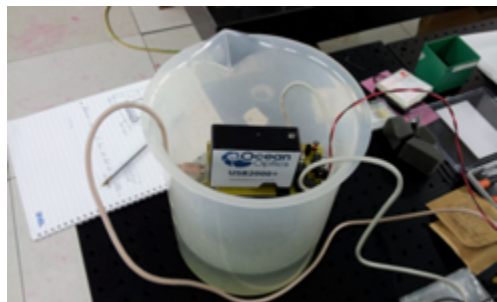


Fig. 20 - Laboratory test of SOMBRERO in algal solution.

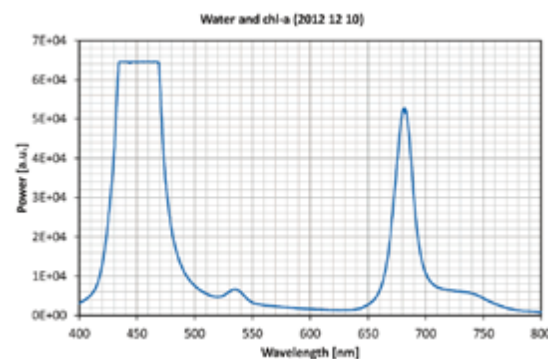


Fig. 21 - Spectrum of Milli-Q water and chlorophyll. The water Raman scattering is peaked at 535 nm. The emission at 680 nm (and 730 nm) comes from the chlorophyll fluorescence. The pigment concentration is proportional to the 680-to-535 ratio.

**Atmospheric Lidar measurements**



The true magnitude of CO<sub>2</sub> emissions from volcanic activity is poorly constrained, limiting our understanding of the natural carbon cycle. CO<sub>2</sub>-sensitive lidars could be used to measure the distribution of CO<sub>2</sub> in a volcanic plume, thereby allowing volcanic CO<sub>2</sub> fluxes to be measured directly. Two recently-begun ERC research projects CO2VOLC and BRIDGE aim to produce such instruments based on the differential absorption lidar (DIAL) technique (Figure 22).

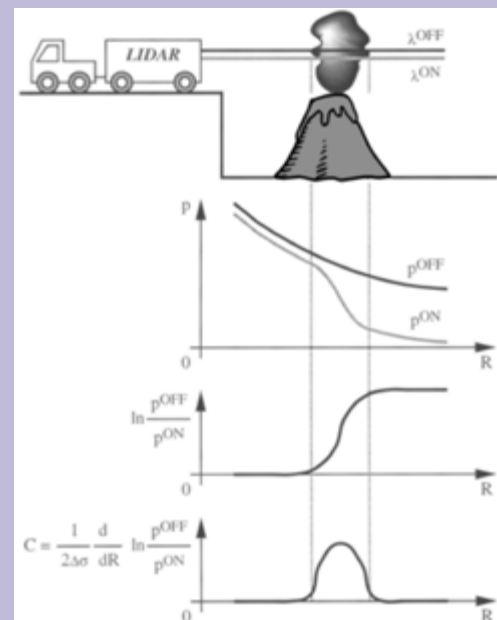


Fig. 22 - DIAL principle of operation. The figure does not represent the actual geometry of the experiment.

Our laboratory has been involved in the realization of two DIAL systems (airborne for CO2VOLC and ground-based for BRIDGE) for the lidar measurement of volcanic plumes.

Both projects are at their beginning and in this first months we investigated the ON and OFF wavelengths which offer optimal CO<sub>2</sub> detection and identify the spectral requirements of the lidar transmitter, in the context of commercially available cutting-edge laser sources. The atmospheric interference, mainly due to water vapor, was studied as well.

Once chosen the suitable ON and OFF wavelengths the lidar signal has been simulated with a numerical model and the following conclusions has been drawn: DIAL measurement of carbon dioxide in volcanic emissions should be performed in the 1.6 or 2.05 μm bands. After examining the absorption coefficient of carbon dioxide and water vapor, five spectral windows have been retained: 1570-1585 nm, 1600-1615 nm, 2005-2020 nm, 2045-2060 nm and 2060-2075 nm (Figure 23).

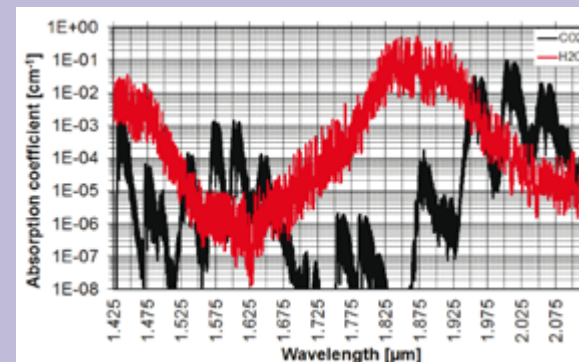


Fig. 23 - Absorption coefficient of CO<sub>2</sub> and H<sub>2</sub>O (1 atm, 296 K) from 1.425 to 2.125 μm.

Eventually, one wavelength per spectral window has been selected for DIAL measurement of carbon dioxide, having in mind to reduce cross sensitivity to water vapor. The observation of the atmospheric absorption coefficient at different altitudes led to the conclusion that laser transmitter should have a linewidth narrower than 0.05 cm<sup>-1</sup>. Beam full angle divergence and pulse duration should be less than 0.5 mrad and 100 ns, respectively, in order to accurately profile volcanic plumes.

**1.5 DIAGNOSTICS FOR CULTURAL HERITAGE PRESERVATION AND FRUITION**

**RGB-ITR: a laser scanner prototype for high-accuracy 3D color imaging of real scenes**

Laser scanning systems are steadily more and more employed for high-resolution 2D (two-dimensional) and 3D (three-dimensional) imaging devoted to an accurate reconstruction and modeling of a real scene. The technique has found widespread application for industrial, civilian and military purposes and, in the last years, also for precise surveys in the field of the Cultural Heritage (CH).

Besides an improved assessment about the preservation state of an artwork, the most advanced variations of the methodology enable also investigations on the pigment status. So, these devices are actually deemed fundamental in the localization of structural damages (surface cracks, delaminations, etc.) and of surface deterioration from physical or chemical agents. Moreover, the quantitative analysis and the processing of the data acquired with these devices can support CH professionals to estimate the amount of material necessary to a possible restoration work.



Fig. 24 - RGB-ITR system assembled in a tower configuration on a mobile platform. On the bottom: the first two boxes host a motion controller of the scanning motors and lock-in amplifiers for laser modulation and signals detection. Inside the next box: laser sources and detectors. On the top: the optical head with the scanning mirror. A laptop is used for the remote operating of RGB-ITR and for the analysis of the acquired data.

Within this framework, ENEA Artificial Vision Laboratory (ArtVisLab) in Frascati (Rome) is since several years involved in the development of electro-optics scanning systems with a particular attention to Amplitude-Modulated (AM) laser optical radars.

In the last times the laboratory efforts are mainly concentrated on remote and punctual diagnosis of cultural heritage, trying to develop instruments suitable for multiple purposes concerning restoration, diagnostics, cataloguing and education. A special attention has been lately devoted to the study of the preservation state of the pigments of an artwork with the purpose of developing a remote and punctual colorimeter.

In order to face this important challenge ArtVisLab has recently realized a new 3D laser scanner prototype called RGB-ITR (Red Green Blue Imaging Topological Radar, Figure 24). It is based on three AM laser sources emitting continuous-wave light with mW power at 450nm (blue), 532nm (green) and 650nm (red) mixed together by dichroic filters for obtaining a single white ray illuminating the investigated target. The system uses a motorized mirror for focusing and sweeping the laser beam onto the target.

Due to construction limits, the actual angle of view of RGB-ITR is  $90^\circ \times 310^\circ$ , with a point-to-point precision of  $0.002^\circ$ . The rate of data acquisition can currently achieve the maximum value of 10000 sample points per second. Five channels of information per each sampled point (pixel) are collected by three avalanche photodiodes and dedicated electronics: two distance measures (high and low frequency) and three target reflectivity signals (red, green and blue channels) with typical modulation frequencies of 190MHz for red, 1–10MHz for blue and 30kHz for green. So, RGB-ITR is a non-invasive, AM, continuous-wave 3D laser scanner that can concurrently acquire information on the range (i.e. form) and native color of the investigated target.

As final result, the device is particularly suitable to reconstruct high-resolution (sub-millimetric), high-quality, dense, accurate 3D color models for a hyper-realistic rendering of colored features on a target such as frescos and for identification of surface irregularities. Specifically, the combination of the five information acquired for each sampled point opens new scenarios for a remote punctual colorimetry allowing reliable diagnoses without the use of scaffolds.

The color information is retrieved by detecting the amplitude of the back-reflected signal from the target. A method for color calibration with the distance has been successfully tested in laboratory and finally adopted during field measurements performed by RGB-ITR for the 3D digitization of artworks.

It is based on the measurement of a reference white target placed at different distances (typically between 2.5m and 21m, approximately corresponding to the standard operating range of the instrument), that permits to obtain specific calibration curves for each color channel depending both on target distance and optical acceptance. Beside the color calibration procedure, in-house developed and copyrighted software packages permit to remote operate the RGB-ITR (ScanSystem) and to process the range and the calibrated RGB data (ITR\_Analyzer), so generating highly faithful and reliable 3D color models that can be exported into the most common 2D/3D file format.

A careful processing of 3D color models acquired is performed in order to optimize the color information. Specifically, this work has been mainly focused on the data involving the vault and the Universal Judgment of the Sistine Chapel (Vatican City, reproduction copyrighted), the Amore and Psyche Lodge (Villa Farnesina, Rome). An example of results obtained before and after the application of the aforementioned color calibration procedure on the recorded RGB-ITR data is reported in Figure 25.



Fig. 25 - 3D color model of the Sistine Chapel after the application of the color calibration procedure: vault (40.5m x 13.5m x 20.5m) and Universal Judgment (13.5m x 18.5m) acquired by RGB-ITR system. This image is shown for scientific purposes only.

A detail of this model is instead shown in Figure 26 along with a table reassuming the main RGB-ITR acquisition parameters during Sistine Chapel campaign. Specifically, the detail is represented by the thin rings of the God's ear in the Adam's creation fresco, that were previously observed only in photos collected at 50cm of distance by a Japanese team, while RGB-ITR acquired this image with similar resolution/accuracy at a distance of about 20m.

A further example of RGB-ITR data processing acquired in Sistine Chapel, still under development, concerns the identification of regions of calcium carbonate in the frescos. Within this framework, a technique has been properly developed. It is based on algorithms already tested successfully on digital mammograms for segmentation of the breast masses. Figure 27 (left) shows a result obtained

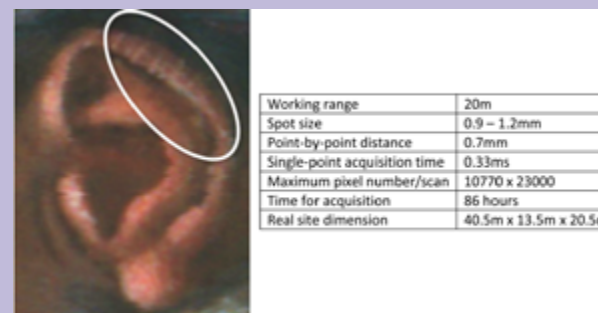


Fig. 26 – A detail on the vault of Sistine Chapel (left). On the right: a table of the main RGB-ITR acquisition parameters.

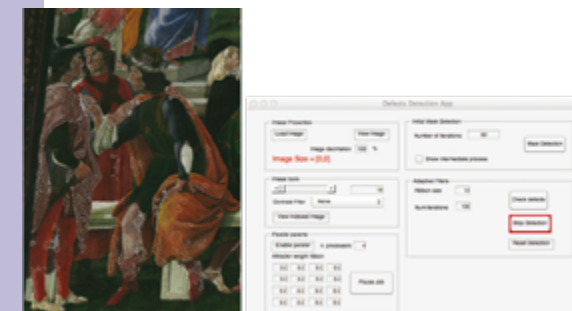


Fig. 27 - Left: segmented cropped image of the "Temptations of Christ" fresco (Botticelli, XV century), acquired by RGB-ITR, showing the results obtained with the developed technique for the detection of calcium carbonate regions enclosed by white lines. Right: graphic interface for the implementation of the developed technique.

by the technique known with the name of Active Contour (AC) applied on a crop of the fresco called "Temptations of Christ" (Botticelli, XV century, 3.45m x 5.55m). Despite the presence of false positives on which we are working, the achieved result is a good starting point for the development of a more robust method devoted to help the restorers in the automatic localization of the painting regions attacked by calcium carbonate. In Figure 27 (right) it is instead shown the graphical user interface that permits the implementation of the developed technique.

Finally, the results of scans of pigments similar to those present in the Sistine Chapel, acquired by RGB-ITR during laboratory tests, are

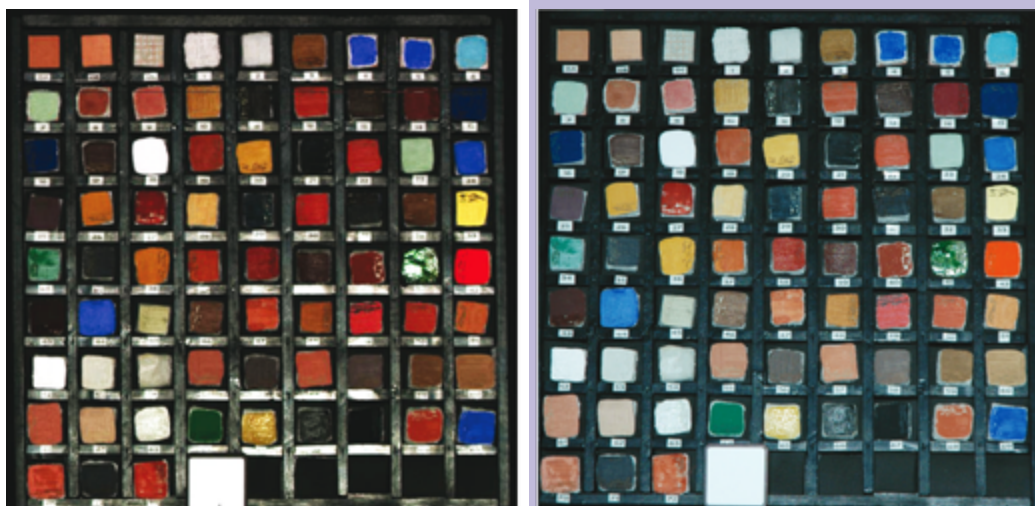


Fig. 28 - On the left: color model of the pigments similar to those present in Sistine Chapel acquired by RGB-ITR system during laboratory tests. On the right: photo (with flash) of the pigments scanned in the laboratory by RGB-ITR. A satisfactory result in terms of color hue and purity has been achieved.

displayed in Figure 28 (left) along with a photo of the pigments (right).

It should be noted that the color calibration procedure, applied to the raw data recorded by RGB-ITR properly referring to the Lambertian white target located in front of the sample holder of the pigments, permits to obtain a satisfactory result in terms of color hue and purity due to no dependency of the RGB-ITR system from external light sources. Future works will be addressed to the development of a further calibration method that takes into account the dependence of the color information on the viewing angle.

#### Development of an innovative subsea 3D laser scanner

2012 has marked a step change in the developmental activity of the amplitude modulated subsea 3D laser scanner. This technique is based on the measurement of the phase delay that a modulated laser beam acquires when back-reflected by a target and allows to record faithful 3D models of immersed objects. We demonstrated that a millimetric spatial

resolution at 10m of distance from the target is attainable depending on the water turbidity.

Within IT@CHA project and finalized to boost the technological innovation in maritime archaeology. The ArtVisLab is called to give momentum to its commitment and to deliver a device which can be effectively deployed in subsea for the inspection of archaeological sites. On the wake of critical inputs and feedbacks from potential end-users several technological and scientific innovations have been identified and studied to realize a less bulky and better performing sensor. To begin with, a new method to transmit electrical signals at Radio Frequency over long distances has been successfully tested in laboratory (Figure 29).



Fig. 29 - The modules for electrical to optical conversion of RF signals.

The method relies on the conversion of the electrical signals into optical ones and their transmission over single mode fibers for getting rid of the electromagnetic interferences. Adopting this solution enables the allocation of most of the electronic equipment on the support vessel thus considerably reducing the weight and the dimension of the immersed stage of the sensor. Another major improvement stems from the installation on the new sensor of two subsea-rated mini cameras (Figure 30) for ensuring visual guidance to the operator and also providing a stereo-vision of the scene under inspection for an early assessment.

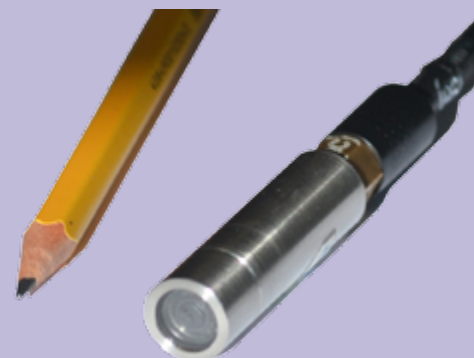


Fig. 30 - The subsea-rated mini camera.

The two cameras come from advanced technological developments in the offshore Oil and Gas sector and the possibility to combine in a modular sensor 3D laser and stereo-vision should be seen as a considerable leap forward in subsea monitoring practices.

Other advanced technological solutions studied and ready to be tested in laboratory include transmission of electrical, optical and Ethernet signals over a subsea rated dry-mateable cable, a detection scheme based on a linear array of optical fibers to enhance the field of view and a compact computer of new conception which could also accomplish the function of up to three lock-in amplifiers as well to generate the low frequency signal to drive the scanning mirror.

All the identified technological solutions have been analyzed and integrated to come up with a preliminary concept-design (Figure 31) of

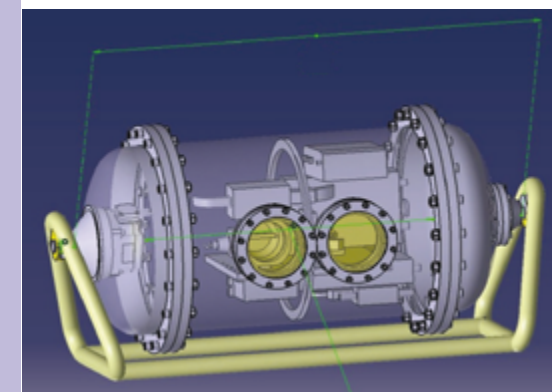


Fig. 31 - Concept-design of the new subsea 3D laser scanner

the new prototype to be developed. The two optical windows (12cm of diameter), are one devoted to the transmission of the laser beam and the other for collecting the optical signal to be processed. The prototype is ultimately intended for installation onboard a Remotely Operated Vehicle (ROV) for multitasking subsea survey missions.

#### Laser Induced Fluorescence for Cultural Heritage diagnostic, preservation and characterization

In the last few years, nanocomposites have been frequently applied for restoration and conservation of artworks. In fact, it has been demonstrated that inorganic oxides nanoparticles, such as silica and titania, improve the performance of materials used in conservation field. In this study, properties of consolidant and protective materials prepared in solutions with homogeneous dispersed nanoparticles have been analyzed after application on marble and travertine samples. To this purpose different solutions of acrylic polymer and silicon-based resins with silica and titania nanoparticles were prepared. New Travertine samples, white and grey Carrara marbles, new and aged in climatic chamber or at open air, provided by UTTMAT-DIAG were used as substrates (Figure 30 left)  $\text{SiO}_2$  and  $\text{TiO}_2$  nanoparticles were produced by  $\text{CO}_2$  laser pyrolysis in the UTAPRAD-MNF laboratory by using tetraethoxysilane and



titanium tetraisopropoxide as precursors, respectively. The nanoparticles were dispersed in solution at different concentrations and used for mixing with acrylic resin (Paraloid B72) and commercial polyalkylsiloxane (Rhodorsil RC80). The obtained solutions were applied on specimens by brushing until manifest refusal to simulate the treatment in real situation (Figure 32).



Fig. 32 - White and grey Carrara samples (top) and application of solutions by brushing (bottom).

Such treated stone samples were submitted to aging processes both in climatic chamber, taking into account temperature and relative humidity, and in solar box, for considering solar light irradiation, in view of simulating a natural open air exposition.

Laser Induced Fluorescence (LIF) measurements were executed before and after the accelerated aging to characterize by a remote diagnostic tool the different materials by means of their fluorescence spectral signatures. In particular, LIF was performed to enhance the database of restoration products with the aim to recognize in future

measurements in field these innovative materials and to test their resistance to the climatic agents.

LIF spectra excited at 266 nm showed that for Rhodorsil RC80 and Paraloid B72 treatments, the addition of  $\text{SiO}_2$  nanoparticles causes an increase of intensity bands respect to the pure polymer matrix. The presence of  $\text{TiO}_2$  decreases the signal intensity, in different bands ratios related to the acrylic and siloxane matrix. Also in the case of travertine  $\text{SiO}_2$  nanocomposites increase the fluorescence efficiency, while  $\text{TiO}_2$  decreases the signal. The photo-oxidative and mechanical aging tests reveal important different degradation processes clearly related to the selected exposure conditions and to the specific chemical and physical nanocomposite properties. The specimens exposure to the Solarbox irradiation shows for the siloxane treatments a good surface resistance due to the minimal morphological variation observed in SEM images and to the permanently characteristic luminescence bands in the acquired LIF spectra. On the contrary, Paraloid B72 irradiated films show in SEM images relevant surface alteration (rise of pores, similar to the pitting phenomena corrosion, loss of the polymeric material, individuated also in presence of nanofiller) and the LIF spectra confirm this weathering: the luminescence band at 330 nm, characteristic of the acrylic polymer, disappears (Figure 33).

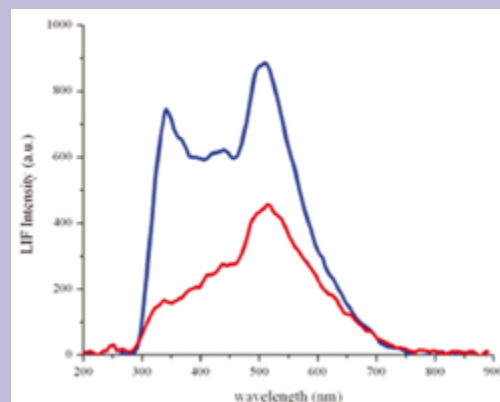


Fig. 33 - LIF spectra of a marble sample treated with a Paraloid B72 nanocomposite before and after Solarbox (S.) aging.

This strong signal decrease can be due to reactions of photochemical degradation. In fact, changes in the molecular structure, as alterations in the unsaturated functional groups, as the carboxylic and carbonylic ones, responsible of the fluorescence processes, could occur.

#### Spectral database of Renaissance fresco pigments by LIBS, LIF and colorimetry

The fast analysis and recognition of fresco pigments by optical methods that are fully non destructive or present a very low invasiveness is an important issue. In fact, the more information on surface materials of a fresco are given to the restorers, the better the restoration works can be carried out. In particular, the used pigments, the followed procedure and eventual successive application of consolidants or modern pigments are the most enquired queries that chemists and physicists receive from art historians, archaeologists and restorers for dating, assignment and investigation of ancient artworks.

During the last decade laser techniques, as Laser Induced Breakdown Spectroscopy (LIBS) and Laser Induced Fluorescence (LIF), have been recognized as unique tools for Cultural Heritage study mainly due to the offered advantages relevant to in situ applicability, capability of remote analysis, minimal or absent invasiveness, and as far as LIBS is concerned, possibility to perform stratigraphic analysis with high sensitivity for a very large number of elements, including light atoms. According to the procedure sketched in Figure 34, a set of about 70 fresco specimens



Fig. 34 - Material and technique used for sample preparation.

has been prepared with pigments and binders typical of the Renaissance period in Rome. Afterward they have been characterized by the LIBS, LIF apparatus developed at the DIM Laboratory and by means of a ColorLite sph850 spectrophotometer (for reflectance and colorimetric measurements) in order to build as much as possible a complete database. Aiming at providing the restorers and art historians with a useful tool for the study of ancient frescoes, the samples have been prepared in agreement with the Cennino Cennini recipes for both materials and procedures. In particular, much attention has been paid to the geographic origin and chemical composition of plaster (intonachino) and pigment components. LIBS measurements have been carried out at 1064 nm, while LIF ones have been performed using two wavelengths (355 and 266 nm), in order to compare the different induced fluorescence emissions.

The results obtained support the choice of combining in the database colorimetric measurements, LIBS data and LIF spectra at two different excitation wavelengths. The results found on applying a multivariate analysis method on data extracted from LIBS spectra prove the necessity and the utility to use this methods to correctly interpret experimental data and to find out from the most important features for clustering and material characterization. In particular the outcomes suggest to use statistical approaches in the analysis of all the acquired data of the database for a smart and quick characterization, that can help in on field analysis of historical frescoes.

### LIBS for underwater material analysis

During the last part of the project AQUALAS in collaboration with the University of Malaga (UMA), aimed to develop a LIBS system for in-situ underwater measurements, a large amount of the previously acquired data was further elaborated. These measurements regard characterization of processes during laser ablation of a metallic target underwater and include the following optical techniques: laser scattering, laser beam transmission and reflection, shadowgraphy, fast photography and LIBS signal detection.

The obtained results fully explain the LIBS signal behaviour inside liquids under dual pulse excitation. Here, the defocusing effect of the vapour bubble (Figure 35) formed by the first laser pulse and reflections at the bubble alter the beam coupling and the detection efficiency.

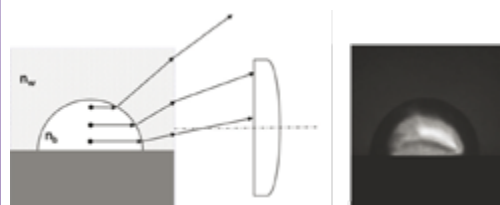


Fig. 35 - Position dependent collection of the secondary plasma generated inside the expanded bubble: left - Illustration; right - photograph of the secondary plasma.

Transitions through the focal volume of the shockwaves generated by the first pulse and reflected by nearby solid objects, change the local refraction index and enhance the LIBS signal produced by the second pulse even for a factor 4X (Figure 36).

By a fast photography we discovered that the primary plasma during ablation in liquids develops in two phases: violent particle expulsion and ionization during the first  $\mu\text{s}$ , followed by slow plasma growth from the ablation crater into the evolving vapour bubble. This second phase of the plasma growth inside liquids, with duration longer than 30  $\mu\text{s}$ , was observed for the first time. Such effect was explained by backward propagation of the

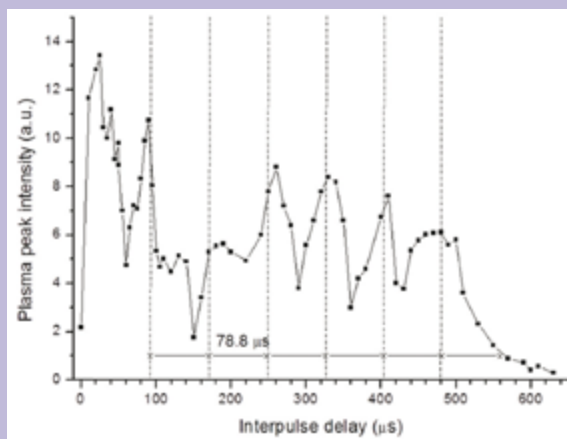


Fig. 36 - Peak intensity of the spectrally integrated plasma as a function of interpulse delay: spacing between the vertical lines indicate the time necessary for round trip sample-cell's wall of the initially formed pressure wave.

initial plasma slowed down by dense media, and the consequent reheating of the sample.

Beside the LIBS spectroscopy, the findings described above are important also for medical applications, underwater imaging, wet material processing and synthesis of nano-materials in the liquid phase.

### 1.6 TECHNOLOGIES FOR ENERGY

#### IVVS - In Vessel Viewing and ranging System for ITER

The "In Vessel Viewing and ranging System" (IVVS) is a fundamental remote viewing equipment, which will be used to achieve a survey of the status of the first blanket wall and plasma divertor facing components in ITER and to make erosion measurements of the vessel during the plasma discharges.

The activities of design and testing of the probe components are ongoing in the framework of a Fusion for Energy (F4E) grant for making the IVVS probe compatible with ITER working conditions such as high temperature, very high magnetic field (8T), ultra high vacuum (UHV), neutron and gamma fluxes (5kGy/hour and integrated dose up to 10MGy). Furthermore,

the IVVS probe dimension must be compatible with the geometrical constraints coming from the space allocated to the system and from the port to access to the vacuum vessel. The IVVS prototype developed at ENEA is a compact amplitude-modulated laser radar able to obtain high-resolution intensity and range images. The probe steers the laser beam through a fused-silica prism attached to the mechanical axes whose rotations allows the scan of the desired area. Two optical encoders accurately measure the angular position of the prism allowing the reconstruction of high-resolution images. Several tests have been performed at ENEA CALLIOPE gamma irradiation facility (dose rate 2.5kGy/h and total dose 4MGy) on piezoelectric motor, optical encoder and fused-silica optical samples in order to verify the dielectric coatings behavior under irradiation (Figure 37).

The PI piezo-actuator under investigation is a rotary stage prototype consisting of two piezo-linear devices U-164 preloaded against a ceramic friction ring. They work as a brake when at rest while during the operation phase they oscillate with ultrasonic frequencies providing a rotation of the ring. The overall tests campaign on IVVS probe will be completed within 2013 exploiting other ENEA facilities. Erosion tests have been also performed on calibrated target (aluminium alloy plate) placed at about 4m of distance from the IVVS laser radar. The metallic plate was eroded on



Fig. 37 - Left: piezo-motor test assembly on Calliope Facility. Right: detail of piezo-motor test assembly.

four different areas (engravings) with various depths (2.1mm, 0.5mm, 0.3mm, 0.1mm) in an attempt to simulate the possible erosion processes of the ITER vessel. The plate under investigation was then sanded to eliminate undesired back-reflections contributions and weighted before and after the erosion process. Thereafter, a series of scans of the target was carried out by means of the IVVS laser radar placing the metallic plate at different orientations with respect to the direction of the incoming laser beam (inclination angles of 0°, 20° and 45°) for acquiring high-resolution, reliable, accurate 3D models of the investigated target. A comparison between the plate loss of weight opportunely evaluated by means of the IVVS laser radar and measured by a high-accuracy balance before and after the erosion has been performed showing a maximum percentage error of 7%. Currently we are going to transfer this technology to the industry for a future delivery of laser viewing and ranging systems for fusion reactors.

#### LIBS detection of H and D in ITER-like tiles superficial layers

High temperature plasma in hydrogen isotopes are peculiar of thermonuclear fusion devices. The study of plasma-wall interaction is of paramount importance for avoiding both damage of plasma facing components (PFCs) and pollution of the plasma. To assure

continuous and fault free operation a strict control must be exerted on the amount of impurities deposited on, and of the fuel retained in the PFCs. These requirements make LIBS (Laser Induced Breakdown Spectroscopy) an ideal candidate for on-line monitoring the walls of the current as well as of the next generation (like ITER) fusion devices. LIBS has become a powerful tool for the fundamental studies of the interaction of laser beams with materials. The spectroscopy of the radiation emitted by the LIBS may be used to obtain the characteristic physical parameters, such as the temperature, the electron number density, the atom and ion number densities, and the relative concentration of different element present in the target. In the framework of the European Fusion Development Agreement (EFDA) task WP11-ETS\_DTM-01 "Dust and Tritium Management" LIBS was used to advance and qualify the operation of a remote system on a ITER relevant experimental set-up, performing Hydrogen and Deuterium inventory on Al and W substrates (single and mix materials). The activity has been carried on in cooperation with UT-FUS Unit.

The optimization criteria considered were the capability of a LIBS system in working at low pressure and remotely, at a distance of some meters from the target to spectrally detect thin coatings of materials of fusionistic interest like the samples here used as targets and specifically prepared to simulate PFCs covered with nuclear fusion fuel and impurity layers.

The apparatus is composed of a vacuum chamber, 35 cm diameter in which the sample is placed vertically on a two axis motorized translation stage remotely controlled for changing the measurement point. All the measurements were carried out in our LIBS laboratory set-up already described in 2011 Activity Report a residual pressure of  $1-3 \times 10^{-5}$  mbar to reproduce plasma emission in high vacuum conditions, as expected in a tokamak. It is not worth noting that in-vacuum plasmas exhibits different behaviors respect to those at atmospheric pressure due to the reduced

electron density and temperature. A set of diamond-like carbon (DLC) layers with two different D concentrations and mixed W:Al:C deposits with W(5-10%):Al(45-48%):C(45-48%) were prepared on W substrates by vacuum arc deposition method by Forschungszentrum Jülich (FZJ, Germany), simulating ITER-like deposits on PFCs, particularly in the divertor zone. Al was used as proxy for Be (not used in these samples due to its toxicity) that, together with W and C will be one of the principal constituent of ITER PFCs. The nominal thickness of the superficial layer was  $\geq 3 \mu\text{m}$ . The samples, round shaped with a diameter of 25 mm, were first characterized by FZJ with Thermal Desorption Spectroscopy (TDS) and Nuclear Reaction Analysis (NRA) to determine the concentration of each element.

The detection of H and D in traces was of principal interest for the present study. We detected H and D via their spectral line  $H\alpha$  and  $D\alpha$  at 656.1 and 656.29 nm respectively. Figure 38 shows the LIBS signal in the spectral region of interest on sample DLC1.

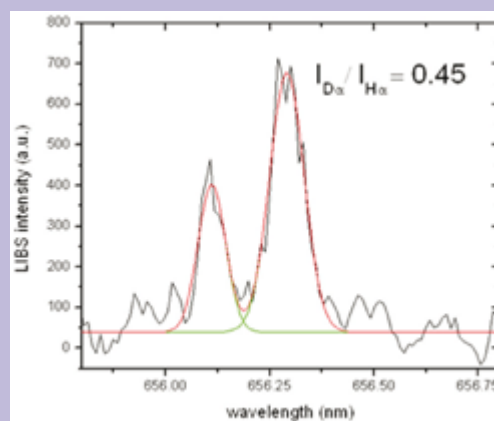


Fig. 38 - LIBS signal from the DLC superficial layer in the spectral region around 656 nm with a detail of spectral region around H and D peaks with the reported intensity ratio.

$H\alpha$  and  $D\alpha$  emissions are clearly visible and well resolved. Through the preliminary NRA measurements, the atomic concentration of D in the surface layer was estimated to be around 3%. The H-D peaks intensity ratio can be used

for the estimation of the relative abundance of the two species. The same procedure could be applied in the case of Deuterium and Tritium under routinely operation. Calibration Free methods have been successfully applied to the determination of several elements present either as major constituents or in traces. The result of its application to the present case is shown in Table 1 and has relevant specific advantages since it not requires any calibration procedures and all the difficulties related with sample preparation are overcome.

Sample #	Element	Nominal value (at/at)	CF
C-W 1	C	70	$70 \pm 12$
	W	27	$27 \pm 12$
C-W 2	C	82	$76 \pm 12$
	W	15	$21 \pm 12$
MIX1	Al	35	$32 \pm 8$
	C	50	$57 \pm 10$
	W	15	$1 \pm 4$
DLC1	D	~3	$5.3 \pm 1$
	C	100	$97 \pm 1$
DLC2	D	~3	$2.8 \pm 2$
	C	100	$96 \pm 1$
	D	~3	$3.9 \pm 4$

Table 1 - Samples nominal content and quantitative determination from CF.

The LIBS apparatus installed on top of the FTU reactor is shown in Figure 39, with details



Fig. 39 - LIBS apparatus installed at the ENEA Fusion facility FTU. In detail, the apparatus and the optical window.

of the optical entrance window for diagnostic. The optical laser beam has been lunched over a target located at 2m distance. The successful results will be used for future design of a new permanent LIBS apparatus as routine diagnostic of the European ITER reactor.

### Mechanism of LIBS signal generation in plasma characterization

It is well known that ablation of solid targets by nanosecond pulsed lasers of high power densities results in rapidly expanding partially ionized vapour clouds (plasma plumes), with electron temperatures in a range from a fraction of eV up to 20 eV. For such laser regimes the observation of prompt electrons with energies above that of the plume, emitted during laser pulse has been observed with the LIBS apparatus. To elucidate the physics of formation of such electrons, experimental evidence concerning their number, details of the energy distribution as well as their dependence on the target material, laser power density and wavelength is necessary. This issue was addressed here through a dedicated study, in collaboration with the "Pietro Caldirola" Institute for plasma physics, afferent to the Italian National Research Council (CNR). Here electrostatic measurements of the charge released from different targets are complemented by detailed spectroscopic studies of the background Nitrogen gas emissions. The latter contains information on the prompt electrons energy distribution and its evolution during their propagation, retrieved by employing a time-dependent collision-radiative model including all the relevant collision (Electron-Energy-Distribution-Function EEDF), quenching and vibrational relaxation rate coefficients that have been recently measured, allowing its application to a wide range of gas pressures. In the layout of the set-up (Figure 40) targets are located in the center of a cylindrical-shaped vacuum chamber, perpendicular to the linearly polarized laser beam.

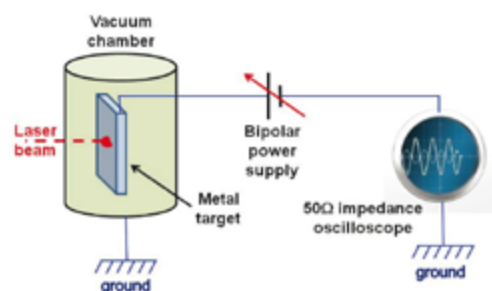
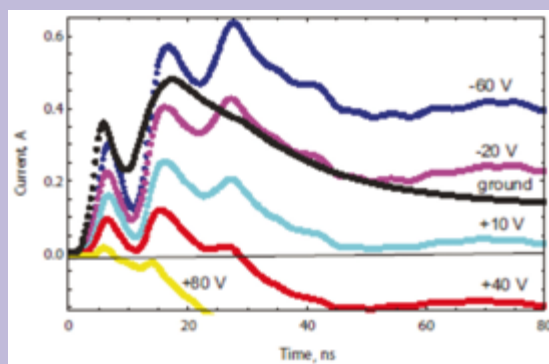


Fig. 40 - Electric circuit.

The beam energy used in the experiments is in the range of 80-140 mJ with a 300  $\mu\text{m}$  laser spot diameter, corresponding to an averaged power density  $I = 10^{10} \text{ W/cm}^2$ . The optical signal is collected at an angle of  $45^\circ$  with respect to the laser beam axis and the optical focus is located at a fixed distance of 8 mm in front of the target to enable spectroscopic measurements. The experiments have been conducted in a flowing  $\text{N}_2$  gas in the pressure range  $p=2 \times 10^{-5} \text{ mbar}$  to  $p=2 \text{ mbar}$  with Tungsten (W), Molybdenum (Mo), Silver (Ag) and Alumina ( $\text{Al}_2\text{O}_3$ ) targets. The targets are biased to both positive and negative voltages by mean of a linear power supply; the current in the circuit is measured by the internal 50 Ohm resistor of a 350 MHz - 4GS/s oscilloscope. Time-resolved spectroscopic data are acquired by an ICCD with a nominal minimum gate width of 25 ns. The gate aperture is triggered by the laser's Pockels cell trigger, and delayed by 1 ns steps. Successive spectra are acquired by incremental delay.

The results reveal that the shape of the spectra and hence of the energy distribution is insensitive to the target material be it conducting or dielectric and also to laser power density; changing of either results only in the variation of the number of the prompt electrons emitted. Fitting of the  $\text{N}_2$  spectra suggests that the energy distribution is narrow, centered at 70 eV or larger. The experimental evidence suggests that collective plasma laser interaction takes place providing a robust frequency matching determining the final energy of the electrons. Electric measurements with all the conducting targets

studied here have revealed a picture similar to that of Figure 41 an always positive pre-peak (implying that prompt electrons have been released from the surface) and a broader part of the curve corresponding to the recollection of the charges from the plume plasma. We point out that while vapour/plasma cloud is formed within a few picoseconds, transport of the plume species back to the target is on longer time scales and dependent on the target geometry and dimensions.

Fig. 41 - Current collected by W target biased at voltage indicated at  $p=1.4 \text{ mbar}$ .

### Energy storage: ProGeo project

The accumulation of electricity from renewable sources (principally from wind power) through the transformation of surplus into "electro-fuels" is becoming one of the most competitive means of energy storage. Of the "electro-fuels" in productions, methane ( $\text{CH}_4$ ) is the front-runner for the simplicity of its production process, its world-wide availability, and the decades of its use. In Italy, construction of a ProGeo 20 kW prototype has been funded by the private firm PLC System and the demonstrative plant will be completed by July 2013 up to the green-methane storage. The ProGeo accumulator is designed to use the "surplus" electricity produced at "low cost", or "not produced", generated by any energy source be it renewable or not, to produce methane by the so-called Sabatier reaction between  $\text{H}_2$  and  $\text{CO}_2$  and to distribute it or to store it for deferred generation of "on-

demand" electricity. Substantially ProGeo will be able to accumulate electricity as chemical energy, transforming it into methane. In doing so ProGeo will satisfy energy "peaks" using the methane produced and stored for generating electricity as required or, if needed, to supply "green-methane" ( $\text{CO}_2$  neutral) directly for transportation applications or to the distribution pipeline for heating or cooking. ProGeo is, therefore, both like a non-conventional "large scale energetic storage" and a "production plant" for  $\text{CO}_2$  neutral fuels. The construction of the prototype plant will create the technological base for other plants of various dimensions, from a few kW to numerous MW. Four fundamental phases of ProGeo's process are foreseen (see Figure 42):

- Electrolysis produces hydrogen and oxygen from water. This process features a passive safety characteristic.
- Methane is created by the Sabatier reaction, using hydrogen and carbon dioxide to make water and methane (the reaction is without energy costs, being self-sustaining.)
- Once methane is obtained, it can be distributed for various uses, among these, transportation, accumulated for long-term storage or for producing deferred cost electricity during peak request times.
- In the last phase, electricity can be produced

using existing and low-cost Internal combustion Engines, or making use of more advanced systems like Fuel Cells of Solid Oxide, or of micro Gas Turbines.

The figure also shows the storage systems and the successive phases of methane combustion and of the oxygen produced, to generate "differed" electric power, with successive treatment of the combustion exhaust. From this general concept, one may discern the configuration of the products, which cover a very wide range of end uses.

The technological advantages of a reliable storage system are manifold. The first of these is the ability to use the surplus of low-cost electricity to produce a clean fuel. This aspect has, not only a technological advantage, but is also a springboard for development, diffusion and an incentive to invest in alternative sources of energy. This detracts nothing from the fact that the proposed technology is applicable, if in reduced scale, to traditional energy plants, carbon for example, having high  $\text{CO}_2$  emission taking advantage of the low night time production costs. The second advantage lies in the development and testing of highly innovative technology (high-efficiency nano-structured electrodes, filter systems

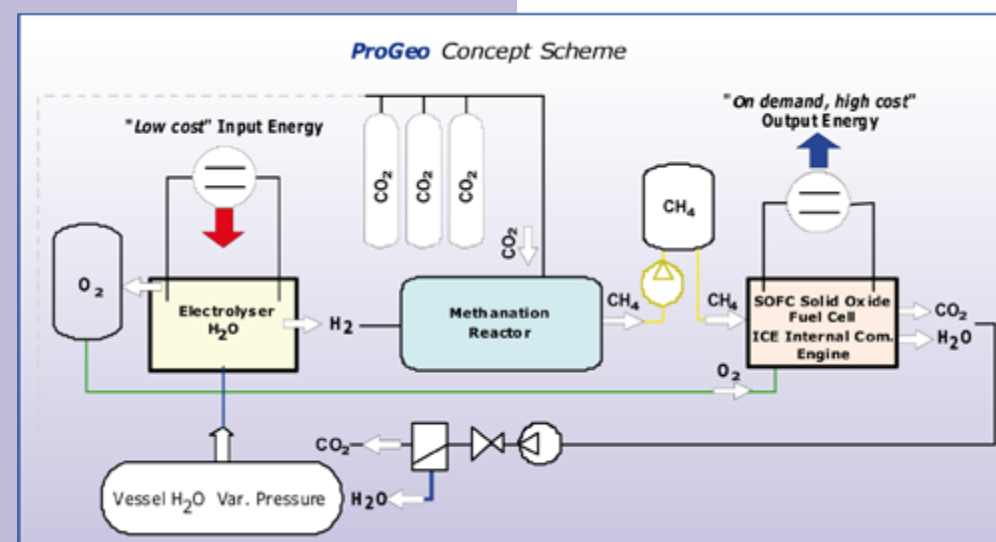


Fig. 42 - Concept Scheme.

for hydrogen made of polymer membranes, methane developed with porous nano-structured matrices) which have technological application ranges from the production of hydrogen to the accumulation of fuel ( $H_2$  and  $CH_4$ ) and the capture of  $CO_2$  (even in minute quantities) but most importantly with production of precious fuels having a neutral  $CO_2$  cycle.

The R&D phase of the electrolyser includes the recovery of heat released in the methanation phase and the use of nano-structured electrodes which increase the efficiency of the electrolysis itself. This activity should end with a “unification” of the two components (upon the recovery of the heat) in a single compact, safe and highly efficient “object”. The strong points of the system lie in the use of nano-structured materials for high efficiency processes under steadily monitored parameters (temperature and pressure) to regulate the quantity of methane produced and maintain the “intrinsic” safety feature during the entirety of both processes. At the moment the first phase of R & D has been completed at the University of Tor Vergata (Rome), Department of Chemistry and Chemical Technologies (Figure 43) with the identification of all the process parameter connected with a specific catalyst. The percentages of  $CO_2$  produced in the methanation reactor will be near 95% and it is also possible to separate the portion of  $H_2$  that do not react with the  $CO_2$  returned to the



Fig. 43: Experimental methanation reactor.

reactor. Nano-material polymer membranes are being developed that better performance and are capable of separating only the portion of hydrogen suspended in the flow composed principally of  $CO_2$  and  $CH_4$ .

At the end of combustion for generation of “on-demand” electricity, the exhaust gasses are cooled and the  $H_2O$  and  $CO_2$  are recycled into the process. In this phase the  $CO_2$  to be stored for later use is separated out. R&D concerns are centred upon the separation and recovery of the  $CO_2$  corresponding.

### 1.7 TECHNOLOGIES FOR INDUSTRY SUPPORT

On demand of one Italian industry, we performed feasibility studies of recognition of dark plastic materials by LIBS technique. The scope of this work is to implement rapid on-line sorting of such materials, thus allowing for their recycling. Presently, affordable sensors for the sorting of dark plastics do not exist in the market.

The measurements were performed on four types of black plastics, namely ABS-FR, ABS-VO, PP e PS. Under optimized experimental conditions and by a proper choice of the spectral parameters and the procedure for the recognition, the excellent results were obtained for the measurements by one laser pulse.

### 1.8 EDUCATION AND KNOWLEDGE DISSEMINATIONS

As in previous years a great deal of attention to knowledge dissemination and to the educational activities at very high level. Indeed, these activities have been recognized by international and national awards. More specifically in the FORLAB Project ENEA is leader of the work package “DISSEMINATION AND EXPLOITATION”. The main objective of this work package is the preparation of the overall strategy for the dissemination plan of the project results and its implementation.

## 2 PHOTONICS MICRO AND NANO-STRUCTURES LABORATORY

### 2.1 MISSION AND INFRASTRUCTURES

Photonics and nanotechnology have been recognised by the European Commission among the Key-Enabling Technologies (KETs) of the next European program Horizon 2020. They play an important role in the R&D, innovation and strategies of many industries and are regarded as crucial for ensuring their competitiveness in the knowledge economy.

The major challenges in the modern world, solution for energy, health, environment, information and communication technology (ICT), safety and security, are driven in their development by the production and manipulation of photons, the basic unit of light. In the last decades, important advances in the field of nanotechnologies enabled major breakthroughs in various scientific domains, due to the possibility of controlling and tuning the physical properties of materials at the nanoscale.

Today one of the main objectives of photonics is the R&D of technologies for miniaturization of optoelectronic devices and optical sensors, including functionalisation with nanomaterials, control of interfaces at nanoscale and engineering of semiconducting-metal-dielectric media of sub-micrometric dimensions for exploitation of light-matter interactions and confinement effects.

At ENEA C.R. Frascati, in the Technical Unit for the Development of Applications of Radiations, the Photonics Micro- and Nano-structures Laboratory (UTAPRAD-MNF) carried out R&D activities on synthesis, characterisation and functionalisation of nanomaterials and on study, realization and characterization of novel light-emitting micro-devices and radiation detectors; they are combined with consolidated expertise in applications of optical fibre sensors for structural monitoring and activities in seismological field.

They found applications in scientific fields and industrial sectors - high-energy physics, biomedical imaging and diagnostics, photonics, cultural heritage, seismic prevention, etc. as well as for innovative energy production systems, including nuclear ones.

In 2012, the activities focused on:

- development of synthesis processes of Si-based nanostructures and electronic characterization of interfaces, with specific interest on scientific research and technological applications in the fields of photonics, electronics and energy, e.g. solar cells and energy storage devices;
- development and optimization of laser assisted pyrolysis synthesis for nanopowders production. Their characterization by morphological and physical-chemistry analysis are carried out together with investigation of their functional properties, e.g. biocompatibility and in vivo and in vitro luminescence, thermal properties of several composites, etc;
- study, realization and optical characterization of novel solid-state luminescent radiation detectors based on films of dielectric (lithium fluoride, LiF), organic (Alq<sub>3</sub>, TPD) and metallic (Al) materials grown on amorphous, crystalline, and plastic substrates by using thermal evaporation technique. They found applications in micro and nanotechnologies, photonics, energy and in the biomedical diagnostics;
- investigation of luminescent materials through laser confocal microscopy and photoluminescence spectroscopy for the development of miniaturized solid state light-emitting devices, including OLED, solid-state lasers and amplifiers in waveguide configurations, optical microcavities and distributed gratings;

- study on the enhanced sensitivity of Raman/SERS spectroscopy in different configurations. This technique is also used to analyze traces of energetic materials and contaminants;
- development of interferometric techniques and benches based on distributed optical fibre sensors for static and dynamic monitoring of infrastructures, in particular in large civil engineering works, cultural heritage and seismic prevention;
- application of methodologies for the evaluation of the seismic hazard on regional and local scale, in order to reduce the seismic risk through the acquisition, interpretation and analysis of geological, geotechnical, geophysical and historical data.

Available infrastructures include well equipped laboratories and advanced instrumentation for material synthesis, light-emitting micro-devices developments and their characterisation:

- evaporators for the growth of dielectric, metallic and organic thin films;
- plants for laser assisted synthesis of nanopowders (LUCIFERO), nanowires and carbon nanotubes;
- electron spectroscopy laboratory;
- optical spectroscopies and confocal laser microscopy laboratories;
- interferometry and fibre optical sensors laboratories.

#### Funding and projects

In 2012 UTAPRAD-MNF carried on R&D activities within the frame of public funded national research programs of industrial research supported by MIUR (Ministero Istruzione, Università e Ricerca) and MiSE (Ministero dello Sviluppo Economico), in collaboration with Italian universities, research institutions and industries.

In the seventh framework programme FP7, UTAPRAD-MNF participate to EU projects,

mainly on Theme 4, NMP – Nanosciences, Nanotechnologies, Materials and New Production Technologies – in collaboration with scientific and industrial partners, and in networking EU actions, MPNS - Materials, Physical and Nanoscience – domain.

Private funded industrial projects devoted to develop innovative products with high technological content were also carried out.

There were frequent and fruitful technical contacts with several small and medium companies operating in the field of optical components, spectroscopy, microscopy, lasers, and vacuum evaporation systems.

## 2.2 NANOSTRUCTURES AND NANOTECHNOLOGIES FOR ENERGY EFFICIENCY

### Band alignment at the CdS/CZTS interface of thin film semiconductor solar cells

In recent years the kesterite compound  $\text{Cu}_2\text{ZnSnS}_4$  (CZTS) has been attracting increasing interest as a thin-film solar cell absorber. This material has a gap close to the single-junction optimum value for maximum energy conversion efficiency and could potentially substitute  $\text{Cu}(\text{In,Ga})\text{Se}_2$  (CIGSe) and CdTe thin-films absorbers because of its lower-cost, earth-abundant and non-toxic components.

Similarly to CIGSe, the p-n junction is obtained by depositing a n-CdS layer on p-CZTS and therefore photogenerated electrons in CZTS move through the CdS/CZTS interface. As most of the solar cells, electronic properties are determined at the emitter/absorber interface and at the absorber/back contact interface. The determination of the band alignment at these interfaces is a crucial point for understanding and optimizing the cell properties. In particular, the relatively low open circuit voltage ( $V_{oc}$ ) of the CZTS solar cells could be

due to an increased interface recombination induced by a cliff-like Conduction Band Offset (CBO) at the CdS/CZTS interface. With this band alignment, the conduction band minimum of the CdS buffer would be located below that of the CZTS and this is equivalent to an interface band gap reduction which favors the recombination processes. Photoelectron emission spectroscopy with tuneable synchrotron radiation and/or with fixed photon energy (X-ray Photoelectron Spectroscopy, XPS, Ultraviolet Photoelectron Spectroscopy, UPS) has been proved to be a powerful technique to study band offsets in semiconductors.

XPS data were acquired at the UTAPRAD-MNF nanoscience and electron spectroscopy laboratory using an ultra-high vacuum system operating at  $4 \times 10^{-8}$  Pa base pressure and equipped with a VG Al  $K_{\alpha}$  monochromatised X-ray source and a CLAM2 hemispherical analyzer working at constant pass energy mode. The total energy resolution resulted to be 0.7eV as obtained from the fit of the Fermi edge of a clean Au sample. In order to reach the CdS/CZTS interface, the samples have been mildly sputtered with 1keV Ar ion energy. A careful investigation of the behaviour of the main XPS core level intensity ratios as a function of sputtering time has allowed to exclude any sputtering-induced effects.

In collaboration with UTRINN-FVC, we have studied the band alignment at the CdS/CZTS interface by XPS core-level spectroscopy and XPS valence band (VB) spectroscopy. In particular, the valence band offset (VBO) has been obtained using information from core-level data and VB data analysis.

The VBO can be calculated with the following formula:

$$VBO = E_{bVB} - E_{aVB} + V_{bb} \quad (1)$$

where  $E_{aVB}$  and  $E_{bVB}$  are the energy positions of the VB edges of species “a” (CZTS) and “b” (CdS) while  $V_{bb}$  is the band bending.

The band bending has been calculated assuming the binding energy (BE) below

the Fermi edge negative. According to the configuration used for our calculations (i.e. CZTS/CdS interface), VBO (CBO) results negative if the valence (conduction) band edge of CdS is lower than that of CZTS.

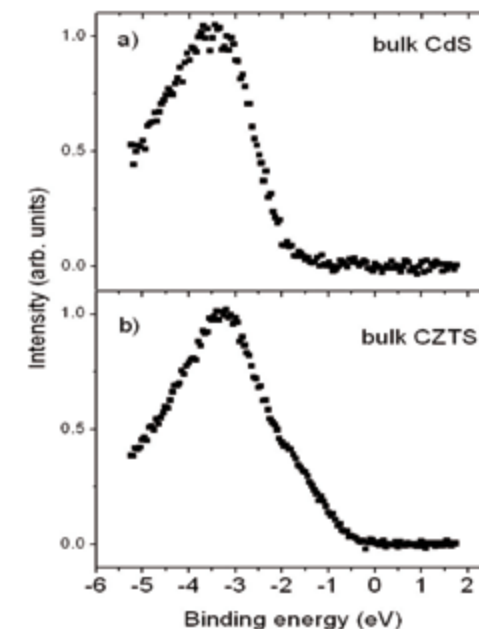


Fig. 1 - VB measured by XPS. a) VB of the clean CdS surface; b) VB of the CZTS substrate.

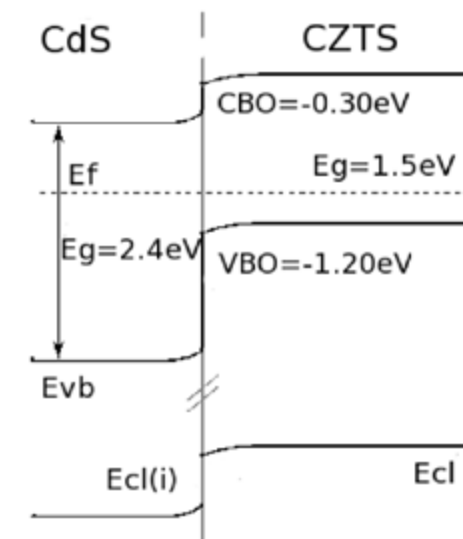


Fig. 2 - Sketch of the band lineup at the CdS/CZTS interface.  $E_g$  is the gap energy.  $E_{vb}$  are the VB edges and  $E_{cl}$  the core energies.

The calculated band bending resulted to be  $(0.14 \pm 0.10)$  eV in good agreement with data reported in the literature.

According to Eq. 1, the VBO extraction requires the knowledge of the CdS and CZTS valence band edges. Figure 1 shows the clean CdS valence band (panel a), and the clean CZTS VB (panel b). These spectra are normalized to the same height. According to Eq. 1, the valence band maximum (VBM) position of the two bulk materials is required to calculate the VBO. The VB onset has been modelled with the convolution product of a Gaussian function and a Heaviside step function, which allows determining the edge position within 0.02eV.

In our samples, the VBM positions relative to Fermi level  $E_f$  for CdS and CZTS resulted to be  $(-1.87 \pm 0.02)$  eV and  $(-0.53 \pm 0.02)$  eV, respectively. Now, all the elements of Eq. 1 have been measured and consequently the VBO can be calculated. Figure 2 shows graphically the result of the band lineup at the CdS/CZTS interface. The obtained averaged VBO value is  $(-1.20 \pm 0.14)$  eV. The CBO can be calculated from the VBO value and the difference of the energy gaps of the two materials:  $CBO = (E_{gb} - E_{ga}) + VBO$ . Using 1.5 eV and 2.4 eV for the CZTS (a) and CdS (b) band gaps respectively, the CBO results to be  $(-0.30 \pm 0.14)$ , pointing to a cliff-like behavior which could be one of the reasons for the Voc limitation in the CdS/CZTS solar cells.

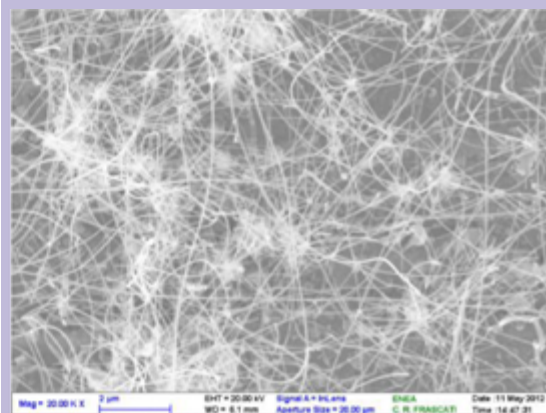
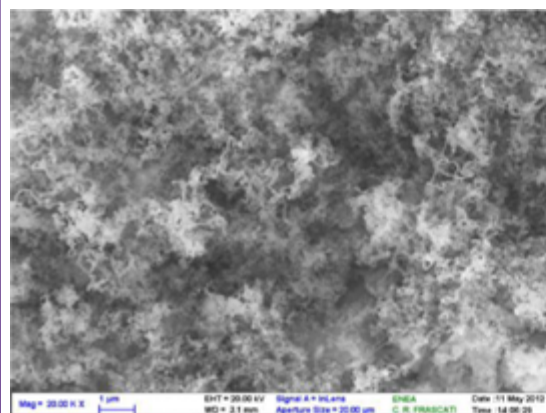


Fig. 3 - (a) SEM images of Si nanostructures CVD grown on a copper substrate. (b) SEM images of Si nanowires CVD grown on a stainless steel substrate.

### Synthesis and development of nanostructured silicon for lithium batteries anodes

In the framework of the cooperation program between ENEA and MiSE-RSE (Ministero dello Sviluppo Economico-Ricerca di Sistema Elettrico), this work has been carried out, in collaboration with UTRINN-IFC, with the purpose of contribute to a proposal for the theme-project "Advanced system for energy storage". The interest in silicon as the active material for lithium-ion batteries anodes is due to its extremely high theoretical storing charge capacity:  $4200 \text{mAhg}^{-1}$ , higher than metallic Li ( $3800 \text{mAhg}^{-1}$ ). Moreover, Si capacity is about 12 times higher than graphite, which is the commonly used material for commercial Li batteries anodes. In this view, the synthesis of silicon electrodes consisting of silicon nanostructures could have the potential to improve dramatically the storage capacity.

The growth of silicon nanowires has been attempted on Cu and stainless steel substrates by Chemical Vapour Deposition (CVD). The substrates have been mounted on a heatable sample holder and exposed to disilane gas at different temperatures and pressures. Figures 3a and 3b show promising preliminary results obtained for Si nanowires grown on Cu and stainless steel substrates, respectively. The Scanning Electron Microscopy (SEM) images were acquired in collaboration with UTFUS-COND.

### Synthesis and characterisation of SiC nanopowders for nanofluids

The need for more efficient and better performing coolants has lately generated considerable interest for the development of nanofluids, that is dilute and stable suspensions of nanoparticles (NPs) in base fluids. In principle, if compared to conventional solid-liquid suspensions, nanofluids should offer several advantages like higher specific surface areas for heat transfer between particles and fluids, reduced clogging when passing through microchannels, better thermal properties. In this context SiC nanopowders for the preparation of selected nanofluids were produced by laser pyrolysis at ENEA Frascati, UTAPRAD-MNF, in the framework of the EU FP7 Project NanoHex, having as objective the development of high performance nanofluid coolants for Data Centres and Power Electronic Components.

The as prepared powders have been characterized also with the collaboration of other ENEA Technical Units and Laboratories (UTTMAT-SUP, UTFUS-COND, UTRINN-IFC, UTTMAT-CHI) by using SEM, X-Ray Diffraction (XRD) and Brunauer-Emmett-Teller (BET) analysis, to study the morphology and the dimensions, by using infrared (IR) spectroscopy to understand chemical properties of particles surfaces, and XPS to study the elemental composition.

At ENEA C.R.Frascati, a set-up for the production of nanopowders by  $\text{CO}_2$  laser pyrolysis, called LUCIFERO, is fit for large scale production (up to 100 g/h) of NPs with different chemical characteristics and dimensions tuned from 5 to 80 nm. LUCIFERO is equipped with an evaporator for using liquid precursors.

Silicon carbide is formed by laser induced reaction of silane ( $\text{SiH}_4$ ) with acetylene ( $\text{C}_2\text{H}_2$ ). The reactive gases are injected into the vacuum chamber in molar proportion 2:1 through use of mass controllers, to produce powders with stoichiometry close to that of pure SiC. The

mean NP size can be varied in the range 20-50 nm by acting on the process parameters, in particular the laser focusing geometries, the reagent fluxes, the laser power, and the inner nozzle diameter. A narrower size distribution of the produced SiC NPs is indeed observed in tight focusing of the laser beam on the reactant flow (see Figure 4).

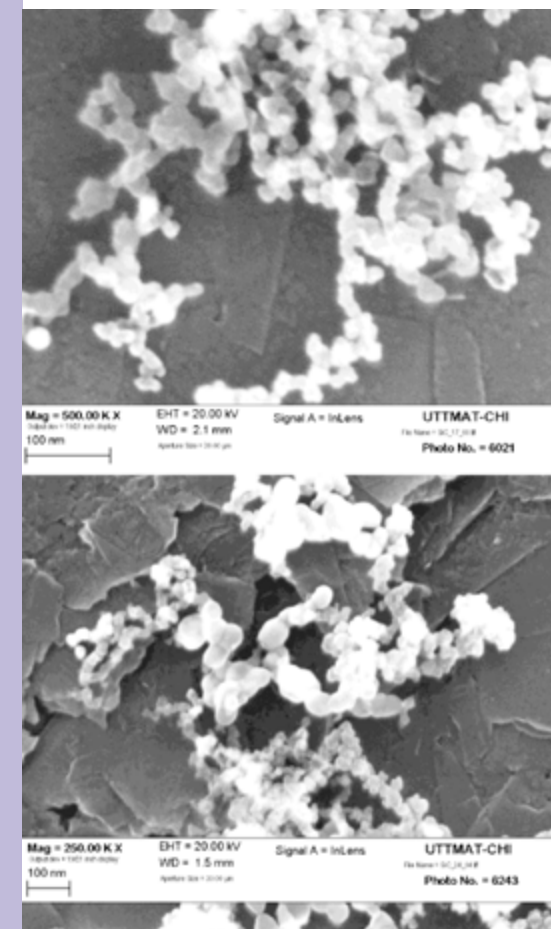


Fig. 4. SEM images of SiC nanoparticles synthesised with different laser focusing geometries: a) large, b) tight.

Typical productivities range between 30-50g/h and reaction yields are about 100%. All these nanopowders present the typical infrared feature of SiC at  $830 \text{cm}^{-1}$  and the XRD patterns of crystalline  $\beta$ -SiC.

In the course of NanoHex project it was found that the presence of free silicon NPs

or free carbon influenced the quality of the dispersion in water or in other cooling fluids and then on the thermal behaviour of the nanofluids. For this reason precursors  $\text{SiH}_4/\text{C}_2\text{H}_2$  ratios and flow rates have been changed to obtain nanopowders with different chemical compositions and sizes.

The XRD and XPS analyses showed that the C/Si ratio in the nanopowder is driven mainly by the composition of the precursors mixture.

### Development of nanofluids for enhanced heat exchange

In the framework of NanoHEX EU project, our SiC NPs were used for the preparation and testing of selected nanofluids, by using as base fluids water, water/ethylene glycol and antifrozen liquid. The partners of the project (University of Birmingham-UK and Royal Institute of Technology-SW) have measured the thermal conductivity and the viscosity of the nanofluids with conventional methodologies.

In cooperation with UTTMAT-SUP, thermal conductivity measurements on  $\text{TiO}_2$  ethanol based nanofluid were performed using an optical technique known as Forced Rayleigh Scattering (FRS), which provides the possibility for in situ monitoring of coolant performances. Moreover, because of its basic feature of contact-free measurement, FRS method has several advantages with respect to the conventional transient hot wire technique, when it is difficult to insert sensors in a sample such as high-temperature corrosive melts. Using FRS, we have found a 5% thermal diffusivity enhancement for ethanol-based nanofluid with 1% v/v  $\text{TiO}_2$  NPs. On this basis, the experimental results are compared with well-known models of nanofluids thermal properties, and are interpreted taking into account the role of the aggregation state, particle morphology and interfacial thermal resistance.

Moreover, in cooperation with UTTEI-TERM, erosion/corrosion tests and evaluation tests of

the heat transfer performance of water based nanofluids containing either  $\text{TiO}_2$  or SiC pyrolytic NPs (in different concentrations) were carried out.

It was found that SiC nanofluids have negligible erosion effect when impact on Al, Cu and stainless steel targets and that the heat transfer coefficient is higher than for the basic fluid, but due to the higher viscosity of the nanofluids, higher pumping power values are required. These conclusions have to be taken into account when considering the perspectives for exploitation of nanofluids in practical applications.

### Synthesis and characterisation of $\text{TiO}_2$ nanopowders for development of porous semiconductor electrodes

The laser pyrolysis method has proven to be a very flexible and versatile technique for the synthesis of NPs because it permits to control the particle-growth mechanism and to tune the final structure and composition of these NPs in view of the new applications in the energetic sectors. Titania NPs were synthesised by laser pyrolysis of an aerosol of titanium tetraisopropoxide (TTIP)  $\text{Ti}(\text{O}i\text{-Pr})_4$  (liquid at room temperature) mixed with either ethylene ( $\text{C}_2\text{H}_2$ ) or ammonia ( $\text{NH}_3$ ) as reaction sensitizer.

In addition, in different runs the gas flows and pressure in the chamber were changed in order to achieve a control on chemical characteristics of the nanopowders. The obtained powders are black or blue for the presence of C contamination that was eliminated by soft thermal treatment in air. When ethylene was used as sensitizer, pure  $\text{TiO}_2$  was obtained with average crystallite size of about 10 nm, the crystalline phase being approximately 30% rutile and 70% anatase, as evinced by XRD, Raman, Transmission Electron Microscopy (TEM) and SEM characterization techniques.

When  $\text{NH}_3$  was used as sensitizer, the resulting nanopowders were N-doped, with an average crystallite size of about 15 nm and

the crystalline phase was mostly anatase, as determined also by Raman spectroscopy. The level of N concentration in the samples was varied by changing the process parameters, as it can be confirmed by the different colour of the nanopowders; after the thermal treatment, the powders colour ranges from white in case of pure  $\text{TiO}_2$  to light yellow and green yellow in case of N-doped  $\text{TiO}_2$  samples with different percentage of doping. In fact N-doping has the effect to shift the optical absorption of titania toward the visible range, as evidenced by their diffuse reflectance (DR) spectra, where the presence of an absorption feature at about 430 nm is apparent in the samples synthesized in the presence of ammonia and confirm the nitrogen doping.

In cooperation with ENEA UTTMAT-SUP and UTRINN-IFC, we are exploring nitrogen-doped titania for applications in photocatalysis and Dye Sensitized Solar Cell (DSSC) electrodes. Preliminary results show that the conversion efficiency of a non-optimised DSSC device using N-doped titania compares well with those of a standard device. Work is in progress to study the transport properties of doped and undoped electrodes, in order to assess their respective electronic performances also in other applications requiring porous semiconductor electrodes as hydrogen generation, sensors, etc.

### Development of nanocomposites for cultural heritage preservation

Applications of nanotechnology to consolidation and restoration of artworks have recently provided clear evidences of the great potentialities of this new science for cultural heritage preservation. The modulation of physical chemical properties of a protective coating can be obtained by a proper blending of the coating material with suitable chosen NPs. In particular, nanosilica and nanotitania were chosen for their physical properties, such as the improved water repellence.

$\text{SiO}_2$  and  $\text{TiO}_2$  NPs were produced by

$\text{CO}_2$  laser pyrolysis at the ENEA-Frascati set-up LUCIFERO, using liquid precursors (tetraethoxysilane (TEOS)  $\text{Si}(\text{OEt})_4$  and TTIP, respectively) and ethylene as sensitizer. Important items were the purity of the nanopowders and low aggregation of the NPs, in order to obtain homogeneous nanocomposites that do not alter the colour of the artworks. For this reason the optimization of process parameters such as laser power and ethylene flux was then performed and the obtained powders have mean size of about 15 nm.

In cooperation of UTTMAT-DIAG and UTAPRAD-DIM, NPs were added as nanometric fillers to two commercial products, largely used as protective coating, an acrylic resin and a silicon-based polymer. In general the synthesis of nanocomposites to obtain a final homogenous dispersion is a tricky step, depending on chosen preparation method, solvent and particles concentrations. To this purpose different solutions of the polymers with dispersed silica and titania NPs were prepared and applied on the surface of two different litotypes, very common in outdoor cultural heritage: white marble (statuary and veined Carrara) and travertine.

Artificial aging processes, both in climatic chamber and in solar box, were carried out to simulate real degradation processes in terms of photo-thermal effects and mechanical damage. The performances of the different nanocomposites were evaluated comparatively by means of several diagnostic techniques. The results demonstrate that NPs enhance the efficacy of consolidant and protective materials because they induce substantial changes of surface morphology of the coating layer and hinder the physical damage observed during artificial weathering, especially in alkylsiloxane products.



## 2.3 LIGHT SOURCES, OPTICAL SENSORS AND TECHNOLOGIES FOR PHOTONICS

### Solid state radiation detectors based on luminescent colour centres in lithium fluoride thin films

Lithium Fluoride, LiF, is a very promising radiation-sensitive material which is widely used in radiation dosimetry, optoelectronics and integrated optics. It is well known that ionizing radiation, such as energetic charged particles (ions and electrons) and photons (X-rays and gamma rays), can generate optically-active aggregate colour centres (CCs) in LiF stable at room temperature (RT).

Innovative radiation detectors (LIRA: Lithium fluoride Radiation detectors) based on the optical readout of the visible photoluminescence (PL) from CCs locally generated in LiF thin films are under development at the Solid State laboratory of UTAPRAD-MNF. The use of thermally evaporated LiF thin films, which are compatible with several substrates, increases the versatility and easiness of use of these detectors, which can be integrated in different experimental apparatus and configurations. LiF thin films of controlled thickness in the range 200-2000 nm are grown by thermal evaporation on glass and Si(100) substrates, kept at a fixed temperature

between 30 and 300 °C during the deposition process, performed under a vacuum pressure below 1 mPa inside the deposition chamber. Figure 5a shows the optical transmittance and reflectance spectra of a LiF film, thickness 1  $\mu\text{m}$ , grown on a glass substrate. The measured interference fringes are due to the refractive index differences between the glass refractive index,  $\sim 1.55$ , and the LiF film one. In Figure 5b the photograph of a LIRA detector, consisting of a LiF film of diameter 10 mm grown on a (12x12)  $\text{mm}^2$  Si substrate, is shown. The Si substrate makes the optically transparent LiF thin film easily visible with the naked eye in daylight.

Enhancement of the optical response of LIRA detectors, up to an order of magnitude, can be obtained by tailoring the choice of the substrate materials and the film thickness in the layered imaging detector by taking into account light confinement effects in the investigated planar microstructures.

Thanks to the versatility of the LiF films, it is possible to realize vertical multilayer structures in order to increase the collection efficiency of the PL signal emitted by CCs during the reading process and, consequently, the sensitivity of the detector. The reflective properties of the substrate help in recovering a relevant part of light emission that would be otherwise lost in the opposite direction of the

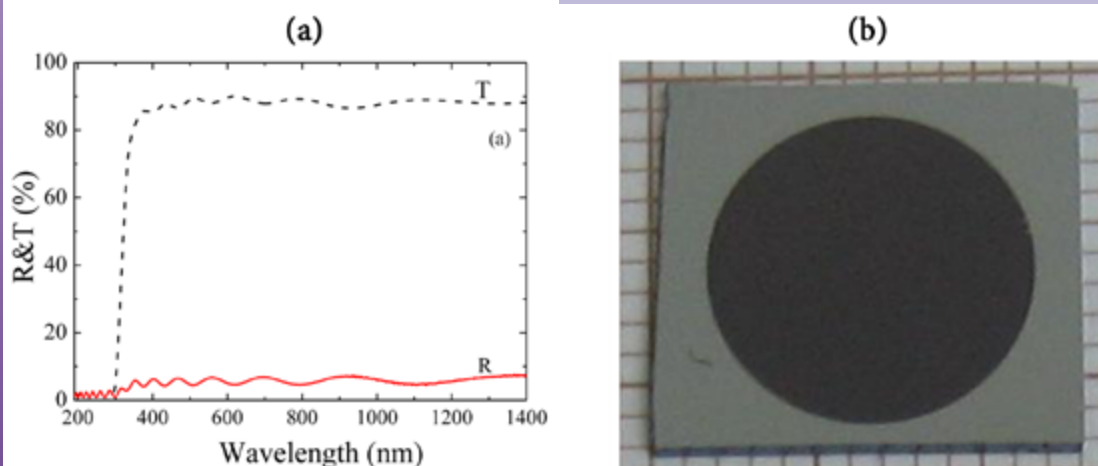


Fig. 5 - Transmittance and reflectance spectra of a LiF film, thickness 1  $\mu\text{m}$ , grown on a glass substrate, a). Photograph of a LiF film grown on Si substrate, b).

observation one. Moreover, this reflected part can constructively interfere with the straight emitted one, and this is true for all the orders of multireflection at all the emission angles, provided the LiF thickness is a suitable one.

Figure 6 shows the CCs PL directly observed by naked eyes under blue lamp light illumination in a fluorescence microscope. The observed sample are a LiF crystal 0.5 mm thick (on the left) and a LIRA thin film detector on a silicon substrate (on the right) previously exposed to soft X-ray from a laser-plasma source (in collaboration with Tor Vergata University, RM) in the same conditions. The photo-induced light emission coming from the LiF film on the Si substrate is significantly larger

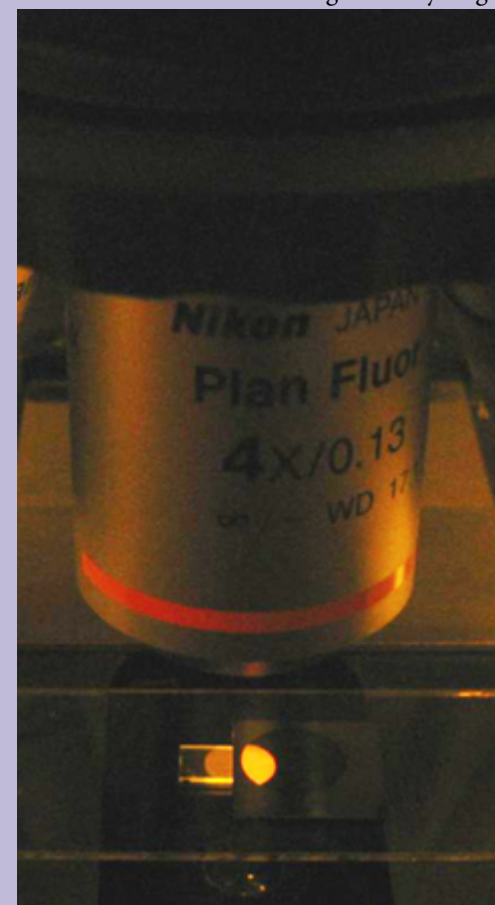


Fig. 6 - CCs PL under blue lamp light illumination in a fluorescence microscope. The observed samples are a LiF crystal and a LIRA thin film detector on a silicon substrate, previously exposed to soft X-ray from a laser-plasma source in a vacuum.

than the one emitted from the LiF crystal. The study of the enhanced formation efficiency of aggregate CCs in polycrystalline LiF films with respect to single crystals is a very promising investigation for nanoscience development. The control of local formation, stabilization and transformation of radiation-induced light-emitting defects is crucial for the development of novel optical active photonic devices and imaging radiation sensors based on LiF material in different forms.

An ENEA patent is pending. A video for the WEB TV ENEA with the title "LIRA, ENEA patent for the analysis of the ultra-small world" has been realized (<http://webtv.sede.enea.it/tecnologie.html>).

### LiF detectors with polycapillary optics in compact X-ray microscopy systems

A great effort in X-ray imaging fields is dedicated to the design of novel optics-detector solutions that aims in creating a compact laboratory X-ray microscopy apparatus. The potential of optics both to concentrate and to shape X-ray radiation enforced by the high performances in terms of spatial resolution/dynamic range of LiF imaging detectors allowed us to use very simple imaging techniques, like the contact one, particularly suitable for these imaging systems.

We explored the possibility to use a low divergent X-ray beam from a polycapillary semilens combined with a micro-source X-ray tube (collaboration with XLab, Istituto Nazionale di Fisica Nucleare - Laboratori Nazionali di Frascati, INFN-LNF) for contact X-ray imaging experiments on LiF-based detectors. This technique was also used to characterize X-ray transmission of the polycapillary optics.

The R&D activities on LiF radiation detectors have been inserted in the EU COST ACTION (COST 4143/12) - MP1203, entitled Advanced spatial and temporal X-ray metrology, in the framework MPNS, Materials, Physical and NanoScience, (16/11/2012-15/11/2016)

([http://www.cost.eu/domains\\_actions/mpns/Actions/MP1203](http://www.cost.eu/domains_actions/mpns/Actions/MP1203)).

### Optical characterization of lithium fluoride detectors for broadband X-ray imaging

An optical characterization of LiF detectors irradiated at the TOPO-TOMO beamline of synchrotron light source Anka (Karlsruhe, Germany) in the energy range (6-40 keV) for different exposure times was performed. Absorption and PL spectra were analyzed to study the optical response of the LiF-based detectors with a white X-ray beam as function of irradiation time. Five commercially available LiF crystals of dimensions (5x5x0.5) mm<sup>3</sup>, polished on both sides, were uniformly irradiated with exposure times of 0.5, 1, 5, 10 and 30s.

The X-ray induced point defects mainly consist of primary F centre and aggregate F<sub>2</sub> and F<sub>3</sub><sup>+</sup> point defects. Optical transmittance of the five uniformly coloured LiF crystals were measured utilizing a Perkin Elmer Lambda 950 UV/VIS/NIR spectrophotometer. The centre densities were obtained from the measured optical density (OD) taking into account the coloration depth of the X-ray radiation in the LiF crystals. The attenuation length of X-rays in LiF is strongly dependent on their energy and raises to 10 mm for 30 keV photons. The mean values of CCs volume densities were reported in Table 1.

X-ray exposure time [s]	F centre density [cm <sup>-3</sup> ]	F <sub>2</sub> centre density [cm <sup>-3</sup> ]	F <sub>3</sub> <sup>+</sup> centre density [cm <sup>-3</sup> ]
0,5	6,8E17	-	1,7E16
1	1,2E18	-	3,0E16
5	4,4E18	2,2E16	9,7E16
10	7,5E18	5,7E16	2,1E17
30	1,3E19	2,0E17	5,9E17

Table 1 - F, F<sub>2</sub> and F<sub>3</sub><sup>+</sup> centre densities in X-ray irradiated LiF crystals for various exposure times.

The PL spectra of the same irradiated LiF crystals, excited with the 457.9 nm line of an argon laser, were performed by a modular spectrofluorometre set-up, equipped with a monochromator and a photomultiplier and based on the lock-in technique. Figure 7a shows the PL spectra of the five X-ray irradiated LiF crystals, corrected taking into account the measuring system response. Deconvolution of the partially overlapping emission bands of the F<sub>2</sub> and F<sub>3</sub><sup>+</sup> centres as the sum of two Gaussian bands gives the mean peak position at 1.844±9E-3eV for F<sub>2</sub> center PL and at 2.306±4E-3eV for the F<sub>3</sub><sup>+</sup> ones. These values are in good agreement with the literature. Figure 7b shows the absorption and PL peak intensities as function of irradiation times for F<sub>2</sub> defect.

A linear increase of both absorption and PL signals was observed in the investigated conditions. For F<sub>2</sub> electronic defects the PL increase is substantially proportional to the absorption increase in the investigated conditions.

For high values of CC volume concentrations, a decrease in fluorescence quantum efficiency with a corresponding PL concentration quenching has been previously observed. The PL quenching phenomena for F<sub>2</sub> starts to become significant for values greater than 5x10<sup>17</sup> cm<sup>-3</sup>. Also the F<sub>3</sub><sup>+</sup> absorption and PL intensities have been shown a linear behavior as a function of exposure times.

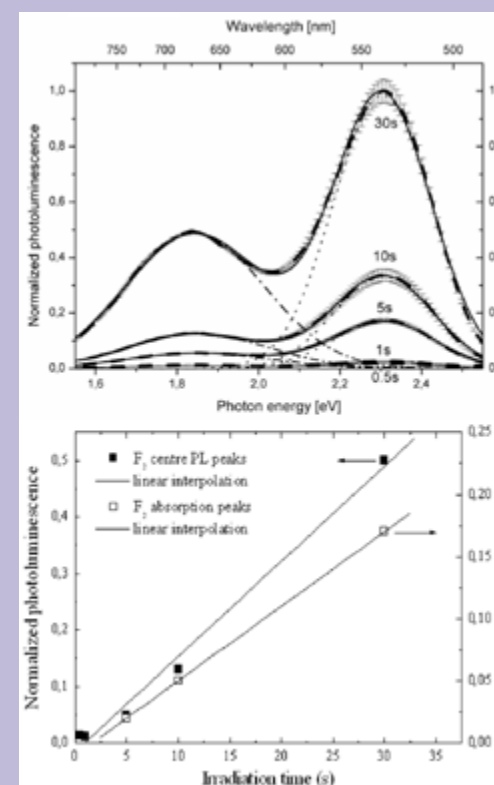


Fig. 7 - RT PL spectra of five LiF crystals X-ray irradiated for exposure times from 0.5 to 30s (dashed curves). The fitting by two Gaussian bands is also reported (solid curves), as well as the F<sub>2</sub> (dash dotted curve) and F<sub>3</sub><sup>+</sup> (dotted curve) centre emission contribution (Top). RT absorption and PL intensities as function of irradiation time for F<sub>2</sub> defects in X-ray irradiated LiF crystals (Bottom).

### Lithium fluoride thin films grown on plastic substrates for EUV imaging

Polycrystalline LiF films, thickness between 500 nm and 1.5 μm, were deposited by thermal evaporation on different substrates, including plastic ones, kept at RT during the growth, using the GP20 deposition system. Despite of the compositions and roughness of the substrates, and the ambient temperature selected for the film growth to avoid damage of the plastic substrates, LiF thin films adhere quite well and are of good optical quality. Figure 8a shows the photograph of a LiF film grown on ENEA plastic badge; the area corresponding to the deposited transparent LiF thin film, 18 mm of diameter, is indicated by a dashed circle.

Figure 8b shows the reflectance spectra of the LiF film grown on ENEA badge and of the uncoated badge. Under exposure to ionising radiations at the EGERIA soft-X ray source (UTAPRAD-SOR), predetermined invisible patterns/codes, based on the stable formation of the visible-emitting F<sub>2</sub> and F<sub>3</sub><sup>+</sup> electronic defects, were locally stored in LiF films. The irradiated LiF films, eventually protected by an additional transparent coating, can be used as tags for the identification and the traceability of goods or products in order to avoid their counterfeiting, including protection of artworks. Due to the optical transparency of the LiF film and the peculiar spectroscopic features of F<sub>2</sub> and F<sub>3</sub><sup>+</sup> colour centres, the marking is invisible under white light illumination, but appears bright orange when illuminated by blue light.

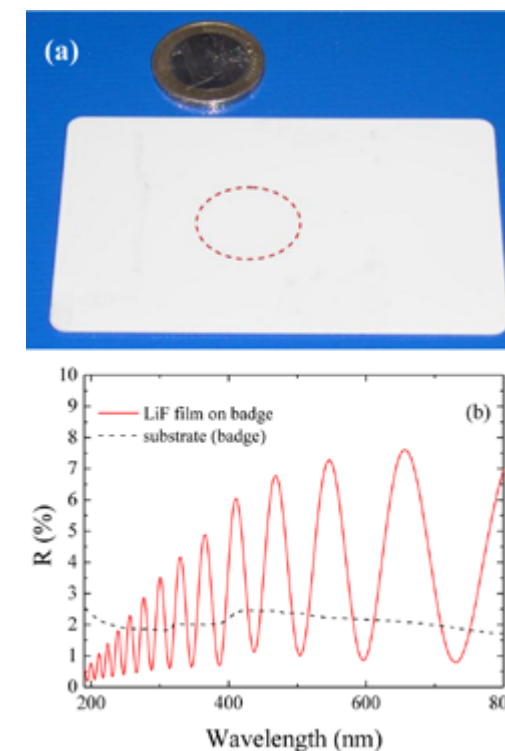


Fig. 8 - Photograph of a LiF film grown on ENEA plastic badge; the area corresponding to the deposited transparent LiF thin film, 18 mm of diameter, is indicated by a dashed circle, a). Reflectance spectra of the LiF film grown on ENEA badge and of the uncoated badge, b).

### Lithium fluoride radiation imaging thin film detectors for proton beams

LiF thin films have been proposed as solid-state imaging detectors for the characterization of high energy particle beams. Preliminary irradiation tests performed by the 3 MeV proton beam injector of TOP-IMPLART (UTAPRAD-SOR) show that these LiF-based detectors are very promising for the proton beam characterization, in particular for the measure of the transverse beam distribution on target, overcoming some limitations of radiochromic dosimeters.

Figure 9a shows a fluorescence image acquired by a confocal laser scanning microscope (CLSM), magnification 4x, of 1  $\mu\text{m}$  thick LiF film grown on a glass substrate irradiated by 1000 pulses of the proton beam. The PL

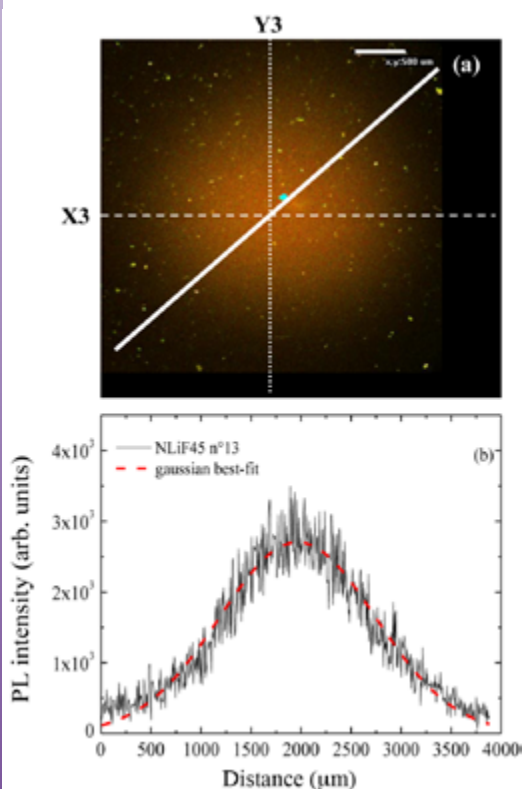


Fig. 9 - Green-red CLSM fluorescence image of the proton-irradiated area from the exposed LiF film, a). PL intensity profile along the diagonal (white solid line in Fig.10a) and its Gaussian best-fit, b).

intensity profile along the diagonal D3 is reported in Figure 9b together with its best-fit by a Gaussian curve, which allows to obtain a FWHM of  $(1560 \pm 15) \mu\text{m}$ .

### Effects of heavy metal doping in lithium fluoride crystals

The radiation-sensitive properties of LiF make it a very appropriate material for radiation detectors and sensors. The presence of impurities in LiF crystalline host matrix, although they are present in small amounts, less than 10 ppm, modifies the structural properties of doped LiF crystals and influences the formation efficiency of electronic defects produced by irradiation with ionising radiations.

In collaboration with the Physics Department of Roma Tre University, the National Institute of Material Physics of Bucharest and CNR-IOM-OGG c/o ESRF GILDA-CRG, the evidence of the incorporation of  $\text{Pb}^{2+}$  ions in the LiF host matrix and their stability during annealing procedures were investigated by optical spectroscopy and X-ray absorption spectroscopy. The influence of the doping on the sensitivity of Pb-doped LiF crystals to ionising radiations is under investigation.

### Broad-band light-emitting waveguides written in lithium fluoride crystals by femtosecond laser

The use of femtosecond laser pulses permits the recording of longitudinally modulated optical waveguides in a broad range of substrates. The high intensity pulses allow higher order transitions in the material and/or material damage in the substrate material, resulting in appreciable changes in the refractive index.

Optical waveguides have been recorded in blank and colored LiF crystals using a femtosecond laser (collaboration with Federal University of Technology, Paran, Brasil). The laser pulses are  $\sim 80$  fs long, with an optical spectrum centred at 810 nm. The obtained

waveguides are characterised using several techniques. Conventional, fluorescence and confocal microscopy are used to obtain the morphology of the recorded structures. Near field measurements are carried out to determine the mode dimension of the propagated light. Optical scattering and insertion loss measurements are done to estimate the waveguide losses (collaboration with University of Rome "Sapienza").

Figure 10a shows the near field profile at the output facet of a waveguides when laser light at 635 nm is launched into their input facet by end-fire coupling. This waveguide shows horizontal half-width of  $\sim 5.5 \mu\text{m}$ , whereas the vertical one is  $\sim 7.6 \mu\text{m}$ , determined from a Gaussian fit.

Using the refractive index changes, a few propagating modes are predicted when using the above dimensions. Figure 10b reports the apparatus recently installed at Solid State laboratory for optical waveguide characterization. Two objectives provide the coupling of injection lasers with the waveguides and the coupling of the guided light with a beam profiler or with spectrofluorometre systems. The sample mounted on the stage in Figure 10b is a CCS waveguide written in a LiF crystal by a fs laser, under coupling with an argon laser.

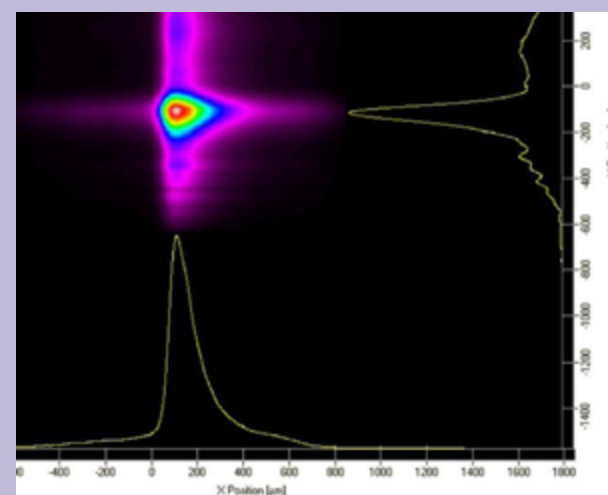


Fig. 10 - a) Near field profile at the wavelength of 635 nm of a waveguide written in a LiF crystal by femtosecond laser.

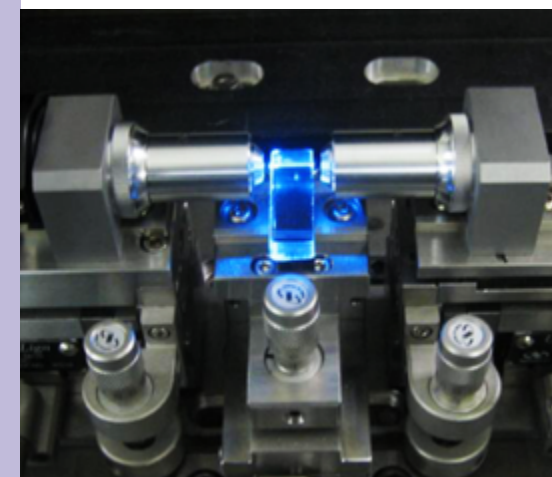


Fig. 10 - b) Apparatus for optical waveguide characterization. The sample mounted on the stage is a CC waveguide written in a LiF crystal by a fs laser and coupled with an argon laser at 458 nm.

### Rapid and ultrasensitive analysis with Raman and surface-enhanced Raman spectroscopy

Raman spectroscopy is obtained by the interaction of laser light with the dipole moment of a molecule. The resulting scattered light is shifted in frequency from that of the original light source, and the magnitude of the resulting shift is recorded as the Raman spectrum. The Raman spectroscopy (RS) has become an important analytical and research tool because the Raman spectrum may be considered the fingerprint of a laser interrogated target by providing specific information on its chemical structure.

At the beginning Raman experiments were carried out only at laboratory level, but in the 1990's a novel generation of lasers, optical notch filters and detectors evolved and smaller, more compact instruments were assembled and the Raman revolution starts. Moreover, the possibility of surface-enhanced Raman scattering (SERS) is currently being explored for trace identification because it is more sensitive than traditional Raman scattering by 6–8 orders of magnitude. Furthermore, because of radiationless deactivation at the

metal surface, fluorescence is quenched. Due to its peculiar property, the RS and SERS can be used for a wide range of applications as materials science, forensic science, polymers, thin films, adulteration of food and pharmaceuticals, semiconductors and even for the analysis of fullerene structures and carbon nanomaterials. At UTAPRAD-MNE, in 2012 the laboratory activity was mainly dedicated to the ultrasensitive detection with surface-enhanced Raman spectroscopy. SERS signal from a single molecule was obtained in a laboratory environment, with the state of the art spectrometry, controlled laser polarization, collimation and angle of incidence chosen to make full use of resonant electromagnetic field enhancement of the plasmonic substrate. For in field applications, carried out in collaboration with UTAPRAD-DIM, it is necessary to obtain high sensitivity relaxing requirements on angle of incidence (focused illumination instead of collimated illumination) and on polarization of the excitation. To this respect, our study was dedicated to the optimization of the SERS detection sensitivity by studying how the SERS signal intensity is affected by some acquisition parameters such as laser beam power scanned

area, laser fluence, to obtain high quality Raman spectra with short acquisition times in view of the possibility to detect substance amounts as smaller as possible. By using lenses with high numerical aperture a more intense Raman signal is obtained although the area probed by the laser is smaller. This finding can be explained because the reduction in the sampled area is counterbalanced by an increased laser fluence. Therefore, the increase of Raman signal can be attributed mainly to an increase of the solid angle using objectives with higher numerical aperture. However, while a linear behaviour of the peak area as a function of laser power was observed, using both 10X (N.A.=0.25) or 20X (N.A.=0.4) objectives, with 40X (NA= 0.6) the linear fit had a poor regression coefficient suggesting the occurrence of a saturation effect. This behaviour indicates that, for smaller amounts of probed analyte, an excessive laser excitation can either evaporate the sample or damage the dried film, giving rise to a "burned" surface layer, the more extended the higher the laser fluence is. The amount of the sampled substance was estimated as the analyte mass density multiplied by the laser spot area, which

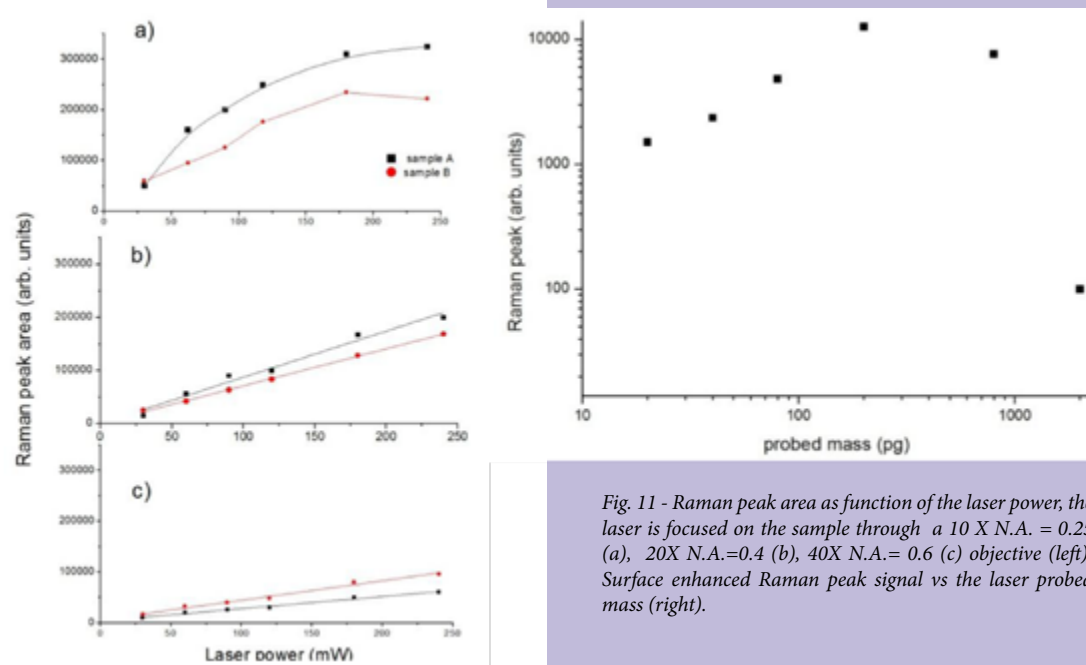


Fig. 11 - Raman peak area as function of the laser power, the laser is focused on the sample through a 10 X N.A. = 0.25 (a), 20X N.A.=0.4 (b), 40X N.A.= 0.6 (c) objective (left). Surface enhanced Raman peak signal vs the laser probed mass (right).

depends on the microscope objective through which the laser is focused. Depending on the concentration of the analyte solution, the mass probed by the laser can be as small as 10 pg. In Figure 11, we reported the behaviour of SERS signal for paracetamol as a function of the probed mass. Contrary to what expected for Raman measurements, the linear behaviour of the Raman signal is observed only up to 200 pg, then the signal strongly decreases. In fact, only the molecules that are in a close contact with the nanostructured surface give enhanced Raman signal; if the analyte quantity is too large a layer is formed covering the SERS spots resulting in a weaker signal. Depending on the compound that we studied, we obtained limit of detection ranging from 10 to 80 pg. These findings support the use of SERS as fast, in situ analytical tool with a sensitivity which competes and, in some cases, overcomes other techniques.

#### 2.4 SPECTROSCOPIC CHARACTERIZATION AND PHOTO-DEGRADATION OF LIGHT-EMITTING ORGANIC FILMS

In last decades organic compounds brought a technological revolution in the field of light sources. The most studied low-molecular weight molecule is a metal-chelate, tris (8-hydroxy-quinoline) aluminum ( $\text{Alq}_3$ ), commonly vacuum deposited as the active layer in green OLED. The degradation processes due to ambient factors as light, moisture and oxygen and their effect on quenching of luminescence are under study.

#### Quenching of photoluminescence of $\text{Alq}_3$ films for organic solid state light sources

The investigation of the PL intensity decay of thermally-evaporated  $\text{Alq}_3$  thin films of different thicknesses, from 50 to 80 nm, kept in air, can be described with four different constant times. This phenomenological behaviour implies the existence of four different species of molecular aggregations, which emit

greenish light with different spectral and time properties. The Four Component Model (FCM), which explains the PL blue shift of  $\text{Alq}_3$  films, their long lifetime, and the effects of annealing processes, works fine up to about 30,000 h, while the emission intensity decays faster than the exponential decay for longer times (see Figure 12a).

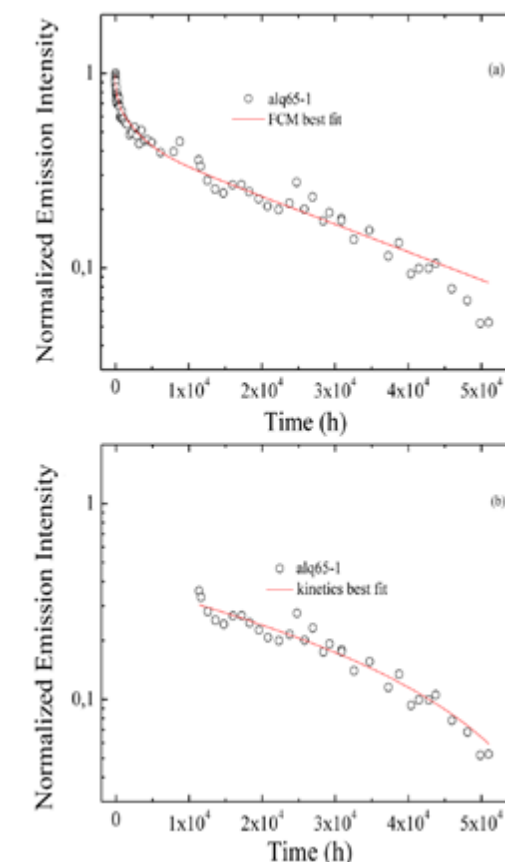


Fig. 12 - a) PL intensity of an  $\text{Alq}_3$  film (55 nm thick), alq65-1, thermally-evaporated on a glass substrate decaying in air, circles, and its best fit with the FCM, full red line. b) PL intensity of sample alq65-1 decaying in air after 10,000 h, circles, and its best fit with a zero + first-order kinetics, full red line.

Another model is coming from a first order approach of chemical reactions. Taking into account only the zero and first order kinetics reaction the decay of the  $\text{Alq}_3$  thin film PL is described by the following expression.

$$I(t, \lambda) = I_1(0, \lambda) e^{-\left(\frac{t}{\tau}\right)} - \alpha \tau \left(1 - e^{-\left(\frac{t}{\tau}\right)}\right)$$

This kinetics approach, applied to several  $\text{Alq}_3$  films, fits in a satisfactory way our experimental data as shown in Figure 12b and provides some clues about the interactions of the different species of  $\text{Alq}_3$  molecular aggregations with the environment.

### Optical spectroscopy of TPB films for particle detectors in Dark Matter search

Tetraphenyl-butadiene (TPB) is an organic material used for the detection of VUV radiation in modern particle detectors based on liquid Argon. In these detectors TPB works as a wavelength-shifter (128 nm  $\rightarrow$  440 nm) as it emits an intense broad emission band peaked at about 440 nm under light excitation at shorter wavelengths. In collaboration with the Italian Institute for Nuclear Physics-Gran Sasso Laboratories (INFN-LNGS), Yale University and Physics Department of Rome

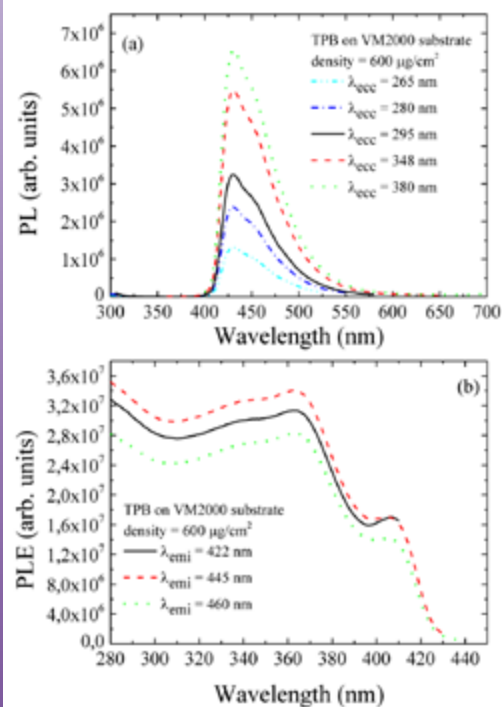


Fig. 13 - a) PL spectra of a TPB layer substrate (surface density =  $600 \mu\text{g}/\text{cm}^2$ ) grown on VM2000, excited at different excitation wavelengths. b) Photoluminescence excitation (PLE) spectra of the same sample acquired at several emission wavelengths.

Tor Vergata University, TPB films grown on different substrates were characterized by linear optical spectroscopy (see Figure 13).

### Upgrade of a thermal evaporator for optical fibre functionalisation

In the framework of a collaboration between UTAPRAD-MNF and Chemistry, Materials and Environment Department of Engineering, Sapienza University (RM), an Edwards-IONVAC deposition system, which is used to grow multilayers of organic thin films, LiF and aluminium on different substrates, was upgraded together with IONVAC Process Srl (Pomezia, RM). An axially rotating fibre-holder was engineered and installed in the vacuum chamber of the thermal evaporator (see Figure 14, top) in order to obtain the deposition of a uniform metal coating on optical fibres. Figure 14 (bottom) shows a fibre covered by a thermally-evaporated aluminium coating. The Edwards-IONVAC deposition system was also equipped with a rotating sample-holder to improve homogeneity in thin film deposition, and with two halogen lamps for substrates heating.

### 2.5 OPTICAL FIBRE SENSORS

The Photonics Micro- and Nano-structures is deeply involved in the development of monitoring systems based on fibre optic technology, aiming at applications ranging from geotechnical engineering to nuclear physics. Sensors based on optical fibre technology have specific features that can make their usage of great advantage with respect to traditional sensors based on electric/electronic technology. Among their best features, we here recall the immunity from electromagnetic disturbances, no requirement of electrical power at the sensing point, in-series cabling of multiple sensors along the same optical fibre, the measurement of different physical and chemical parameters by use of the same analysis technique of the optical signal. The laboratory works both to develop new type

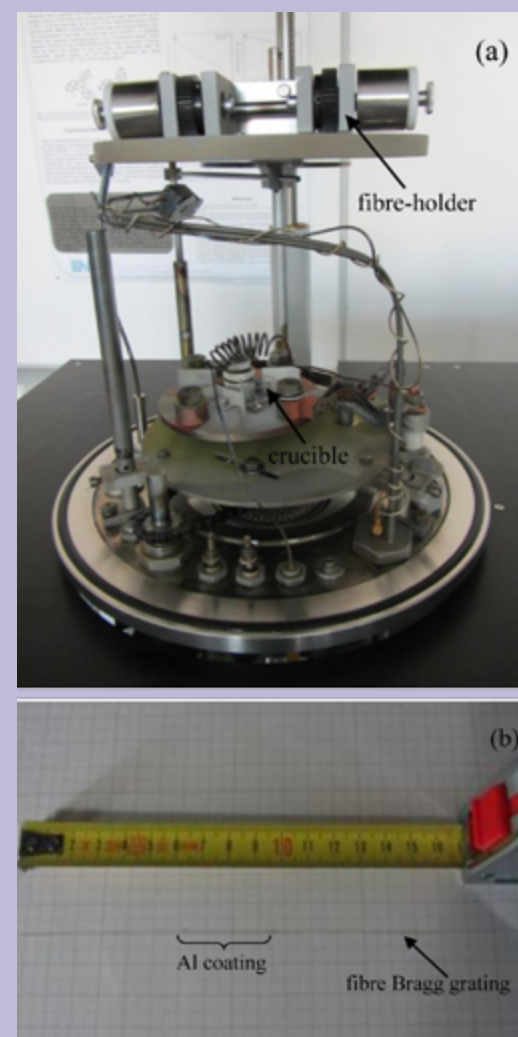


Fig. 14. Inside of the vacuum chamber of the Edwards-IONVAC deposition system equipped with the fibre-holder, (top). Fibre Bragg grating covered by a thermally-evaporated Al thin film, (bottom).

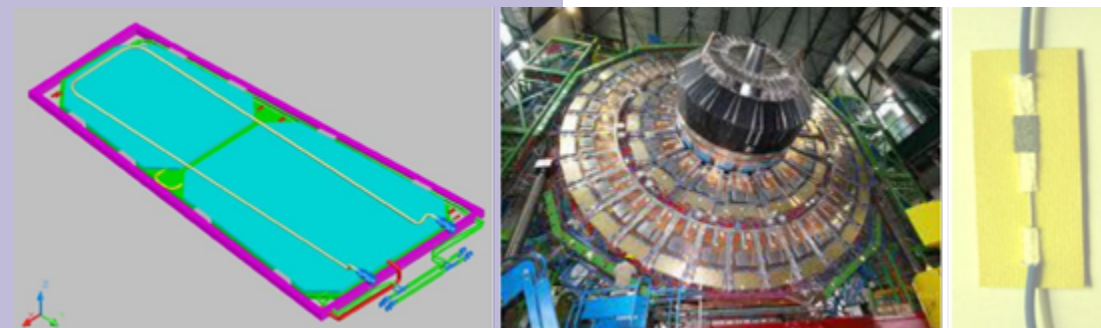


Fig. 15 - Lay-out (left) of RPC chamber of the large CMS experiment (centre) run at CERN; fibre optic sensors (right) are being tested to develop a temperature and relative humidity sensing system for RPC chambers.

of sensors and novel and efficient practical solutions to use and apply these type of sensors, whose usage is well assessed.

### Development of sensors for nuclear and high energy physics experiments

For High Energy Physics experiments, work has been carried on with the aim of developing a distributed sensing system devoted to monitor the working conditions of gas-ionising elementary particle detectors. Such detectors require a precise control of the temperature and the relative humidity of the circulating gas, as they can seriously affect the efficiency of the detectors. The work is particularly addressed to the Resistive Plate Counter (RPC) of the large experiment CMS (Compact Muon Solenoid) currently run at CERN (European Centre for Nuclear Research; Geneva, CH). Prototypes of the proposed sensor system have been realised using in fibre sensors based on the FBG (Fibre Bragg Grating) technology. Prototypes are currently being tested and qualified at the ASTRA experimental facility, where a RPC detector is available for R&D activity (see Figure 15). Achieved results show that the use of FBG as sensing device makes the proposed sensor well suited to develop a full-scale distributed real-time monitoring systems to be installed on a huge volume detector such as CMS, which operates in high electromagnetic fields. As a matter of fact, FBGs are fully immune from electromagnetic disturbances and allow simplified wiring by in-series interconnection of tens of them along a single optical fibre.

### Development of sensors for biomedical applications

For electro-medical applications, a distributed temperature monitoring system has been developed and applied to assist R&D activity aiming to better characterise the application of LITT (Laser-induced interstitial thermotherapy) for ablation purpose to human pancreas surgery. LITT has been recently applied to pancreas in animal models, but assessment of thermal effects due to the laser-pancreatic tissue interaction is a critical factor in validating the procedure feasibility and safety. A monitoring system made of 18 FBG (Fibre Bragg Grating) sensors has been developed to measure the temperature distribution during the application of LITT on ex-vivo porcine pancreas. Thank to the minimal invasiveness, the very small dimension and the very low thermal inertia of the sensors, the temperature distribution in vicinity of the ablated tissue has been acquired with high time and space resolution, with no appreciable perturbation inferred by the mass of the monitoring system. Special array of FBG sensors on bare optical fibres had to be used, in order to succeed in having temperature probes as small as 3mm in length and 0.5mm in diameter, placed at less than 10mm far from each other. Moreover, the array of the temperature probes had to have both the required mechanical robustness to allow insertion into the organ and the required resistance to thermal stress. The demanding

features have been met by adopting special pure silica monomode fibre with thin polyimide recoating. The activity has been carried on in cooperation with the Dept. of Biomedical Engineering of the University Campus Bio-Medico of Rome, during experimental LITT ablation assisted by X-ray CAT (Computed Axial Tomography) scan (Figure 16).

### Development of innovative sensing solutions for the industry

Within the commercial offering of high technological services, a feasibility study aimed at the development of an innovative Weigh In Motion system was done. The system has been first tested on a small-scale experimental set-up installed on a working bench, and later optimised and tested by use of chariots on a reduced-scale prototype installed in a experimental hall. Results addressed the production of a full scale prototype which is currently under test for qualification and optimisation. The full scale prototype is currently being tested on the road in a controlled traffic area in the ENEA Research Centre of Frascati (Figure 17). Experimental results are being analysed aiming at the design of a pre-industrialised system to test in a non-controlled commercial traffic environment. Results are addressing the plan of an industrial system with large potentialities of penetration in the commercial market. The activity, funded

by a private industry, shows the availability in the laboratory of key knowledge in the field of fibre optic sensors that can help industry in developing new and competitive products.



Fig. 17 - Transit tests on an instrumented plate to develop a Weigh In Motion system in the ENEA Research Centre of Frascati. Commercial activity of technological services funded by private industry.

### 2.6 ACTIVITIES IN ENVIRONMENTAL AND SEISMIC SECTORS

Regarding the MS activity, the study on the Frosinone territory has been completed (Level 1 of MS analysis); in May 2012, in collaboration with the Dept. of Scienze della Terra University of Rome "Sapienza" and Geological Survey of Lazio Region; the final reports of Alvito, Cassino, Gallinara, Sora and Isola del Liri were delivered (see Figure 18).

MS analysis, only for reporting and cartographic results, is still underway for some reatino municipalities (Antrodoco, Borgo Velino, Fiamignano and Petrella Salto). The MS activity was conducted following the methodology and procedures expressed by the Italian Civil Protection Department, i.e. collection and analysis of historical data, analysis and processing of geological information related to previous campaigns, environmental noise measurements, data processing by GIS procedures.



Fig. 18 - Cover of Isola del Liri MS final report.

### Liquefaction phenomena in Emilia Romagna region, May 2012

Concerning the May 2012 Emilia earthquakes, geological surveys on the environmental effects caused by this earthquake were carried out in cooperation with the Geological Survey of Lazio Region. Two contributions on this topic are reported in EIA n 4-5/2012 focused on the Pianura Padana Emiliana Earthquake, relative to an analysis of the seismic sequence and the liquefaction phenomena (see Figure 19).

### Cultural heritage protection

On Cultural Heritage a special software for data processing resulted from the shaking table has been developed and then applied to the 1:6 model Lateran Obelisk during a work carried on in cooperation with UTTMAT. Furthermore two contributions published in EAI 2012 Special Issue on "Knowledge, Diagnostics and Preservation of Cultural Heritage" are devoted to the seismic preservation of a small town historical centre and to natural hazard analysis on Machu Picchu Inca citadel.



Fig. 16 - Use of fibre optic sensors for assessment of thermal effects due to the laser-pancreatic tissue interaction during LITT (Laser-induced interstitial thermotherapy): experimental research activity on ex-vivo porcine pancreas aimed to human surgery application.



Fig. 19 - Surface effects in San Carlo area (Sant'Agostino Municipality, Ferrara Province).

### Environmental hazard

An analysis of environmental hazards on the landslide hazards in Messina area (Sicily) has been conducted. In particular, the statistical correlation between soil erosion and rapid mud and debris floods was made, together with a probabilistic analysis of susceptibility to the triggering of landslides, collapse, rapid casting, rotational and translational.

### Development and management of databases, WebGIS and warning systems



Fig. 20 - Model Lateran Obelisk placed on the shaking table

Several activities has been conducted by computer analysis and Web GIS tools on the topics listed below:

- design and implementation of a "Spatial Data Infrastructure" and staff training for the town San Giuliano di Puglia;
- design and implementation of a database and spatial coding of parallel computing for the automatic extraction of hydrographical data from digital elevation models. Within the project RITMARE – Marine Italian Research Project, coordinated by CNR,

the target was the study of the river basins sediment, the activity was conducted in collaboration with UTPRA-PREV;

- implementation of a WebGIS procedure to support the study and cliffs monitoring in Favignana Island;
- software update of databases and ENEA accelerometric data;
- software update databases and ENEA velocimetric data;
- study of early warning for the identification of critical deformations of the components of the fence in the Memorial Park of San Giuliano using instrumentation based on optical fibre sensors;
- participation to the Working Group Open Source GIS available in ENEA GRID, and Group for design and implementation of a "Spatial Data Infrastructure" on ENEA computing systems, as Task Force GIS.

### 2.7 EDUCATION AND KNOWLEDGE DISSEMINATION ACTIVITIES

On the basis of high-level scientific competencies and the fruitful collaboration with national and foreign universities and prestigious Italian and international research institutions, the MNF staff carried out technical and professional training of researchers and students (Bachelor, Master and PhD levels). Great deal of attention was devoted to high-level educational activities (invited seminars and lessons, practical teaching lessons) and knowledge dissemination.

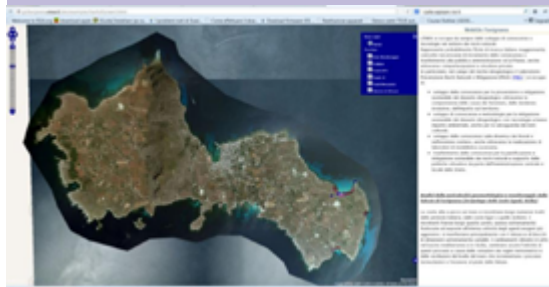


Fig. 21 - WebGIS procedure supporting the study monitoring of cliffs on Favignana island. See internet site: [gisfavignana.enea.it](http://gisfavignana.enea.it)

## 3 MATHEMATICAL MODELING LABORATORY

### 3.1 MISSION AND INFRASTRUCTURES

Main objectives of the Laboratory are to develop advanced Mathematical Methods for the study of the classical and quantum optics, and for modeling the transport of charged particle beams, to study and modeling of complex systems, including biological systems.

Competences available in the Laboratory are originated from expertise in different scientific disciplines as charged beam dynamics and transport, accelerators, RF structures, lasers, free electron lasers, optics and resonators, mathematical modeling.

UTAPRAD-MAT is currently involved in the development of the SPARC free electron laser test facility at LNF-INFN.

The activity of UTAPRAD MAT during 2012 has been developed along the following directions

- Free Electron Lasers
- Design of electron Sources
- Theoretical Physics
- Applied Mathematics

### Funding and projects

The research activities of the UTAPRAD-MAT Laboratory are mainly funded in the frame of National research programs (MIUR) as partner of collaborations (SPARX).

### 3.2 FREE ELECTRON LASER ACTIVITY

The activity on Free Electron Laser has been devoted either to the SPARC experimental activity and to the design of new FEL sources.

### SPARC experimental activity

During 2012 particular effort has been devoted to the development of COMB FEL that has

produced innovative results in particular in the operation of the FEL with two electron pulses at slightly different energies which have been injected inside the undulator chain to produce synchronous or delayed FEL SASE pulses with two different frequencies ("two colors FEL" TCF) for applications in pump and probe experiments.

The electron phase space distribution at the entrance of the undulator is reported in Figure 1 and 2.

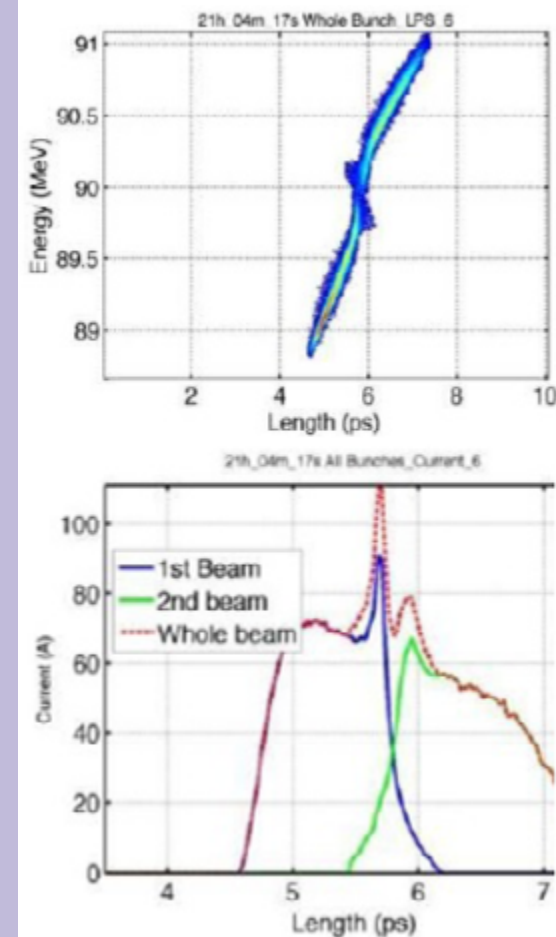


Fig. 1- Longitudinal phase space distribution for the SPARC two color experiment.

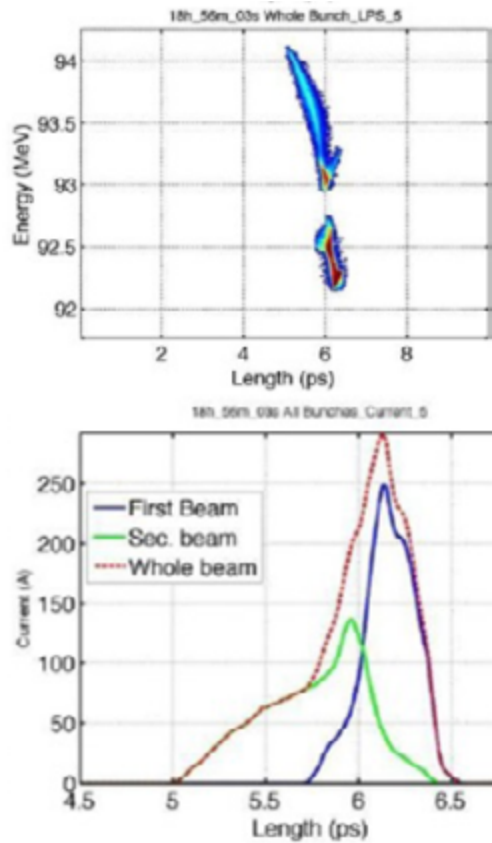


Fig. 2- Longitudinal phase space distribution for the SPARC two color experiment.

The FROG images reporting relevant to the temporal and spectral distribution of the pulses are reported in Figs. 3.

The experiment has confirmed the possibility of operating the FEL on two different colors and has provided the possibility of manipulating the pulses in order to achieve very short time durations. A further important achievement has been development of a diagnostic system, referred to as “speckle heterodyne method”, for measuring the transverse coherence of laser sources. The device has been exploited to study the coherence properties of the SASE FEL SPARC beam and the relevant diagnostic images are reported in Figure 4.

The experimental activity have achieved fairly important goals, which have clarified important aspects of the FEL physics and have opened new scenarios towards the development of laser sources consisting of trains of very short pulses.

**Beam Transport**

Particular attention has been devoted to the development of systems of diagnostic and control, either for the radiation and the e-beam propagating inside the SPARC transfer

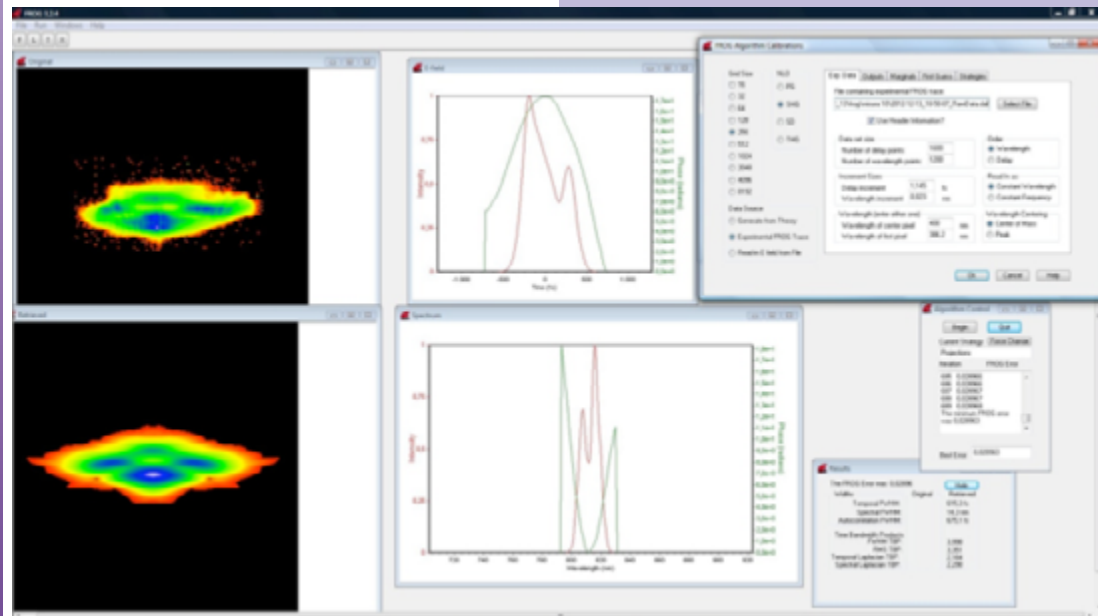


Fig. 3 - FROG Traces for the SPARC two color experiment.

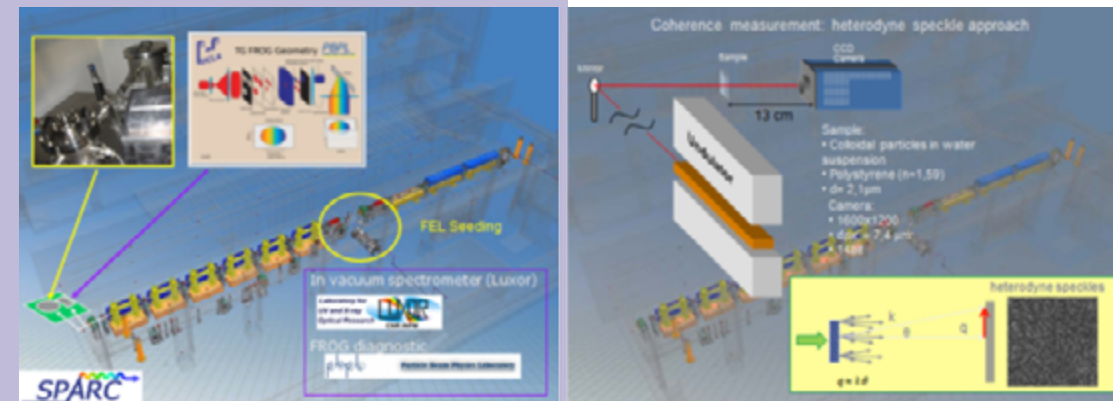


Fig. 4 - SPARC-SPECKLE heterodyne diagnostic.

line. One of the lines of research has been the construction of a “diagnostic” system capable of visualizing the evolution of the e-beam on the screen target inside the transport line. The procedure consists of “real” and “simulated” diagnostics. The simulated diagnostic is the result of a theoretical analysis merging the electron beam and the laser intensity evolution, as indicated in Figure 5.

The effort has been that of confronting in real time the measured and calculated quantities and get on line feedback, like the corrections to quadrupole current, if problems of transport arise. In Figure 5 we have reported the beam section snapshots at different locations in the transport line and the FEL intensity growth along the undulator line.

**Realization of a Magnetic Undulator**

Within the SPARC project a role of particular importance has been played by the design and construction of magnetic undulators.

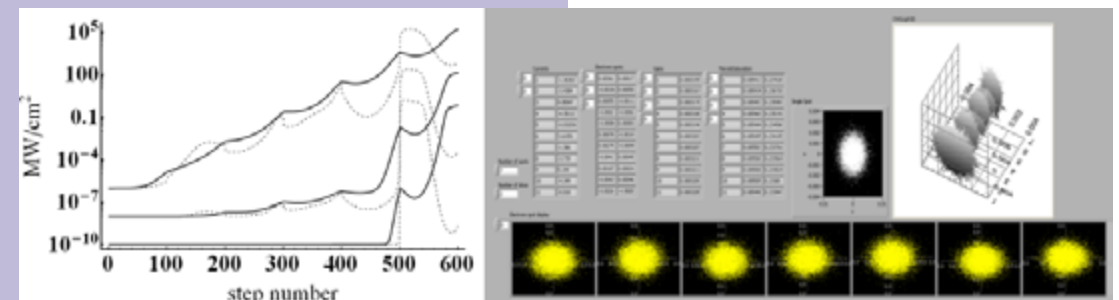


Fig. 5 - Power evolution along the undulator line with different focusing elements and Snap-shots of the electron beam inside the electron beam inside the SPARC transport line.

The undulators of the SPARC line have been designed by ENEA and have been realized by the ACCEL factory and successively they have been tested and characterized by ENEA.

Further developments of the SPARC project have demanded for the development of a short period undulator for the operation at higher harmonics.

This undulator with a period 1.4 cm length and with K values larger than 1 has been designed by the UTAPRAD MAT and realized in Collaboration with Kyma, the relevant images are reported in Figure 6. The measurement and the characterization of the device have been completed in Frascati and examples of measured field distributions are reported in Figure 7.

**Design of new FEL sources**

A new FEL sources for operation in a wide spectral range, from IR to X-ray has been proposed and is under design. The source



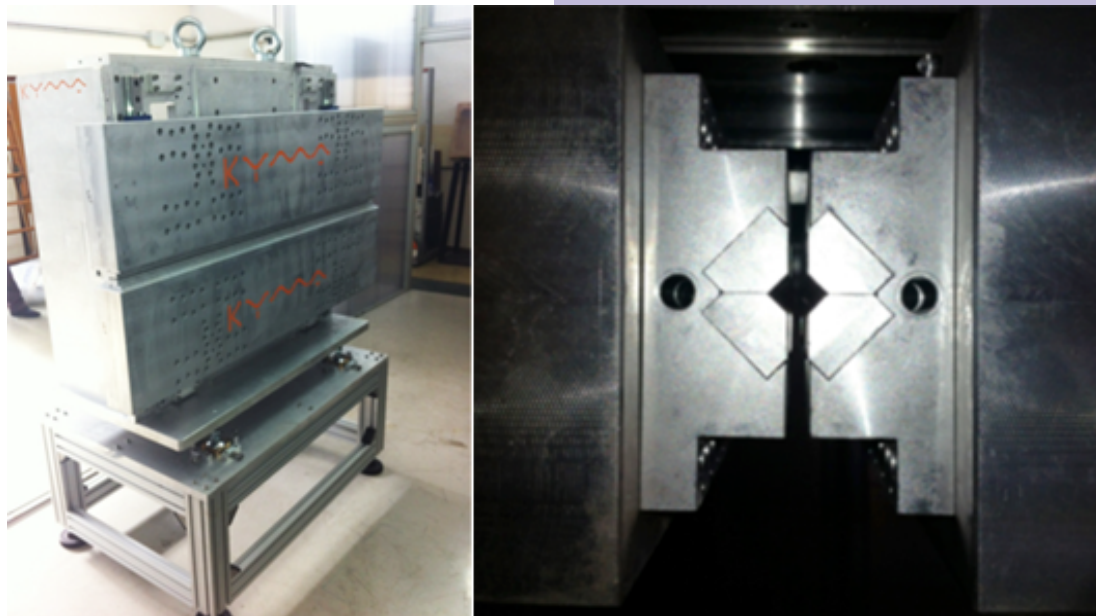


Fig. 6 - The SPARC short period undulator.

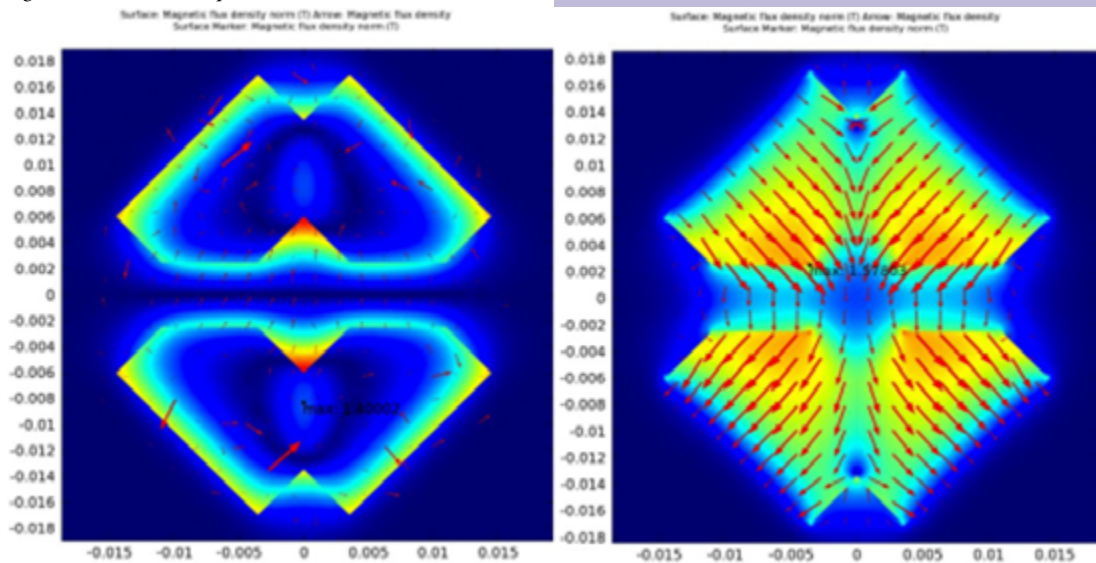


Fig. 7 - Surface Magnetic Flux density.

conceived as an integrated device is conceived to provide in its final stage high brightness radiation in the X-ray region and is supposed to operate with a superconducting linac with a maximum energy of 3 GeV.

The architecture of the device called IRIDE to be developed in cooperation with INFN at LNF, is reproduced in Figure 8, where we have reported

- a) Two S-C-LINACS with 1.5 GeV maximum energy
- b) Between the two Linacs a double FEL oscillator, with a manifold role, is inserted
- c) The undulator chain can be powered by the beam operating at full energy (3-GeV) or less
- d) A second FEL oscillator is added for the operation in the UV region and for intra-

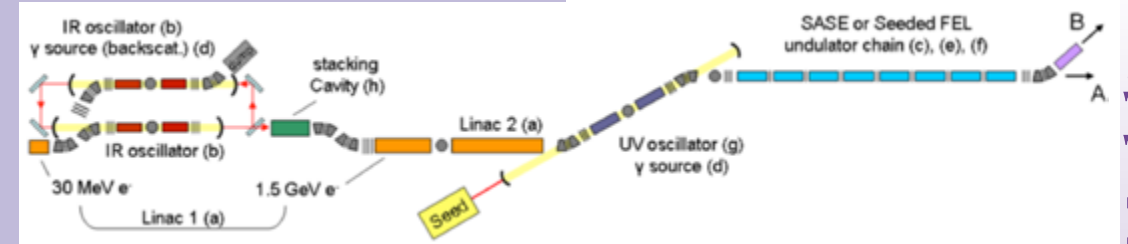


Fig. 8 - IRIDE FEL Architecture.

cavity backscattering for the realization of a gamma source to be exploited for Nuclear Physics studies and the production of polarized electrons

- e) The third FEL section may operate in SASE or SEDEED mode
- f) The seeding will be achieved by exploiting a conventional seeding procedure or by using the self- seeding scheme based on a kind of oscillator-amplifier device, according to the ENEA patent
- g) An oscillator with mirrors at can eventually be considered for the operation at short wavelength seeding

The IRIDE device is designed to provide a facility for different research areas, including Nuclear and elementary particle physics. The scientific case and the detailed cost analysis are under study.

### 3.3 DESIGN OF ELECTRON AND CARM SOURCE

In the past decade the research programs in nuclear fusion has had a significant progress thanks to the international collaboration (Europe, America, Japan and Russian Federation) for ITER project.

Italian activities are coordinated by UT FUS at ENEA, because of specific expertise available in RF heating. One of the greatest problem of the fusion and the power transfer for starting the self- sustaining nuclear fusion reaction. The problem was considered at MAT.

There are several methods to transfer power to the plasma but the most efficient of them is

the transfer through the RF resonance. The RF power is lunched into the plasma by a set of antennas. The minimal radio frequency power requirements to support the ignition and to stabilize the bulk of the plasma for the ITER machine is ~1 MW at ~170 GHz as reported in Figure 9.

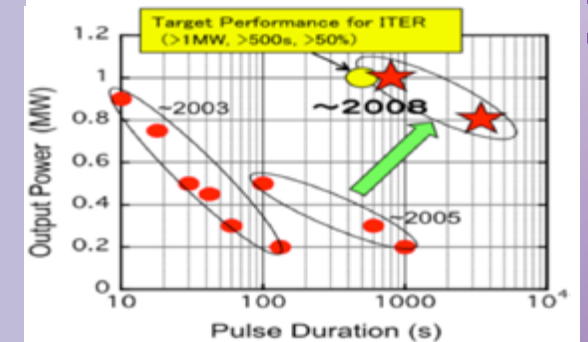


Fig. 9 - Gyrotron evolution during the last decade.

Till now a wave of 170 GHz was generated by a gyrotron device, producing hundreds of KW power for a few seconds as reported in fig 9. The latest model gyrotron developed by the Japan Atomic Energy Agency is able to produce radiation at 170 GHz with a power of 0.9 MW for 70 seconds or 1.1 MW for 5 seconds with 60% maximum efficiency. These results stresses the intrinsic limitations of the gyrotron sources when higher frequencies are required, as a consequence of the operation with an over-moded cavities and very high magnetic fields. Efficient heating of the plasma in ITER-like devices, may, however, occur through a radio frequency field operating at frequencies and power larger than 240 GHz and 1MW, respectively.

Heating sources different than gytrons have been therefore actively studied. One possible solution is the Free –Electron Laser (FEL), which, however, is limited by the low intrinsic efficiency of the process itself and requires therefore 99% beam recovery. Experiments performed within such a respect failed in either demonstrating long pulse operation at high efficiency. An alternative solution by a Cyclotron Auto-Resonance Maser (CARM). As in the case of FEL it uses a relativistic beam but has an intrinsic higher efficiency and, with a modest beam recovery, could bring the overall efficiency up to 50-60%.

For the overmoded cavity where the radio frequency is generated, the crucial point of a right operation for a CARM generator, lies at high quality of electrons beam in terms of the longitudinal velocity spread ( $\delta v_{||}$ ) and pitch-ratio ( $\alpha=v_{\perp}/v_{||}$ ). In table 1 the parameter values that should be respected by our CARM design are reported.

A conceptual design of a high voltage electron gun as a driver of high power millimetre wave gun oscillators was developed taking in mind the important role played by the gun geometry in the generation of a high quality beam.

Anode-cathode distance( $D_a-D_c$ )/2	200mm
Magnetic field along the cavity	7 T
Pitch ratio $\alpha = v_{\perp}/v_{  }$	<0.5
Axial and transverse velocity spread	<0.1+0.3 %
Cathode potential	650+750 kV
Electric field at the cathode surface( $E_c$ )	<10kV/mm

Table 1 - The design project parameters.

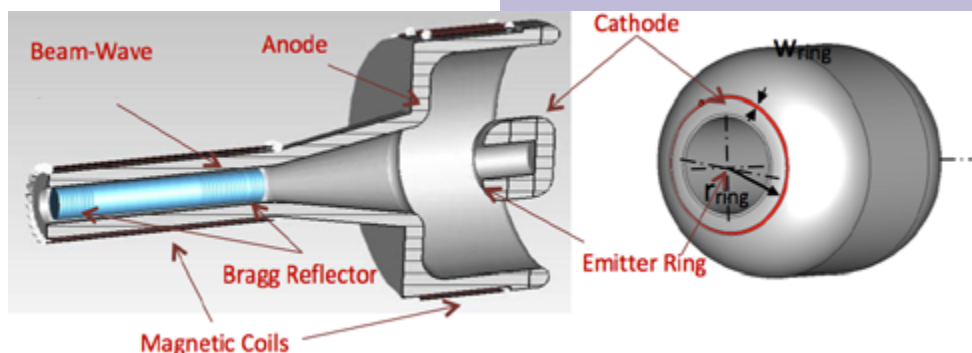


Fig. 10 - Gun design for CARM.

In Figure 10 and table 2 are reported the gun design and the most important parameters values, necessary to respect the requirement of the project; a very short emitter ring as a circular crown with a width of 2mm is necessary in order to reduce the velocity spread, produced from the thermo-ionic emission.

Gun Parameters	
Anode Radius	310 mm
Cathode Radius	112 mm
Emitter Ring Width	2 + 4 mm
Emitter Ring Radius	45 + 55 mm

Table 2- Geometric parameter value of the gun.

Using the commercially available code CST, with particle tracking package, we performed a numerical simulation of the gun configuration reported in Figure 10. The magnetic field guiding the beam is generated by an analytical axial profile computed considering two coils. The first one, the gun coil, is located at the gun part. It produces a low magnetic field of about  $B_c \approx 0.2T$ .

The second one is positioned along the cavity and produces a magnetic field( $B_0$ ) up to 7T.

In Figure 11 we report the results of the

simulation in terms of the electrostatic 2D map and the longitudinal axial profile of the magnetic field. The first attempt to design a high voltage electron gun shows optimistic results.

However the velocity spread and especially

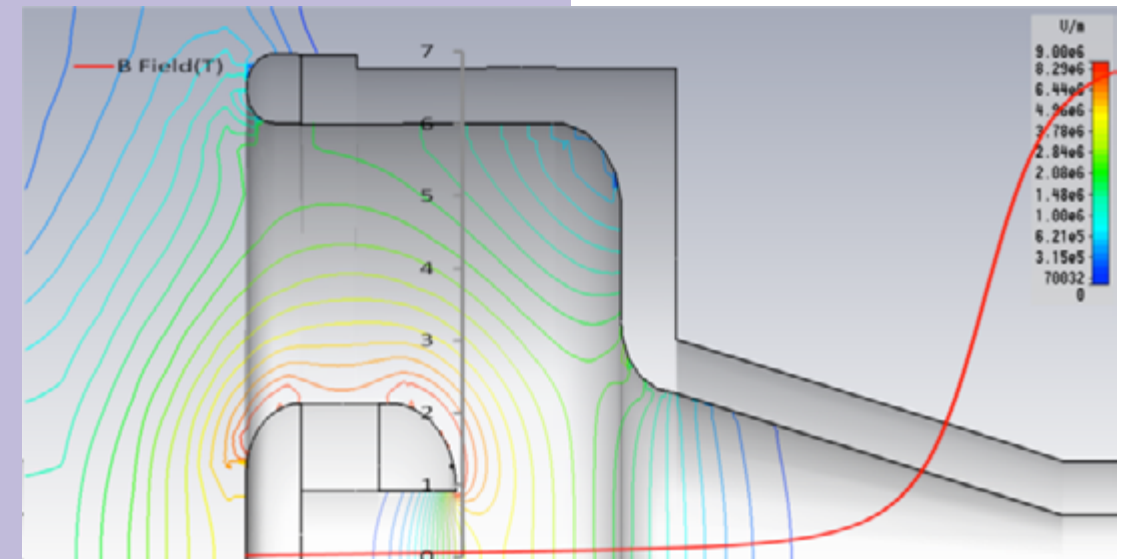


Fig. 11- 2D map of absolute value of electrostatic field, the axial magnetic field profile.

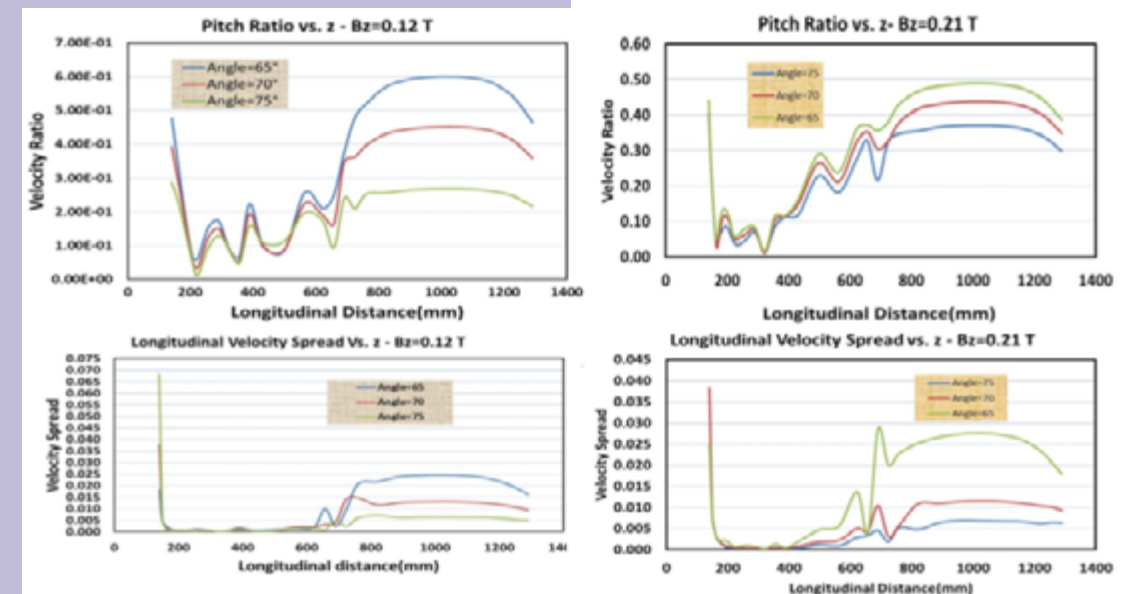


Fig. 12 - Trend of the logitudinal velocity spread and pitch ratio varying the magnetic field on the cathode.

the transverse one and the cathode surface field are still above the values required by the project as reported in Figure 12.

### 3.4 THEORETICAL PHYSICS

A significant part of the activity of the unit has been devoted to the analysis of problems concerning the theoretical treatment of problems relevant to the evolution of ensemble of relativistic particles under the effect of external forces. The problems have been treated either for classical and quantum devices.

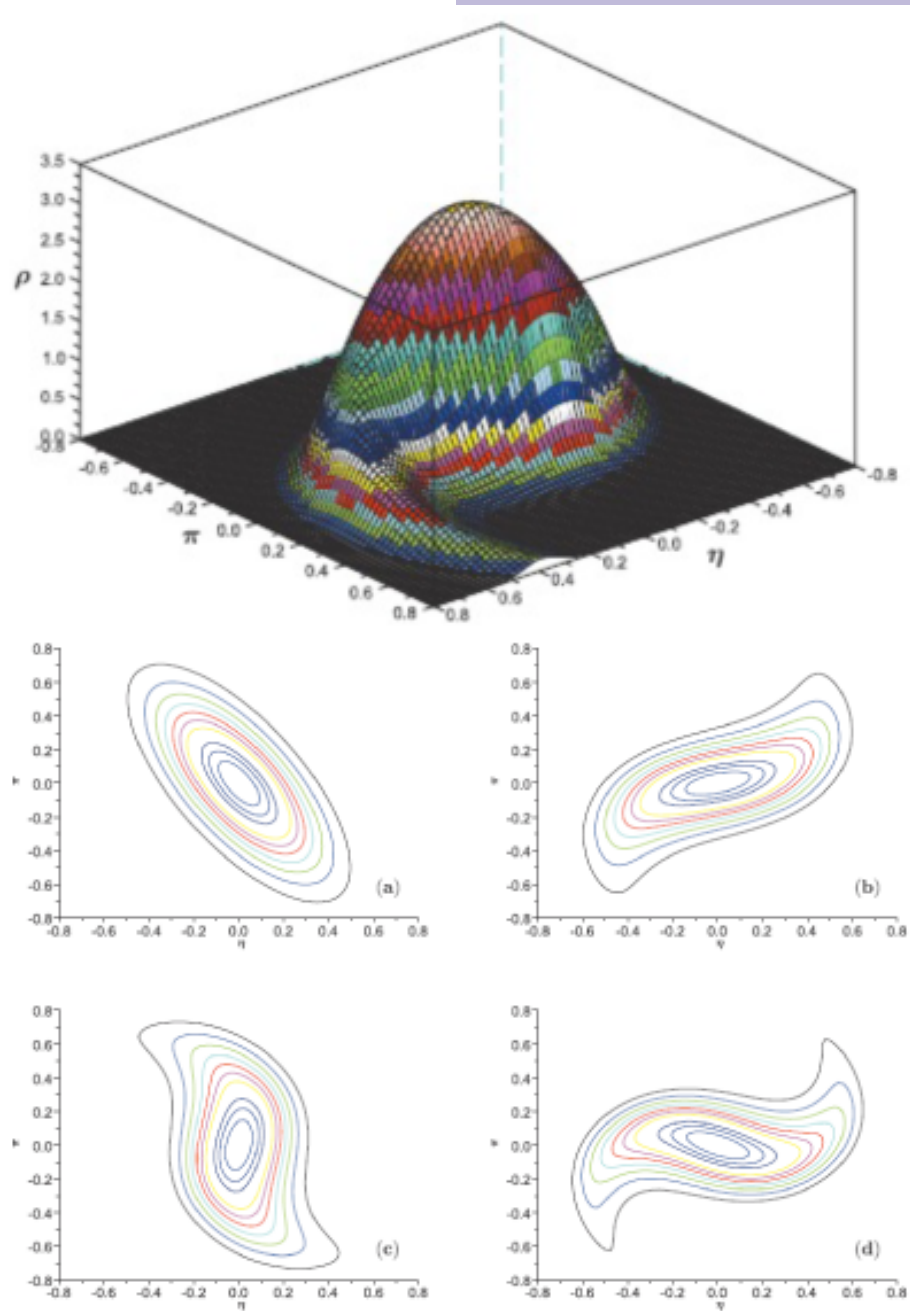


Fig.13 - Relativistic phase space distribution for an ensemble of particles ruled by a quadratic potential, the upper plot represents the 3-D Liouville distribution the lower plots the level curves at different times.

A particular effort has been devoted to the analysis of the so called relativistic harmonic oscillator.

The analysis have been aimed at correcting some miss-conceptions arising within the framework of the treatment of relativistic Liouvillian problems and the method put forward to treat the evolution of classical relativistic phase space distributions has been achieved by an innovative algebraic integration algorithm.

Examples of relativistic phase space evolution have been reported in Figs. 13.

The method has been extended to the solutions of relativistic Schroedinger and to Klein Gordon equations. The results obtained have been exploited to treat problems concerning either the relativistic transport of charged particles and the simulation of quantum process as e. g. the so called trembling (zitter-bewegung) motion in Dirac relativistic particles.

Different methods to generalize the Dirac relativistic equation have been studied and in particular we have stressed their importance for the so called fractional calculus.

We proceeded as illustrated in the following. It is well known that the formulation of the relativistic Dirac equation is based on a factorization of the square root which allows to write the Pythagorean theorem in the form

$$\sqrt{B^2 + C^2} = B \hat{\sigma}_j + C \hat{\sigma}_k, \quad j \neq k = 1,2,3$$

with  $\hat{\sigma}_j$  being the Pauli's matrices. The previous identity is justified by the following well known properties of this family of matrices

$$\begin{aligned} \hat{\sigma}_j^2 &= \hat{1}, \\ \hat{\sigma}_j \hat{\sigma}_k &= -\hat{\sigma}_k \hat{\sigma}_j, \\ \hat{\sigma}_1 &= \begin{pmatrix} 0 & 1 \\ 1 & 0 \end{pmatrix}, \hat{\sigma}_2 = \begin{pmatrix} 0 & -i \\ i & 0 \end{pmatrix}, \hat{\sigma}_3 = \begin{pmatrix} 1 & 0 \\ 0 & -1 \end{pmatrix} \end{aligned}$$

We can extend the same idea to the sum of three squared terms and accordingly the relevant square root can be written as the following linear combination of Pauli matrices

$$\begin{aligned} \sqrt{A^2 + B^2 + C^2} &= A \hat{\sigma}_l + B \hat{\sigma}_j + C \hat{\sigma}_k, \\ l \neq j \neq k &= 1,2,3 \end{aligned}$$

The realization of such a factorization is not unique. The use of the Hamilton quaternion can be efficiently used for this purpose and this is by no means surprising, a purely imaginary quaternion can indeed be written as

$$\begin{aligned} Q &= a \hat{i} + b \hat{j} + c \hat{k}, \\ \hat{i}^2 &= \hat{j}^2 = \hat{k}^2 = -1, \\ \hat{i} \hat{j} \hat{k} &= -1 \end{aligned}$$

and can be realized, in terms of Pauli matrices, according to

$$\hat{i} = i \sigma_1, \hat{j} = i \sigma_2, \hat{k} = i \sigma_3$$

It is therefore evident that the key tool of the game is the use of the Clifford algebras, at least if we limit ourselves to the case of square roots.

We have therefore tried an extension of the Dirac factorization method allows the following extension of the Pythagorean identity to cubic roots, namely

$$A = \sqrt[3]{B^3 + C^3} = B {}_1\lambda_1 + C {}_1\lambda_2$$

Where we have used the matrices (the reason of the sub-index "1" on the left will be clarified below)

$${}_1\lambda_1 = \begin{pmatrix} 0 & 1 & 0 \\ 0 & 0 & 1 \\ 1 & 0 & 0 \end{pmatrix}, {}_1\lambda_2 = \begin{pmatrix} 0 & \varepsilon_1 & 0 \\ 0 & 0 & \varepsilon_2 \\ 1 & 0 & 0 \end{pmatrix},$$

$$\varepsilon_1 = -\frac{1}{2} + i\frac{\sqrt{3}}{2}, \varepsilon_2 = -\frac{1}{2} - i\frac{\sqrt{3}}{2},$$

along with the following properties of the cubic roots of unity

$$\varepsilon_j^3 = 1, j = 0,1,2$$

$$\sum_{j=0}^2 \varepsilon_j = 0, \varepsilon_0 = 1$$

which are crucial in getting the following condition

$${}_1\lambda_j^3 = 1$$

$${}_1\lambda_j^2 \lambda_k + {}_1\lambda_j \lambda_k + {}_1\lambda_k \lambda_j^2 = 0,$$

$$j \neq k = 1,2$$

If we add to  ${}_1\lambda_{1,2}$  the diagonal form

$${}_1\lambda_3 = \begin{pmatrix} \varepsilon_1 & 0 & 0 \\ 0 & \varepsilon_2 & 0 \\ 0 & 0 & 1 \end{pmatrix}$$

we can realize the factorization

$$\sqrt[3]{A^3 + B^3 + C^3} = A {}_1\lambda_j + B {}_1\lambda_k + C {}_1\lambda_l,$$

$$j \neq k \neq l = 1,2,3$$

The previous set of matrices provides an extension of the Pauli matrices, but they are not the only possible triples, for example we can pick the following combination

$${}_2\lambda_1 = \begin{pmatrix} 0 & \varepsilon_1 & 0 \\ 0 & 0 & \varepsilon_2 \\ 1 & 0 & 0 \end{pmatrix}, {}_2\lambda_2 = \begin{pmatrix} 0 & \varepsilon_2 & 0 \\ 0 & 0 & \varepsilon_1 \\ 1 & 0 & 0 \end{pmatrix}, {}_2\lambda_3 = \begin{pmatrix} \varepsilon_1 & 0 & 0 \\ 0 & \varepsilon_2 & 0 \\ 0 & 0 & 1 \end{pmatrix}$$

The case of the Dirac factorization for a generic n, namely

$$A = \sqrt[n]{B^n + C^n} = B t_1 + C t_2$$

can be afforded using the same strategy as before, i. e. the search for the associated matrices by means of the properties of the roots of unity. In the case of n odd we find

$$\hat{t}_1 = \begin{vmatrix} 0 & 1 & 0 & \dots & 0 \\ 0 & 0 & 1 & \dots & 0 \\ \dots & \dots & \dots & \dots & \dots \\ 0 & 0 & 0 & 0 & 1 \\ 1 & 0 & 0 & 0 & 0 \end{vmatrix}, \quad \hat{t}_2 = \begin{vmatrix} 0 & \varepsilon_1 & 0 & \dots & 0 \\ 0 & 0 & \varepsilon_2 & \dots & 0 \\ \dots & \dots & \dots & \dots & \dots \\ 0 & 0 & 0 & 0 & \varepsilon_{n-1} \\ 1 & 0 & 0 & 0 & 0 \end{vmatrix}.$$

where  $\varepsilon_r$  are the n-th roots of unity, satisfying the conditions

$$\sum_{r=0}^n \varepsilon_r = 0, \prod_{r=1}^{n-1} \varepsilon_r = 1,$$

$$\varepsilon_0 = 1$$

determining identities generalizing the Dirac factorization of the Pythagorean identity to the n-th order.

As in the previous case the matrices  $t_{1,2}$  are not the only allowing the factorizations, the following example shows how the other matrices can naturally enter into the game.

A fairly immediate consequence of the previously outlined procedure is that we can "linearize" the

equation  $\partial_t F = \sqrt[n]{\partial_x^n + a^n} F,$

to obtain the following Dirac like form  $\partial_t \Phi = (t_1 \partial_x + t_2 a) \Phi$

with  $\phi$  being a vector with n-components.

### 3.5 APPLIED MATHEMATICS

The study of fractional differential equations has a deep physical motivation mainly in connection with the anomalous diffusion. For this reason a strong effort of the unity has been devoted to pursue the relevant activities in collaboration with INFN, University of "Paris Sud" at Jussieu, Paris XIII and the Polish academy of science. The anomalous transport characterizes different processes in different fields including physics, ecology, social science, economy...

In normal diffusion variance of transported distributions grow linearly with time, while in anomalous diffusion their time dependence is characterized by exponents larger than unity. This means that "anomalous" spreading may occur in short time, as it has been observed in the spreading of infectious disease, in the spreading of tumor metastasis, or human and animal movements for food foraging.

The equation describing such a behavior are partial differential equations of the type

$$\partial_t F(x,t) = -D_\alpha \partial_x^\alpha F(x,t),$$

$\alpha = \text{non - integer}$

And the natural solutions are provided by the so called Levy distributions, characterized by long tail (see Figs. 14)

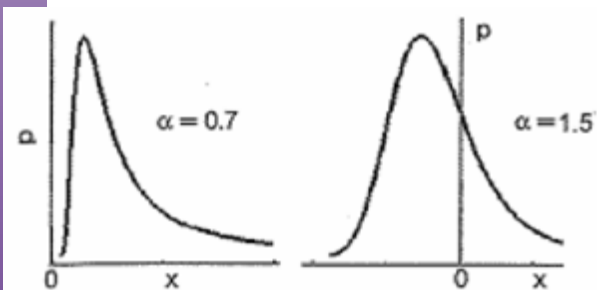


Fig. 14 - Examples of Levy distributions

and by the fact that their moments  $\langle x^\mu \rangle$  exist only for  $\beta \leq \mu$ .

These concepts apply to the decay of photoluminescence of silicon nanocrystals, an activity which has been actively studied in UTAPRAD.

The analysis of the experimental data have supported the interpretation of the "microscopic" processes leading to photoluminescence decay in terms of super-diffusive mechanisms and further modeling is in progress.

## 4 RADIATION SOURCES LABORATORY

### 4.1 MISSION AND INFRASTRUCTURES

The Radiation Sources Laboratory (UTAPRAD-SOR) performs R&D work in the fields of coherent radiation sources and in the acceleration of charged particles.

Research activities include emerging technologies in photonics and microlithography, development of laser systems and accelerators for scientific, industrial and medical applications.

Current activities are focussed on the development of:

- High energy-per-pulse excimer lasers, plasma driven X-ray sources and their applications;
- Free Electron Laser (FEL) sources for the generation of electromagnetic radiation in the Far InfraRed and in the Terahertz region;
- Low-energy electron accelerators for material processing, medical applications and as a driver for FELs;
- Medium-energy proton accelerators for cancer therapy
- Cybernetic models, artificial vision and automation systems.

These research areas are undergoing a rapid development worldwide with an increasing number of applications such as microlithography in the extreme ultraviolet, X-ray microscopy of biological systems, effects of electromagnetic radiation, imaging systems applied to material characterization, biology, biomedicine and, more recently, art conservation studies.

The facilities developed by UTAPRAD-SOR and utilized for current activities include:

- Excimer laser laboratory
- Soft X-ray plasma sources laboratory
- Compact FEL (90 – 150 GHz)
- FEL-CATS (400 – 700 GHz)
- TOP-LINAC
- 5 MeV Electron LINAC

### Funding and projects

In 2012 important steps forward were made in the submission and launch of new projects in the fields of nano-fabrication and "nano-patterning" by EUV radiation, and in the field of accelerators.

In particular, the effort devoted over the past two years to the implementation of an agreement with the Regional Government of Lazio for the construction of the new accelerator for proton therapy IMPLART, a project carried out in collaboration with the National Institute of Health and IFO (Institute Physiotherapy Hospital, Rome), lead to the provision by the Regional Government of Lazio of the first part (2.5 MEuro) of the total funding of 11 MEuro at the end of November.

Moreover the Radiation Sources Laboratory was actively involved in the realization of the SPARC/X FEL, a joint project between ENEA, CNR, INFN and the University of Rome "Tor Vergata", aimed at the development of a Free Electron Laser in the VUV and X-ray regions.

In the following a brief review of the above activities is reported together with the most recent results and perspectives.

## 4.2 SHORT-WAVELENGTH SOURCES AND APPLICATIONS

In the extreme ultraviolet (EUV) spectral region (20 eV – 280 eV) laser-plasma and discharge-plasma sources can produce energies per pulse and repetition rates sufficient to be considered a valuable alternative to synchrotrons and short-wavelength free-electron lasers (X-FELs) in many applications, namely when the peak power and the brightness are more important than the average power and when a narrow spectral band is not required.

In past years the SOR Laboratory has developed a Micro-Exposure-Tool (MET) for micro- and nano-lithography. The MET is a complex apparatus comprising a laser-driven plasma source called EGERIA, a debris mitigation system, an optical collector and an accurate optical projection system able to print a pattern with a spatial resolution better than 100 nm. Detailed information can be found on the website:

[www.frascati.enea.it/Impianti/SorgenteRi-X%20da%20laser-plasma/SorgenteR-Xdalaser-plasma.html](http://www.frascati.enea.it/Impianti/SorgenteRi-X%20da%20laser-plasma/SorgenteR-Xdalaser-plasma.html).

It is worth recalling the exploitation of the EUV radiation for the development of a novel anti-counterfeiting system based on an invisible writing method which uses lithographic techniques on luminescent materials.

The experimental results have shown that this patent-pending technology is suitable to fabricate robust anti-counterfeiting tags, which are almost impossible to counterfeit and can be applied to almost every kind of objects, independent of their shape and size. In the ultraviolet spectral region, the long-term expertise on the development and application of high-peak-power excimer lasers continues focusing on laser-matter interaction studies, particularly regarding the surface coloration of linen textiles for reproducing archaeological images.

### Discharge-plasma source of EUV radiation

In 2012 the research activity on the Extreme Ultraviolet (EUV) radiation source based on a Discharge Produced Plasma (DPP) has been mainly dedicated to two tasks: optimization/characterization of the source and treatment of different samples with the EUV radiation. As far as the first task is concerned, a numerical code has been developed to simulate the behaviour of the high voltage power supply of the source with the aim of studying the possibility of a further improvement of the source stability and power. An analysis of the source physics and its characterization have been widely described in an ENEA technical report.

As far as the second task is concerned, the DPP source has been employed to produce some sample tags based on the ENEA anti-counterfeiting technique. In particular, several invisible markings have been obtained on plastic cards, like the identification pass used by ENEA personnel, and on a new flexible and adhesive tag.

A new application regarding the irradiation by EUV radiation of novel photoresist materials for microelectronics and nanofabrication was also started in collaboration with the Material Engineering Dept. of Padova University (Italy). In particular, some samples of titania “ex situ” (a material loaded by 15-nm-diameter  $\text{TiO}_2$  nanoparticles) and of titania “in situ” (an alcoxide based network) have been exposed to the radiation source. A good response has been demonstrated through these preliminary tests, as shown in Fig. 1.

The result is much better than expected on the basis of former experiments of UV exposures. As it can be seen, a periodic pattern of 400 holes/inch has been reproduced on the titania in-situ photoresist (as well as on the ex-situ one) by exposing it to 4000 shots of the DPP source, operated at 10 Hz, at a distance of approximately 10 cm. The corresponding EUV dose is approximately  $0.6 \text{ J/cm}^2$ . In this experiment the radiation has been filtered

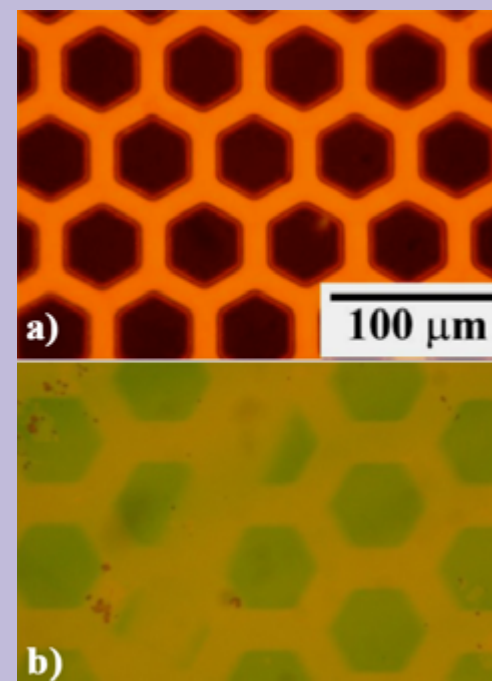


Fig. 1 - Example of photoresist EUV exposure with the ENEA DPP source: (a) a copper grid of 400 holes/inch used as contact mask and (b) the same mask reproduced on a titania “in-situ” photoresist after an exposure to 4000 shots of the DPP source.

by a 150-nm-thickness zirconium filter in order to limit the spectrum to the 10-20 nm range and to avoid artefacts (the shadow of a 36- $\mu\text{m}$  nickel wire, supporting the Zr filter, is recognizable in Fig. 1b). No dose or process optimization have been done yet.

The research activity in this field will be extensively developed during the next two years in the frame of a national project, funded by “Cariplo Foundation” and coordinated by the Chemistry Dept. of Pavia University (Italy). The project, entitled “New materials for direct nanopatterning and nanofabrication by EUV and soft X-rays exposures” involves ENEA and the above mentioned two Universities. It aims at the development of innovative photoresists characterized by particular functional and structural properties. The expected ENEA contribution to the project is the irradiation of the above mentioned innovative photoresists in different experimental conditions to determine both their sensitivity to the EUV

radiation as well as their spatial resolution properties. Both the DPP and the Laser Produced Plasma (LPP) sources, already operative in the ENEA Laboratories, will be utilized to reach the project objectives.

### Anti-counterfeiting ENEA technology: new applications

As previously reported, the Laboratory UTAPRAD SOR has patented an apparatus which consists of an extreme ultraviolet radiation source writing invisible patterns on thin films of alkali halides. The markings written using this method are almost impossible to counterfeit, and offer a much better protection against fakes than the available anti-counterfeiting techniques.

Our technique is based on the capability of EUV radiation to alter the electronic structure of a class of dielectric materials, like alkali halides. Depending on the EUV irradiation conditions, a permanent visible pattern on alkali halides can be obtained. However, in particular conditions the radiation can locally produce a controlled density of color centers, thus printing a trace which is invisible to the naked eye and also at the microscope observation.

Thanks to the atomic-scale interaction and to the short EUV wavelengths, the writing process allows to achieve an extremely high spatial resolution of the stored image, down to the sub-micrometer scale which is not attainable, e.g., using fluorescent inks deposited by the current ink-jet printer technology. The security level of this technology can be further increased by the digital encoding of the image, applying the state-of-the-art cryptography techniques. In this case, the control relies not only on the physical reading of the image, but also on its decoding with the appropriate digital key/algorithm.

We can increase even more the security level of the technology by structuring the crystalline film as a series of thin layers separated each other by non-luminescent materials, the

thickness of these layers increasing from the layer facing the ionizing radiation under writing process to the opposite side of the luminescent structured material, so that, after irradiation, the spectral energy of the used ionizing radiation affects the luminescence ratio of the different layers, and therefore a mark imprinted with a ionizing radiation having a spectral energy different from a pre-determined one can be identified.

So far, we have used this invisible marking to tag electronic components, credit cards and containers of radioactive waste. However, the protection level, the cost and the production yield associated with our technique suggest that the ideal field of application be the traceability and the protection of artworks against fakes. Accordingly, we have deposited a LiF film on transparent and adhesive plastic substrates which can be stuck on the object to be protected without altering it. Obviously, a good anti-counterfeiting tag should change its status/pattern-visibility when it is torn away from the original object, in order to easily recognize if it has been moved to a faked object. After

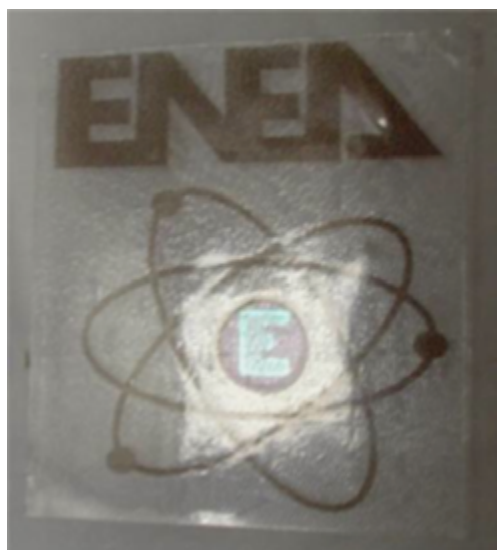


Fig. 2 - The adhesive tag photographed after being pulled off the original metal substrate and re-attached to another surface. The patterned letter E, which was originally invisible, is now visible under ambient light illumination. The LiF film was thermally evaporated on the transparent and adhesive plastic substrate by the MNF Laboratory.

writing an invisible “E” in a LiF film deposited on a transparent tag, we have checked what happens when slowly and carefully pulling off the adhesive tag and attaching it to another surface. The result, shown in Fig. 2, shows that the letter “E” patterned by EUV radiation (originally invisible at the naked eye) becomes visible when observed at ambient light after the tag was pulled off the original surface.

As a test to check the applicability of our AC tags to archaeological objects, we stuck a tag similar to that of Fig. 2 to a copy of a bronze statue, known as “Hero four-eyes and four-arms”, see Fig. 3. The original statue was found in the Nuraghe Village at Abini (Nuoro, Sardinia) and dated back to the tenth century B.C.

Figure 3 provides evidence that the patterned letter “E” is absolutely invisible to the naked eye, while it is easily detected by a proper illumination and filtering.

When seeking for practical uses of our technology, an important issue is the durability of the invisible writing on AC tags. In general, LiF is a rugged material, hard and almost non-hygroscopic. Our tests show that the irradiated films can be touched many times without significantly damaging or altering the visibility of the pattern. When the tags are exposed to severe conditions (heavy and uncontrolled scratching or abrasions), a protection film can be applied on the tag.

In order to build up an industrial prototype producing our AC tags one needs:

- The ENEA patents and the related know-how;
- A 50-W average power EUV source (DPP commercially available);
- A contact mask with the barcode/logo/picture (made, e.g., by lithography, or using a laser, or by chemical erosion);
- A suitable alkali halide film sensitive to EUV deposited on a flexible transparent plastic substrate (commercially available).

There are several parameters that influence

the number of tags written per unit time, including the time to accurately align the contact masks on tags, the maximum number of tags that can be irradiated in the same irradiation run, and the area to be irradiated (which depends on the size of the patterns). A conservative estimation, based on a system made by assembling commercially available parts, gives a potential production yield of

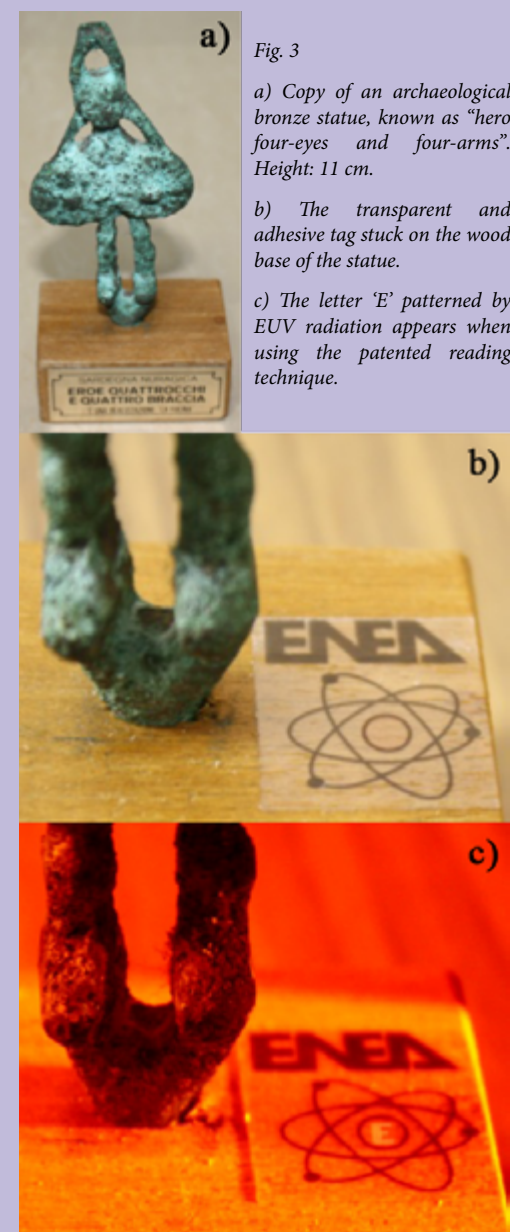


Fig. 3

a) Copy of an archaeological bronze statue, known as “hero four-eyes and four-arms”. Height: 11 cm.

b) The transparent and adhesive tag stuck on the wood base of the statue.

c) The letter ‘E’ patterned by EUV radiation appears when using the patented reading technique.

about 50-100 tags/hour, each tag having a patterned area of 0.4 cm<sup>2</sup>. In summary, we have developed and patented a new anti-counterfeiting/tracking technology based on EUV lithography on luminescent materials. An arbitrary pattern can be transferred as an invisible image on thin tags, which in turn can be put on or embedded in any object to be protected or traced. A compact and cheap device can read the luminescent image and check the authenticity of the tags. In contrast with the use of fluorescent inks, our patterns are obtained by illumination of alkali halides materials with EUV radiation rather than by ink jet writing. Consequently, our patterns can reach a better spatial resolution, down to the sub-micrometer range. Our writing tool is complex and expensive (especially in the case of projection imaging, giving sub-micrometer resolution) and it requires an experienced and skilled team to be optimized. As a consequence, it is highly unlikely that a counterfeiter can build up and operate a similar writing tool. On the other hand, the reading system is cheap and simple so that it can be easily check the presence of watermark patterns to verify if the good is genuine. The complexity and safety level of our hidden patterns can be further enhanced and adjusted by encoding patterns by cryptography techniques, and/or by structuring the fluorescent film as a series of thin layers, each separated by non-luminescent materials, with a variable thickness. Our anti-counterfeiting tags are resistant to normal conditions of use, and can be protected by a standard thermoplastic film, when exposed to severe conditions. Our tags cannot be detached from the original object and stuck on another object, because in this case the pattern becomes visible, see Fig. 2. The feasibility of the application of this technology to artworks has been demonstrated, see Fig. 3.

The ENEA technology can be used alone or in conjunction with other anti-counterfeiting/tracing methods. The level of security of our technology can be evaluated by the following standard criteria:

- very high cost to break;
- high probability to detect a clone;
- very low probability of false negatives;
- no privacy risks.

Concerning vulnerabilities, at the moment we are not able to find practical ways to fool the product authentication. ENEA is presently looking for industrial companies and research partners interested in a joint scientific/engineering development, and/or license agreement, and/or testing new applications.

### Optical systems for solar technologies

The Radiation Sources Laboratory has recently applied its expertise in optics to the positioning of concentrating solar systems with respect to the sun and to innovative linear concentration schemes. To this aim, the Laboratory has developed a simplified analytical algorithm that allows the astronomical calculation of the sun position with an accuracy of about 1 minute of arc. Such algorithm can be easily implemented in a microprocessor. The algorithm, based on an analytical solution of Kepler's laws.

To test the algorithm-microprocessor, and to develop a linear concentration panel prototype based on such microprocessor for the cogeneration of electricity and heat, the Laboratory has issued to different Italian companies a request for an expression of interest to cooperate on these topics.

As a result, a meeting with the companies Arca, Telicom srl., Atec Robotics, Anaf Spa, and Archimede Srl, was organized with the participation of ENEA colleagues from Laboratories involved in research on solar energy (ENEA Portici and ENEA Casaccia UTRINN-PCI). Following an indication of UTRINN-PCI, contacts were established with the company D.D. s.r.l. (Udine) for experimenting the ENEA sun tracking algorithm/microprocessor on a prototype of single-axis parabolic concentrator for solar thermal power.

The research activity in 2012 on optical systems

for solar technologies has been mainly devoted to the development of a sun tracker (SIMO) for a photovoltaic streetlight in collaboration with Elettro Rail s.r.l., and to the development of a new high-precision solar compass.

The research provided in the contract with Elettro Rail s.r.l. (Frosinone) about the sun tracking system SIMO is based on the above mentioned astronomical algorithm/microprocessor. ENEA has completed its scheduled activities:

- a) calculation of the energy collected by solar panels characterized by various tracking motions types (mono-axial, bi-axial, fixed) and by different latitudes.
- b) development of an electro-mechanical device for driving the movement of the solar panel of the photovoltaic streetlight. This device consists of a low-voltage electric motor controlled by the above mentioned algorithm implemented in a microprocessor, which is equipped with a GPS device that provides the geographic coordinates of the place where the streetlight is positioned.

An example of the calculations of the energy daily collected by a solar panel is shown in Fig. 4, while a picture of SIMO during preliminary tests is shown in Fig. 5.

Any sun tracking system exclusively based on astronomical calculations of the sun position requires an accurate orientation of its base during its installation phase. Starting from this necessity and considering that the equations of the above mentioned astronomical algorithm can be inverted, a new high precision solar compass was developed and patented (patent application number RM2012A000664).

The innovative sun compass is based on:

- a particular sun image detector;
- the above mentioned microprocessor (with inverted equations) connected to a GPS device for accurate knowledge of the local time and geographical coordinates;
- a pointing optics (a telescope with pointing

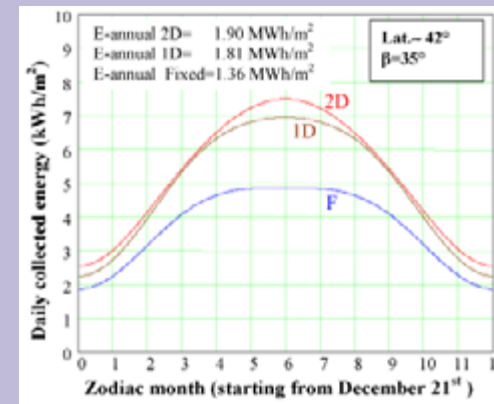


Fig. 4 - Calculation of the energy daily collected by a solar panel, placed at Frascati (Rome), for different tracking motion types: bi-axial rotation (2D), where the panel is always perpendicular to the sun rays; single-axis rotation (1D), where the panel is facing toward the sun but laying on its rotating axis which is tilted by  $\beta$  degrees with respect to the horizontal plane and oriented along the N-S direction; a fixed panel (F) oriented to South and tilted by  $\beta$  degrees with respect to the horizontal plane.

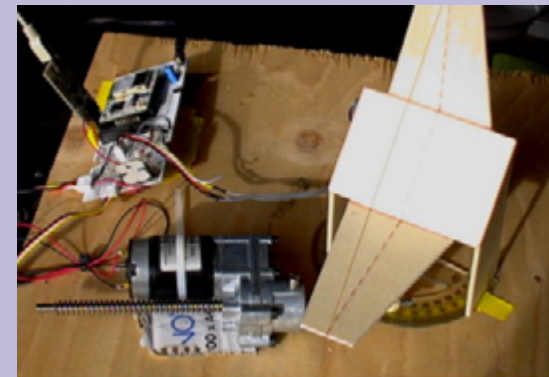


Fig. 5 - First test bed of SIMO during preliminary tests: a low voltage motor (bottom), controlled by the microprocessor (top-left), orientates a small wooden panel (right) toward the sun, while the shadow of thin wire, at about 7 cm from the panel, demonstrates that a correct orientation is maintained.

- cross);
- a high-accuracy digital goniometer (connected to the microprocessor too) for the measurement of the angle between the image detector and the pointing optics.

After pointing at any object with the telescope and turning the image detector approximately (within few degrees) toward the sun, the

microprocessor immediately calculates the direction (azimuth) of the observed object with respect to the true geographic South or North with an accuracy of one minute of arc.

A prototype of the compass, developed by using instruments and materials already available in the lab, has demonstrated an absolute accuracy better than 3 minutes of arc. Fig. 6 shows the

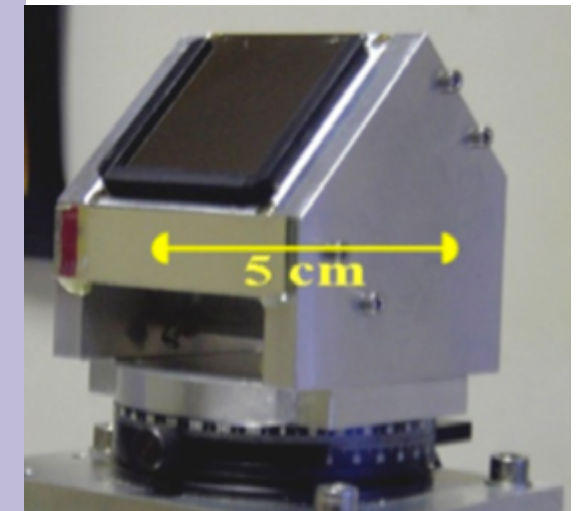


Fig. 6 - Detail of the image detector of the compass prototype. For this prototype a conventional goniometer has been used rather than a digital one.

key element of this prototype.

To verify the accuracy of the azimuth values obtained from the compass, it should be necessary to know the true azimuth to be compared. Although it is almost impossible to get this information, a theoretical azimuth value can be obtained starting from the geographical coordinates of both the compass and the observed object as extracted from satellite maps, and by elaborating them according with an ellipsoidal Earth model.

The results are reported in Table 1, where the experimental azimuth values (with respect to the South direction, positive clockwise) are compared with the corresponding theoretical ones (Azimut-T) obtained from satellite maps of two different web sites: Google Earth (GE)



Objective	Distance from compass	Experimental Azimuth (degrees)	Azimet-T GE (degrees)	Azimet-T FA (degrees)	$\Delta$ GE minutes of arc	$\Delta$ FA minutes of arc
1 Antenna Telecom Roma Laure.	15.1 Km	+80.691°	+80.658°	+80.662°	+2.0'	+1.7'
2 Cupola chiesa Ss. Pietro&Paolo	17.4 Km	+93.978°	+93.945°	+93.932°	+2.0'	+2.8'
3 Castello Orsini	23.7 Km	-171.482°	-171.489°	-171.464°	+0.4'	-1.1'
4 Silos	20.8 Km	-169.555°	-169.573°	-169.567°	+1.1'	+0.7'
5 Campanile M.C	5.7 Km	-75.021°	-75.057°	-75.018°	+2.2'	-0.2'

Table 1 - Comparison between experimental and theoretical values of the observation direction of different objects in Rome area seen from the Frascati ENEA Research Center. The values are taken positive moving clockwise with respect to the South direction.

and Faureargani (FA), available at:

<http://www.google.it/earth/index.html> and <http://www.faureragani.it/mygps/getlatlonita.html>, respectively.

The table shows that, despite the use of not optimized components, which implies an estimated accuracy around 0.1°, the experimental errors are smaller than 3' (0.05°), that is just three times higher than the best achievable accuracy allowed by the algorithm, and are also better than those claimed by any compass currently on the market. On the other hand, as evident in the table, errors at the level of 1'-2' can also be present on the azimuth theoretical values, depending on which source is used for the determination of the objectives geographical coordinates.

This kind of high-accuracy compass can be fruitfully applied in many fields such as:

- Topography
- Archaeological sites surveying
- Radar installations (for airports)
- Concentrating solar power installations
- Remote shuttle control
- Magnetic compass calibration in navy
- Calibration of any other compass type (this sun compass can be used as a primary standard)
- Buildings orientation accurate measurements

A new prototype is currently in progress to approach the best theoretical accuracy of

this compass design, and also to demonstrate that the compass can be easily integrated in conventional topographic instruments like theodolites or total stations.

#### 4.3 TERAHERTZ SOURCES AND APPLICATIONS IN THE BIOLOGICAL FIELD

ENEA has a long term expertise in the construction of powerful short-pulse mm-wave and THz free electron laser (FEL) sources. Various electron-wave interaction schemes were successfully tested in the past, ranging from Cerenkov to Smith-Purcell radiators and to undulator devices. Two THz FEL sources are currently available, covering altogether the spectral range from 90 GHz to 0.7 THz. Recently, a novel Electro-Magnetic pulser, capable of providing both nanosecond THz electromagnetic (EM) radiation pulses as well as electrostatic (ES) pulses with identical time duration in one device, has been designed and is currently under development. Many experiments and epidemiological studies have been performed to understand the effects of the electromagnetic field (EMF) on biological systems, mainly human and animal cells or organisms. However, apart from thermal heating effects on cells and tissues, a missing gap was the mechanism of transformation of EMF energy into a biological effect. It is well known that short electrostatic pulses can modify the cell membrane permeability. The goal of our research is to demonstrate that

a similar effect can be achieved by means of an electromagnetic field carried by a wave instead of a static electric field. Using an EM wave instead of a pulsed ES field would greatly expand the applications in the biomedical field.

For this reason, in 2012 the SOR laboratory joined the "International Bioelectrics Consortium", coordinated by the Frank Reidy Center for Bioelectrics at Norfolk (VA), USA. The proposed work-program involves the investigation of the lipid layer dynamics under the simultaneous action of electric and electromagnetic fields. We expect to reveal a non-linear behaviour of the interaction process, that could lead to a rectification effect, due to the fact that the polarization vector cannot react to the fast oscillations of the electric field. A first evidence of this was shown a few years ago in the framework of the EU project THz-BRIDGE, coordinated by ENEA, by performing a series of measurements on artificial membranes with the ENEA Compact-FEL at 130 GHz. Permeability changes in cationic liposomes (a good model of the cell membrane) were observed irradiating the samples with sufficiently high peak power, which yields peak electric field values greater than 2 kV/cm at the sample surface. Further experiments of this kind are planned to be carried out using different radiation sources already available or under development at the ENEA.

#### Terahertz Free Electron Lasers

At the ENEA-Frascati Research Center two FEL sources operating in the THz spectral region are currently available. The first device is based on a 2 to 5 MeV Microtron accelerator powered by a 2.5 MW magnetron. The set-up shows a straight line electron transport channel leading to a vacuum chamber designed to host different interacting structures, like metal gratings (Smith-Purcell FEL), dielectric loaded wave-guides (Cerenkov FEL) and short-period undulators. When operating with an 8-period

permanent magnet undulator ( $\lambda u=2.5$  cm) the emission frequency ranges from 90 to 150 GHz, with a peak power of about 1.5 kW on 4  $\mu$ s pulses. A second device makes use of a 2.5 MeV RF Linac as electron source, in a special configuration which optimizes the energy extraction from the electron beam in a single pass, exploiting the mechanism of coherent spontaneous emission, avoiding the necessity of an optical cavity. This source emits high power ( $\sim 1$  kW) radiation in the range 0.4-0.7 THz. The first device was already utilized to perform measurements on liposomes at 130 GHz with encouraging results. We are currently putting back into operation the second device to perform similar measurements. In 2012 measurements for biological applications have been carried out utilizing the 150 GHz device, in the coherent spontaneous emission configuration (wide band), in collaboration with CNRS-IGR, University Paris-Sud and with CNR-IFT, Rome.

#### Electromagnetic pulser for biological applications

An ideal source for a direct comparison of EM and ES pulses on biological system is the novel Electro-Magnetic pulser that has recently been designed at ENEA (Fig. 7). This device is based on a short pulse electron gun, capable of providing both nanosecond THz electromagnetic (EM) radiation pulses as well as electrostatic (ES) pulses in the same device,

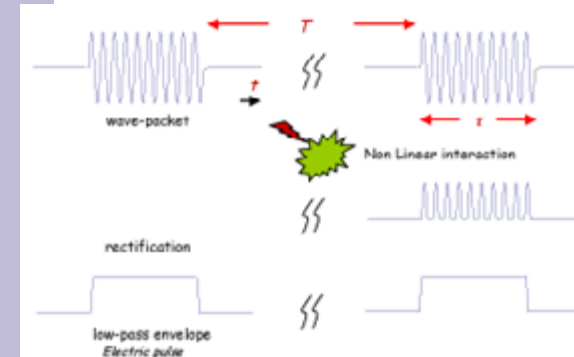


Fig. 7- Schematic diagram of the Electromagnetic Pulser.

with identical time duration. The pulser is designed to produce peak electric fields in the samples that are significantly higher than any reported to date, while keeping the average power low enough to avoid sample heating.

The pulser was described in detail in the 2011 Annual Report. The device is driven by a 20 kV power supply charging a capacitor bank that acts as the primary energy reservoir. In order to reduce the pulse length from 1  $\mu$ s down to about 30 ns, simultaneously rising the voltage up to 350 kV, a six-stage magnetic pulse compressor is used. The final condenser of the compressor is then connected to a transmission-line transformer made by coaxial cables charged in parallel and discharged in series on a mismatched diode load, resulting in adding the voltages on each cable. Utilizing this method it is possible to raise the voltage up to about 1 MV.

Due to the high peak current (about 5 kA) this device is the ideal electron source for a compact high power FEL. The electron beam generated by the cathode is transported into a beam-wave interaction region by means of a solenoidal magnetic field, used to minimize the space charge effects.

Both a magnetic undulator and a Cyclotron Auto-Resonance Maser (CARM) structure have been considered for this device. The undulator is identical to the one presently in use in the 2.5 MeV Microtron based Compact-FEL. At a gap value of 8 mm a field of about 3.5 kG is obtained on-axis with a parameter  $K = 0.8$ . Preliminary simulations have shown that the described source is capable of reaching saturation at megawatt level at a central frequency of 200 GHz. Details of the CARM design and a schematic layout are reported at paragraph 3.3.

#### 4.4 ACCELERATORS DEVELOPMENT

The field of particle accelerators involves a variety of multidisciplinary technologies and is cross-sectional to many activities. Accelerator R&D deals with physical technologies based on ionising particles and X-rays, which are employed in special applications ranging from materials science to medicine. Electron accelerators are also used as a powerful driver of non-ionising radiation source, such as Free Electrons Laser (FEL).

In the following, we briefly describe the main results of the activities carried out in the field of protons and electrons accelerators at the ENEA Frascati Research Centre for different applications: industrial and medical applications and generations of FEL radiation.

##### Electron accelerators at ENEA-Frascati

The Radiation Sources Laboratory currently operates three electrons accelerators:

- 5.3 MeV Linac for irradiation with electrons and X-rays from "Bremsstrahlung";
- 5 MeV Microtron used as a driver for the Compact-FEL
- 3 MeV Linac used as a driver for the THz radiation source FEL-CATS

During 2012 the radio-frequency structure of the 5 MeV Linac has been modified installing a new modulator and magnetron. In the framework of the development of dosimeters, several tests on ionization chambers of the National Institute of Health were performed.

In the framework of the partnership with ADAM-Geneva, a spin-off company of CERN, dedicated to the development of compact high-frequency linear accelerators (C Band -5712 MHz) for medical applications, ENEA trained the company staff and assisted commissioning tests on a jointly developed Linac dedicated to X-rays production. The experimental tests were done in a bunker at CERN in Geneva, while the activity of training and data analysis was carried out in part in Geneva and in part

at ENEA-Frascati.

The 5 MeV Microtron operating in S-band (3 GHz) continued to be used as a driver for the Compact-FEL for the generation of electromagnetic radiation in the millimetre-wave region (90 - 150 GHz). A stable performance was obtained with 0.3 A, 4  $\mu$ s pulses at a repetition frequency of 10 Hz.

The 3 MeV Linac, equipped with a particular device for the manipulation of the e-beam, used as pilot for the generation of electromagnetic radiation in the sub-millimeter (0.4 - 0.8 THz) by means of a magnetic undulator (FEL-CAT), is currently being refurbished to host a novel THz imaging setup.

##### Proton accelerator facility (ISPAN and TOP-IMPLART Projects)

**The ISPAN Project.** In 2012 the ISPAN program was brought to completion. It was conducted by ENEA in collaboration with the national industry (NRT and CECOM) and the National Institute of Health (ISS) and concerned the construction of a radiobiology facility with two beam outputs: a 17.5 MeV horizontal beam for small animals irradiation, and a variable energy (up to 7 MeV) vertical beam for cells irradiation.

The facility is based on the use of the commercial accelerator PL7 manufactured by Accsys-HITACHI, currently installed at

ENEA-Frascati and composed by a source of protons of duoplasmatron type followed by two linear accelerators operating at 425 MHz, a RFQ up to 3 MeV energy and a DTL up to an energy of 7 MeV. In 2012 the horizontal and vertical transport lines were mounted, aligned and tested with the beam (see Fig. 8): the horizontal line consists of four magnetic quadrupoles and the vertical line includes a dipole magnet, whose pole pieces and vacuum chamber were designed at ENEA, placed between the first and the second doublet of quadrupoles.

The proton beam produced by the injector has been used in several irradiation experiments and in particular:

- dosimeters of CR39 type supplied by ISS were irradiated in order to perform a dosimetric characterization for the use of the beam on cellular samples;
- detectors based on LiF films deposited on glass, provided by the Photonics Micro- and Nano-structures Laboratory (UTAPRAD-MNF), were irradiated to explore the possibility of using such detectors for the transverse characterization of the beam and in the future for proton dosimetry. The fluorescence images of the samples were subsequently acquired with a confocal optical microscope at the UTAPRAD-MNF Laboratory, to check the linearity of this type of detector in a wide range of total delivered charge, given by a number

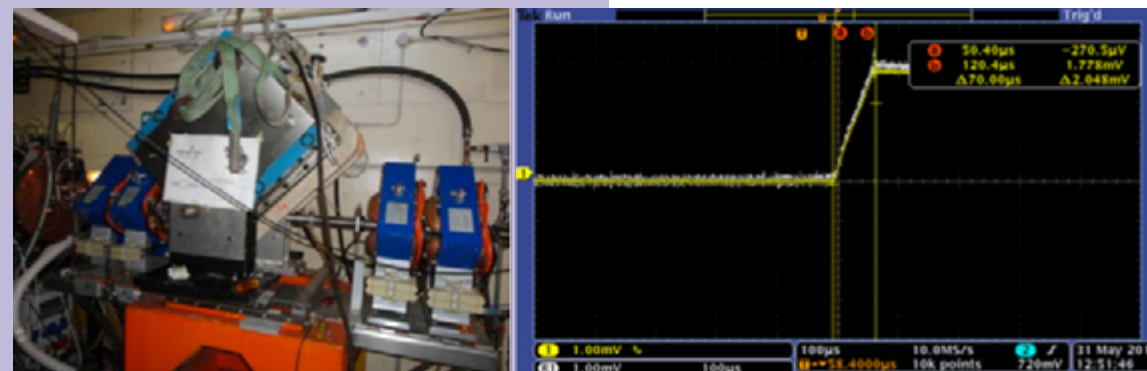


Fig. 8 - (Left) Horizontal and vertical transport lines at the exit of PL7 injector; (Right) Signal proportional to the proton beam charge: white trace (horizontal beam), yellow trace (vertical beam).

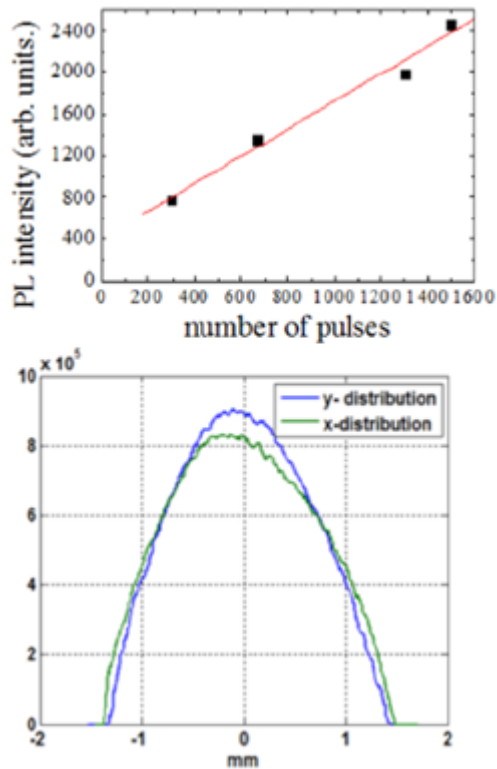


Fig. 9 - (Top) Average luminescence signal vs number of pulses; (Bottom) Horizontal and vertical distribution of the beam spot on LiF film irradiated by 1300 pulses:  $\sigma_x=0.66$  mm  $\sigma_y=0.614$  mm

of pulses between 300 and 1500 with 6 pC/pulse (Fig. 9).

Other activities concerned the development of the first module of the accelerator that will be injected by the PL7 7 MeV proton beam: a 2997.92 MHz 7-11.6 MeV SCDTL structure provided with a permanent magnet focusing

quadrupole system. The structure has been manufactured by CECOM and NRT on ENEA design and tuned on a RF bench (Fig. 10). An innovative measuring system particularly suitable for the measurement of the multipolar content of the field produced by high-gradient (~200 T/m) small-aperture permanent quadrupoles has been set up for a fast and precise characterization of 11 demountable permanent magnet quadrupoles (PMQs) realized by BJA-Magnetics on ENEA design. They will be used for focusing the beam of

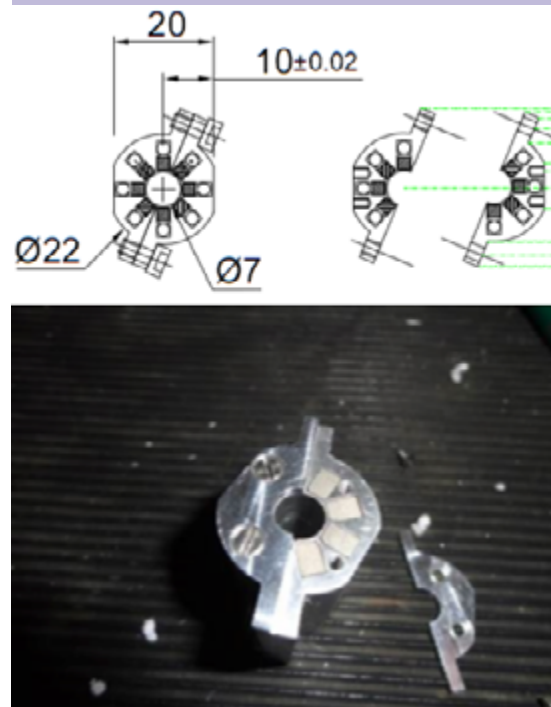


Fig. 11 - Demountable PMQ for SCDTL-1 module: (Top) design (Bottom) PMQ manufactured by BJA.

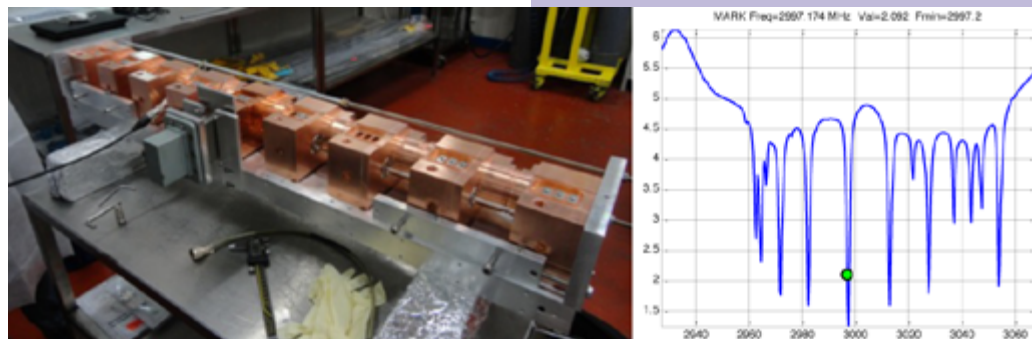


Fig. 10 - (Left) SCDTL-1 module (Right) Measured (in reflection) resonant modes from the central tank.

protons within the SCDTL module (Fig. 11). The measurement system is shown in Fig. 12: the PMQ is placed on a lathe where it is put in rotation and a 9-turns, 40-mm long and 1.4-mm wide coil is placed on a XY translational stage. The measurement procedure is as follows: the PMQ is rotated and the induced voltage on the coil is measured and recorded. The data are analyzed by FFT to obtain the harmonic field component amplitude. The interval between two trigger spikes marks the beginning and the end of a PMQ revolution: this interval corresponds to two complete oscillations (typical of a quadrupole behaviour), while on the quadrupole axis it corresponds to one complete oscillation due to the residual dipole. This setup allows the evaluation of the center of rotation with micrometer precision.

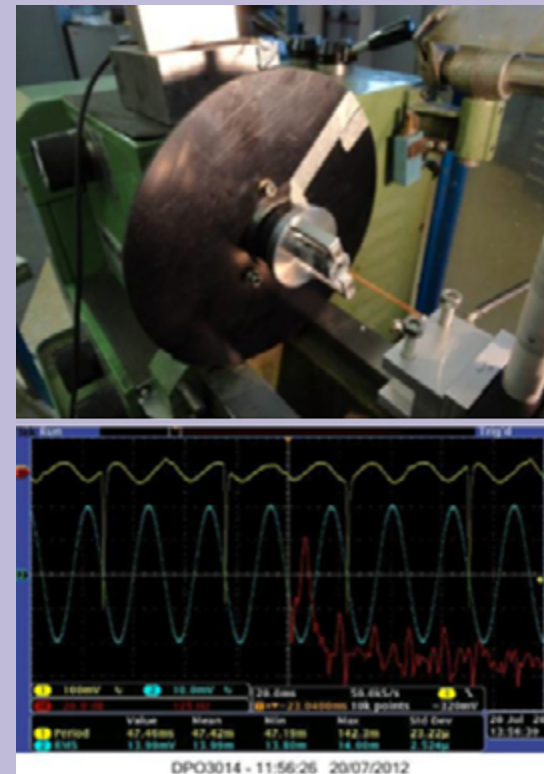


Fig. 12- (Top) PMQ Measurement setup, (Bottom) Measurement at R=1mm on quadrupole #8 (oscilloscope screen: the cyan trace is the voltage on the coil, the yellow one is the trigger signal and the red one is the FFT).

**The TOP-IMPLART Project.** At the end of November 2012 the Regional Government of Lazio released the first part of the financing for the TOP-IMPLART Project (2.5 M€ over the total allocated funding of 11 M€ expected in three years). The TOP-IMPLART Project, a collaboration between ENEA, the Institute of Health and the Regina Elena National Cancer Institute-IFO, Rome, is aimed at realizing an innovative system for proton therapy, called IMPLART (Intensity Modulated Proton Linear Accelerator), based on a proton accelerator of 230 MeV of maximum energy to be installed at IFO in Rome.

The regional funding, which will be also used to promote national technological companies, will allow to implement and test the accelerator section up to 150 MeV at the ENEA Research Center in Frascati before the transfer to its clinical user IFO. The infrastructure and clinical facilities will be provided by IFO. The program foresees a first milestone (operation at 30 MeV) after the first two years of the project upon the release of a second part of the financing of 2 M€ foreseen for the end of 2013.

#### 4.5 “OLOCONTROLLO EMULATIVO” TECHNOLOGY

During 2012 GIASONE, the cybernetic model of synthetic intelligence, was analyzed in its aspects concerning the mental processes, that from an imaginative step lead to ambulation, and that are sustained through the interaction of proprio-ceptive and proprio-emissive mechanisms of the Biological Organic System.

In particular, we have taken into consideration the reconstruction of the ambulative sequences, how the sequence of interior postures is created from these sequences, and how the execution of the trajectories of motion in the environment is allowed.

Extensive research has been carried out on the so called “places of the mind” and their holonomic representation.

Among the activities on the Vision System

VISIO, the group was invited to participate in a workshop organized on the occasion of exhibition "Gunther Von Hagen 's Body Worlds", with a great media feedback. The Central Unit on Relations and Promotion of ENEA Projects is taking care of promotional material for this application.

Within the "ADAPTIVE PROSTHESIS"

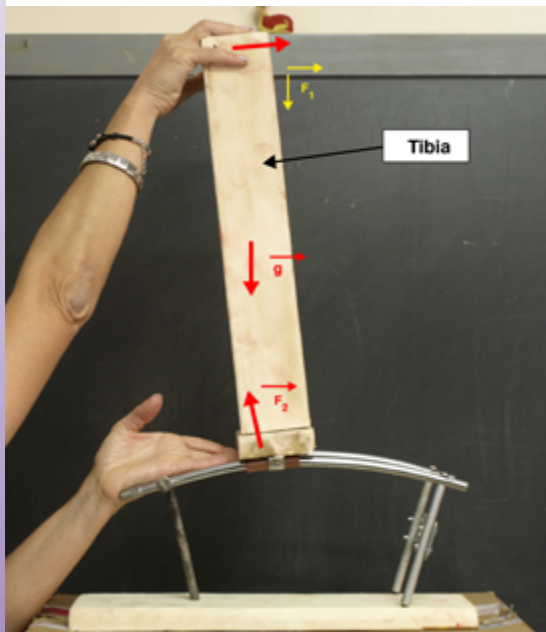


Fig. 13 - Movement femur-tibia.



Fig. 14 - Roto-translation of the knee.

Project, which aims to re-establish the connection between intentionality and proprioception of movement during all phases of walk, restoring the proprioceptive feedbacks consistent with previous memories of the amputee, and numerous laboratory prototypes for experiments on the kinematics of the step were performed, to deepen the mutual movement femur-tibia, (see Fig. 13), the roto-translational of the knee, (see Fig. 14), the rotation and flexion of the foot, (see Fig. 15), the "desmodromic" action of the ankle, (see Fig. 16).

A further laboratory model was designed to house the mechanical actuators. The model

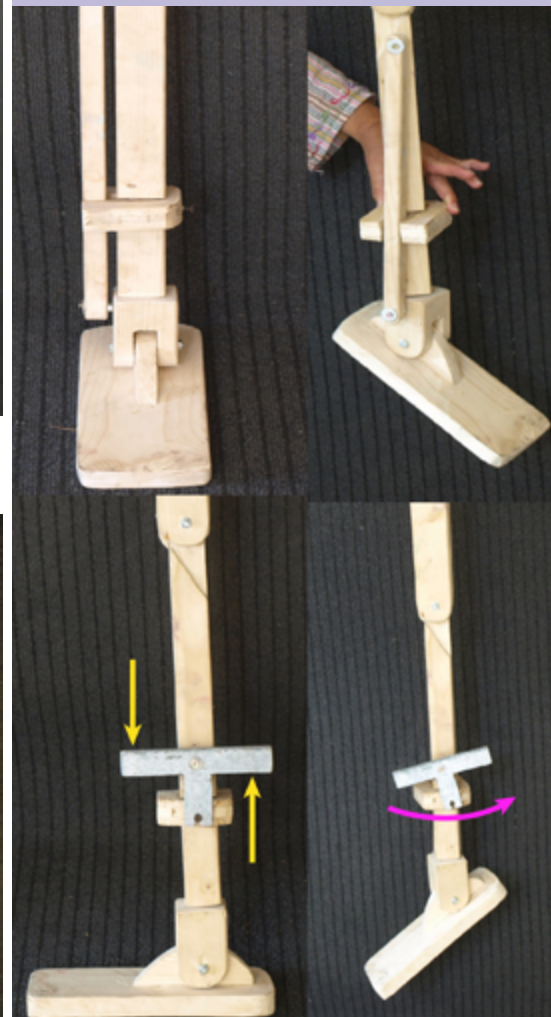


Fig. 15 - Rotation and flexion of the foot.

was made using the pneumatic pistons controlled by solenoid valves (Fig. 17).

In addition, the activities of the project FLEX-PROD, carried out in collaboration with the CALEF Consortium, were initiated.

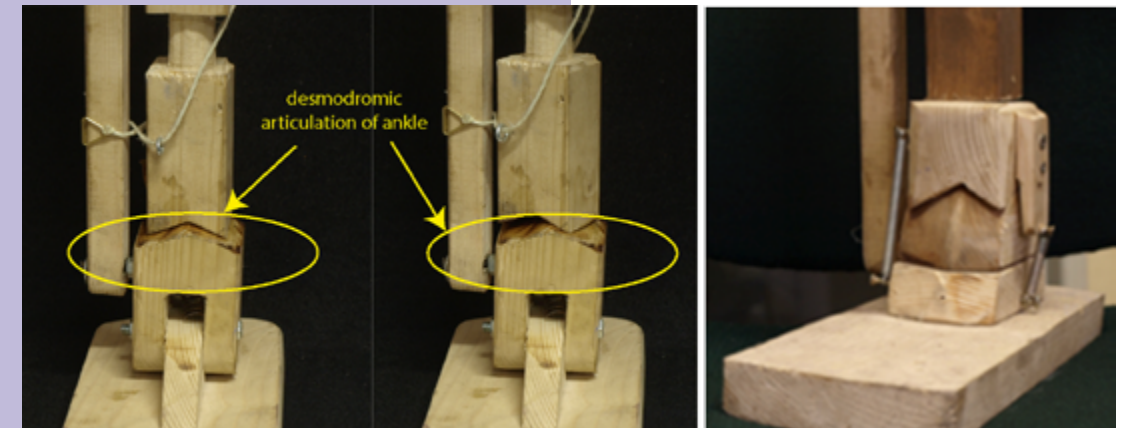


Fig. 16 - "Desmodromic" action of the ankle.

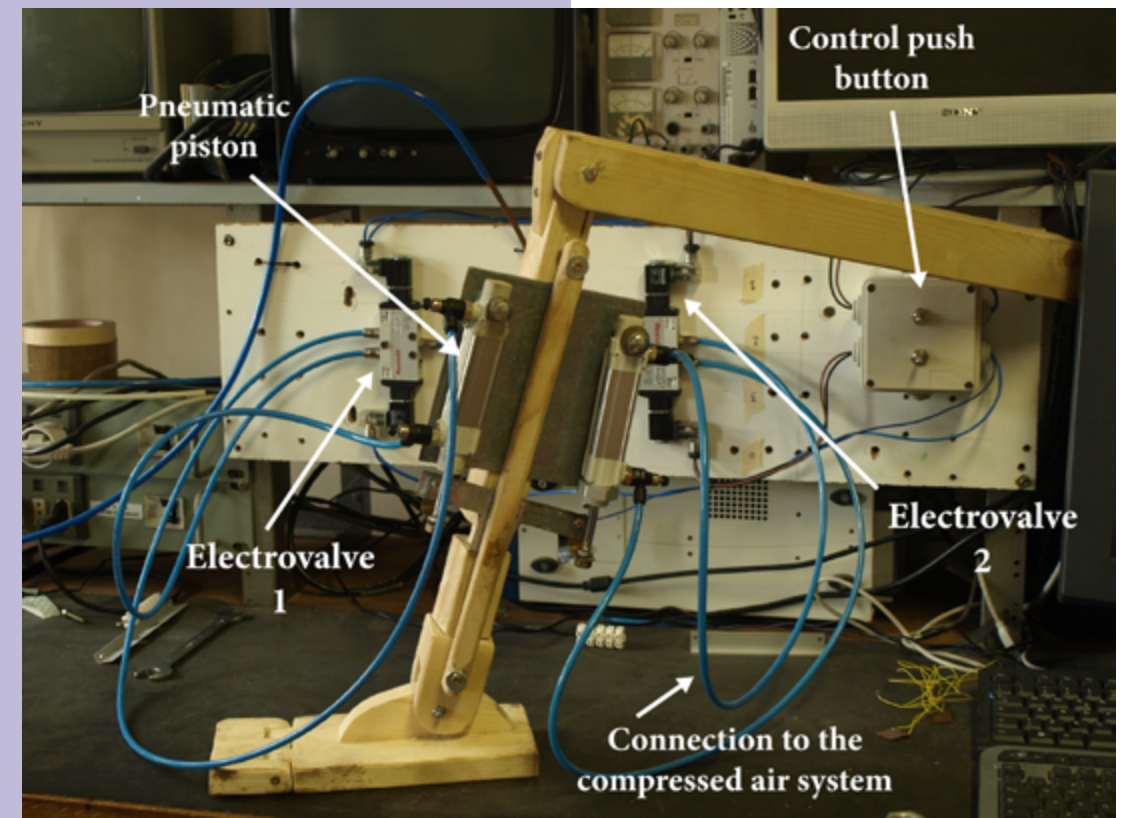


Fig. 17 - Mechanical actuators controlled by solenoid valves .

#### 4.6 CONTRIBUTIONS TO OTHER PROJECTS

##### SPARC-LAB

In 2012 the SOR Laboratory continued the long-term collaboration with the SPARC accelerator group at Frascati National Laboratories of INFN.

In the framework of the activities of SPARC-LAB, ENEA participated to the optimization of machine parameters, experimental test and measurements analysis related to the generation of 800 nm radiation using a FEL driven by a double pulse of high brightness electron beams in different configurations. In particular two limit conditions were explored: temporally superimposed pulses and separated in energy (around 1 MeV), and temporally separated pulses (a few picoseconds) at the same energy. In the first case self-amplified radiation (SASE) at two distinct wavelengths was produced and characterized.

##### Gamma Source - ELI-NP Project

A cooperation agreement between ENEA and Sapienza University of Rome was signed for research and development of "Sources of Radiation". The agreement was defined in the framework of a more general agreement between the two institutions that governs the relationship of cooperation on matters of common interest aimed at training, development and exploitation of research. The specific collaboration agreement concerns the development of an innovative source for advanced applications in the field of photonics within the European project "Gamma source for ELI-NP (Extreme Light Infrastructure-Nuclear Photonics)" coordinated by the University "La Sapienza" and INFN.

The project is aimed at creating an innovative source of gamma rays based on Compton back-scattering of an intense laser and a high brightness electron beam produced by a 720 MeV linac to be installed in Romania.

In this context, the SOR Laboratory coordinated the activities of a study group on the optimization of the photoinjector and contributed to the preparation of a Technical Design Report, required for the participation to an international tender for the allocation of European funds in 2013.

##### FORLAB Project

In 2012 the Radiation Sources Laboratory has contributed to the design of the LIF sensor components related to the scene illumination, that is the choice of the laser source, the design of the laser beam delivery optics, the selection of the collecting optics features and the scanning parameters.

The chosen laser source is a very compact KrF excimer laser (system dimensions: 57x2x25 cm<sup>3</sup>, weight: 15 kg) emitting 248-nm-wavelength pulses with 16 mJ energy at a maximum repetition rate of 500 Hz.

The 248-nm ultraviolet radiation can efficiently excite most substances of interest and the high repetition rate allows a fast scanning of the surveyed area. Moreover, the rectangular beam shape (output beam dimensions: 6x3 mm<sup>2</sup>) well fits with a flat surface covering. Therefore, this laser system satisfies all the requirements expected by the project: portability, efficient excitation, fast scanning capability.

Also, the laser coupling with both the beam delivery optics and the signal collecting CCD camera has been analysed: an optical arrangement has been proposed where a wide-angle-lens CCD camera observes and records the overall scene, while the laser beam, properly enlarged by a telescope and directed by a two-axes rotating mirror, performs a scan on the same field of view, allowing the illumination of the full area in few minutes.

The selected laser beam shape permits an efficient excitation of the scene at least up to 20 m distance from the LIF sensor, giving rise to fully detectable potential fluorescence signals.

Since the whole system stands at given height

and distance from the area of interest, the analysis took into account the image deformation on the CCD camera due to perspective and the distortion of the beam dimensions when projected on the ground at different distances from the source (Figs. 18 - 19).

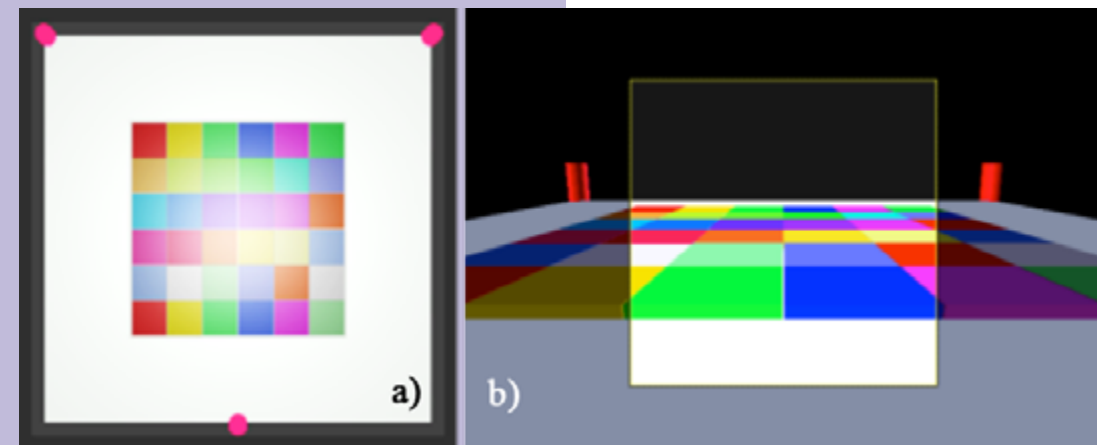


Fig. 18 - Example of a possible scene (12x12 m<sup>2</sup> at a distance of 5 m) as seen a) from the top, b) from position A by the wide-angle-lens CCD camera placed at an height of 2 m.

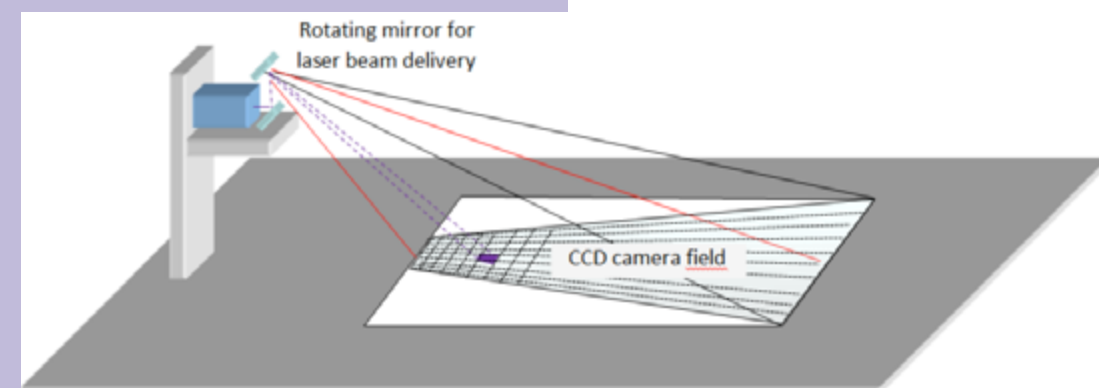


Fig. 19 - Schematic of the laser beam scanning on the field of interest.

## 5 LIST OF PERSONNEL

### Technical Unit for the Development of Applications of Radiations (UTAPRAD)

Director Roberta Fantoni (roberta.fantoni@enea.it)

#### Direction staff members

Fabio Avello, Emilia Batisti, Elisabetta Borsella, Andrea Capriccioli, Paola Chiappini, Giorgio Fornetti, Anna Pagliardini, Luigi Picardi, Iliaria Sergi, Giulio Tuccinardi.

### UTAPRAD-DIM (Diagnostics and Metrology Laboratory)

Director Antonio Palucci (antonio.palucci@enea.it)

#### DIM staff members

Lorella Addari, Salvatore Almaviva, Federico Angelini, Paolo Aristipini, Florinda Artuso, Rodolfo Borelli, Luisa Caneve, Roberto Carletti, Dario Cataldi, Roberto Chirico, Massimiliano Ciaffi, Francesco Colao, Luigi De Dominicis, Antonella De Ninno, Giovanni Di Poppa, Mario Ferri De Collibus, Luca Fiorani, Massimo Francucci, Gianfranco Giubileo, Massimiliano Guarneri, Antonia Lai, Violeta Lazic, Giovanni Leggeri, Giacomo Lorenzoni, Salvatore Marullo, Ivano Menicucci, Marcello Nuvoli, Marco Pistilli, Roberto Ricci, Valeria Spizzichino, Laura Teodori.

#### DIM research fellows

Adriana Puiu

### UTAPRAD-MAT (Mathematical Modelling Laboratory)

Director Giuseppe Dattoli (giuseppe.dattoli@enea.it)

#### MAT staff members

Franco Ciocci, Emanuele Di Palma, Luca Gianessi, Marcello Quattromini, Alberto Petralia, Elio Sabia, Ivan Panov Spassovsky, Amalia Torre.

#### MAT Co.Co.Co

Mario del Franco, Vincenzo Surrenti

### UTAPRAD-MNF (Photonics Micro and Nano-structures Laboratory)

Director Rosa Maria Montereali (rosa.montereali@enea.it)

#### MNF staff members

Francesca Bonfigli, Sabina Botti, Luciano Cantarini, Michele Arturo Caponero, Rosaria D'Amato, Roberto D'Imperio, Stefano Libera, Guido Martini, Valerio Orsetti, Salvatore Paolini, Alessandro Peloso, Andrea Polimadei, Flaminia Rondino, Antonino Santoni, Gaetano Terranova, Maria Aurora Vincenti,

Alessandro Zini.

### UTAPRAD-SOR (Radiation Sources Laboratory)

Director Gian Piero Gallerano (gianpiero.gallerano@enea.it)

#### SOR staff members

Alessandro Ampollini, Rosanna Balveti, Maria Laura Bargellini, Marco Battaglia, Sarah Bollanti, Ezio Campana, Mariano Carpanese, Gemma Casadei, Domenico De Meis, Paolo Di Lazzaro, Andrea Doria, Antonio Fastelli, Alessandra Filippini, Francesco Flora, Emilio Franconi, Emilio Giovenale, Giovanni Messina, Luca Mezi, Daniele Murra, Gian Luca Orlandi, Loredana Puccia, Concetta Rosinvalle, Davide Vicca, Giuseppe Vitiello, Consuelo Zampetti.

### UTAPRAD-STG (Administration and Management Service)

Director Tiziana Giuli (tiziana.giuli@enea.it)

#### STG staff members

Maria Luisa Mori, Tiziana Pigiani, Tiziana Vari.

## 6 RESEARCH PRODUCTS

### 6.1 PATENTS

1. Patent ENEA n. 768, deposito nazionale N. RM2012A000660, "Sistema per la Rilevazione di Esplosivi", inventori Roberto Chirico, Antonio Palucci, Francesco Colao, Luca Fiorani, Salvatore Almaviva, Marcello Nuvoli, Daniele Murra, depositato presso U.I.B.M. di Roma il 21/12/2012.
2. Patent ENEA n. 752, deposito nazionale N. RM2012A000183, "Dispositivo Semplice ad Elevata Efficienza per la Rivelazione di Radiazione Ionizzante basato su Film Sottile di Fluoruro di Litio Luminescente, e relativi Metodi di Preparazione e Lettura del Dispositivo", inventori Rosa Maria Montereali, Francesca Bonfigli, Enrico Nichelatti, Maria Aurora Vincenti, depositato presso U.I.B.M. di Roma il 27/04/2012.
3. F. Flora, S. Bollanti, D. De Meis, P. Di Lazzaro, A. Fastelli, G.P. Gallerano, L. Mezi, D. Murra, A. Torre, D. Vicca: "Bussola solare elettronica ad alta precisione" (Ufficio Italiano Brevetti e Marchi, RM2012A000664, depositato il 27 Dicembre 2012).

### 6.2 PEER REVIEW PAPERS

1. Martin A. Montes-Hugo, Luca Fiorani, Salvatore Marullo, Suzanne Roy, Jean-Pierre Gagné, Rodolfo Borelli, Serge Demers and Antonio Palucci: A Comparison between Local and Global Spaceborne Chlorophyll Indices in the St. Lawrence Estuary, *Remote Sens.* 2012, 4, 3666-3688; doi:10.3390/rs4123666
2. V. Lazic, S. Jovicevic, M. Carpanese, Laser induced bubbles inside liquids: Transient optical properties and effects on a beam propagation, *Appl. Phys. Lett.* 101, (2012) 054101. IF 3.844
3. L.M. Cabalín, A. González, V. Lazic, J.J. Laserna, Laser induced breakdown spectroscopy of metals covered by water droplets, *Spectrochim. Acta Part B*, 74–75 (2012) 95–102. IF 2.876
4. S. Guirado, F.J. Fortes, V. Lazic, J.J. Laserna, Chemical analysis of archaeological materials in submarine environments using LIBS. On-site trials in the Mediterranean Sea, *Spectrochim. Acta Part B* 74–75, (2012) 137–143. IF 2.876
5. Colao F., Fantoni R., Caneve L., Fiorani L., Dell'Erba R., Fassina V. Diagnostica superficiale non invasiva mediante fluorescenza indotta da laser (LIF) sulle pitture murali di Giusto De' Menabuoi nel Battistero di Padova (in Italian) Fassina V. (ed.), *Da Guariento a Giusto De' Menabuoi. Studi, ricerche e restauri*, Antiga Edizioni, Crocetta del Montello, Italy (2012) pp. 101-116
6. M. Guarneri, M. Ferri De Collibus, G. Fornetti, M. Francucci, M. Nuvoli, R. Ricci "Remote colorimetric and structural diagnosis by RGB-ITR color laser scanner prototype" *Advances in Optical Technologies*, Vol. 2012, Article ID 512902, doi: 10.1155/2012/512902 (2012), 1 – 6.
7. M. Crippa, P.F. DeCarlo, J.G. Slowik, C. Mohr, M.F. Heringa, R. Chirico, L. Poulain, F. Freutel, J. Sciare, J. Cozic, C.F. Di Marco, M. Elsassner, N. José, N. Marchand, E. Abidi, A. Wiedensohler, F. Drewnick, J. Schneider, S. Borrmann, E. Nemitz, R. Zimmermann, J.L. Jaffrezo, A.S.H. Prévôt, U. Baltensperger, Wintertime aerosol chemical composition and source apportionment of the organic fraction in the metropolitan area of Paris, *Atmos. Chem. Phys. Discuss.*, 12, 8, 22535-22586, 2012. I.F.=5.520
8. C. Chou, O. Stetzer, T. Tritscher, R. Chirico, M.F. Heringa, Z.A. Kanji, E. Weingartner, A.S.H. Prévôt, U. Baltensperger, U. Lohmann, Effect of photochemical aging on the ice nucleation properties of

- diesel and wood burning particles, *Atmos. Chem. Phys. Discuss.*, 12, 6, 14697-14726, 2012. I.F.=5.520
9. M.F. Heringa, P.F. DeCarlo, R. Chirico, A. Lauber, A. Doberer, J. Good, T. Nussbaumer, A. Keller, H. Burtscher, A. Richard, B. Miljevic, A.S.H. Prevot, U. Baltensperger, Time-resolved characterization of primary emissions from residential wood combustion appliances, *Environmental Science & Technology*, 46, 20, 11418-11425, 2012. I.F.=5.228
10. M.F. Heringa, P.F. DeCarlo, R. Chirico, T. Tritscher, M. Clairotte, C. Mohr, M. Crippa, J.G. Slowik, L. Pfaffenberger, J. Dommen, E. Weingartner, A.S.H. Prévôt, U. Baltensperger, A new method to discriminate secondary organic aerosols from different sources using high resolution aerosol mass spectra, *Atmos. Chem. Phys.*, 12, 4, 2189-2203, 2012. I.F.=5.520
11. C. Mohr, P.F. DeCarlo, M.F. Heringa, R. Chirico, J.G. Slowik, R. Richter, C. Reche, A. Alastuey, X. Querol, R. Seco, J. Peñuelas, J.L. Jiménez, M. Crippa, R. Zimmermann, U. Baltensperger, A.S.H. Prévôt, Identification and quantification of organic aerosol from cooking and other sources in Barcelona using aerosol mass spectrometer data, *Atmos. Chem. Phys.*, 12, 4, 1649-1665, 2012. I.F.=5.520
12. G. Giubileo, F. Colao, and A. Puiu, "Identification of standard explosive traces by infrared laser spectroscopy: PCA on LPAS data", *Laser Physics* (2012) 22, 1033-1037
13. A.Puiu, G.Giubileo, S.Nunziante Cesaro, "Vibrational spectrum of HMX at CO2 laser wavelengths: a combined DRIFT and LPAS study", *International Journal of Spectroscopy*, Volume 2012, Article ID 953019, 4 pages, doi:10.1155/2012/953019
14. Giuseppe Dattoli, Emanuele Di Palma, Alberto Petralia, and Julietta V. Rau, "SASE FEL Storage Ring", *IEEE Journal of Quantum Electronics*, vol. 48(10), October (2012), pp.1259-1264. (IF=1.879)
15. M. Quattromini, M. Artioli, E. Di Palma, A. Petralia, and L. Giannessi, "Focusing properties of linear undulators", *Phys. Rev. ST Accel. Beams* vol. 15(8), 080704 (2012).
16. D. Babusci, G. Dattoli, E. Di Palma and E. Sabia, "Complex-Type Numbers and Generalizations of the Euler Identity", *Adv. Appl. Clifford Algebras*, vol.22(2) (2012), pag. 271–281. (IF 0.496)
17. G. Marcus, M. Artioli, A. Bacci, M. Bellaveglia, E. Chiadroni, A. Cianchi, F. Ciocci, M. Del Franco, G. Di Pirro, M. Ferrario, D. Filippetto, G. Gatti, L. Giannessi, M. Labat, A. Mostacci, A. Petralia, V. Petrillo, M. Quattromini, J. V. Rau, A. R. Rossi, and J. B. Rosenzweig, *Appl. Phys. Lett.* 101, 134102 (2012) IF=3.844
18. L. Giannessi, M. Artioli, M. Bellaveglia, F. Briquez, E. Chiadroni, A. Cianchi, M. E. Couprie, G. Dattoli, E. Di Palma, G. Di Pirro, M. Ferrario, D. Filippetto, F. Frassetto, G. Gatti, M. Labat, G. Marcus, A. Mostacci, A. Petralia, V. Petrillo, L. Poletto, M. Quattromini, J.V.Rau, J. Rosenzweig, E. Sabia, M. Serluca, I. Spassovsky, and V. Surrenti, "High Order Harmonics Generation and Super-radiance in a Seeded Free-Electron Laser", *Phys. Rev. Lett.*, vol. 108(16), 164801 (2012) (IF 7.37)
19. G. Dattoli, K. Gorska, K. Penson, D. Babusci, G.H.E. Duchamp, *Phys. Rev. E* 85 E, 031138-031141 (2012) (IF 2.255)
20. G. Dattoli, M. Delfranco, M. Labat, P. L. Ottaviani and S. Pagnutti, "Introduction to the physics of Free Electron Laser and Comparison with conventional Laser Sources", Book edited by Sandor Varro, ISBN 978-953-51-0279-3- Published March 14, 2012 (INTECH) (Total of down loads 1578)
21. G. Dattoli, L. Giannessi, P. L. Ottaviani and S. Pagnutti, "Energy phase correlation and pulse dynamics in short bunch high gain Free Electron Lasers, *Optics Communications*", Volume 285, Issue 5, p. 710-714 (IF 1.356)
22. G. Dattoli, V. Petrillo and G. V. Rau, "FEL SASE and Wave Undulators", *Optics Communications*, 285, 5341-5346 (2012) (IF 1.356)
23. G. Dattoli, P. L. Ottaviani, S. Pagnutti and V. Asgekar, "Free Electron Laser oscillators with tapered undulators: Inclusion of harmonic generation and Pulse Propagation", *Phys. Rev. ST*, 15, 030708 (2012) (IF 1.52)
24. G. Dattoli, M. Del Franco, A. Petralia and E. Sabia, "Beam matching strategies in undulators for

- SASE FEL operating devices”, Nucl. Instrum. Meth. 671 A, 82-93 (2012) (IF 1.072)
25. G. Dattoli, E. Sabia, C. Ronsivalle, M. Del Franco, A. Petralia, Slice Emittance, projected emittance and properties of the SASE FEL radiation, Nucl. Instrum. Meth. 671 A, 51-61 (2012) (IF 1.072)
  26. G. Dattoli, D. Babusci, K. Gorska and K. Penson, “The Relevance of the Ramanujan Master Theorem and its Implication for Special Functions, Applied Mathematics and Computation”, 218, 11466-11471(2012) (IF 1.338)
  27. D. Babusci, G. Dattoli, M. R. Martinelli and P. E. Ricci, “Integrals of Bessel Functions” Appl. Math. Letters, 26, 351 (2012) (IF 1.238)
  28. D. Babusci, G. Dattoli, G. H. E. Duchamp and K. A. Penson, “Definite integrals and operational methods”, Appl. Math. Comput., 219, 3017 (2012) (IF 1.338)
  29. D. Babusci, G. Dattoli, M. Quattromini, “On Integrals Involving Hermite Polynomials”, Appl. Math. Lett. 25, 1157 (2012) (IF 1.238)
  30. E. Allaria, R. Appio, L. Badano, W.A. Barletta, S. Bassanese, S.G. Biedron, A. Borga, E. Busetto, D. Castronovo, P. Cinquegrana, S. Cleva, D. Cocco, M. Cornacchia, P. Craievich, I. Cudin, G. D’Auria, M. Dal Forno, M.B. Danailov, R. De Monte, G. De Ninno, P. Delgiusto, A. Demidovich, S. Di Mitri, B. Diviacco, A. Fabris, R. Fabris, W. Fawley, M. Ferianis, E. Ferrari, S. Ferry, L. Froehlich, P. Furlan, G. Gaio, F. Gelmetti, L. Giannessi, M. Giannini, R. Gobessi, R. Ivanov, E. Karantzoulis, M. Lonza, A. Lutman, B. Mahieu, M. Milloch, S.V. Milton, M. Musardo, I. Nikolov, S. Noe, F. Parmigiani, G. Penco, M. Petronio, L. Pivetta, M. Predonzani, F. Rossi, L. Rumiz, A. Salom, C. Scafuri, C. Serpico, P. Sigalotti, S. Spampinati, C. Spezzani, M. Svandrlik, C. Svetina, S. Tazzari, M. Trovo, R. Umer, A. Vascotto, M. Veronese, R. Visintini, M. Zaccaria, D. Zangrando and M. Zangrando, “Highly coherent and stable pulses from the FERMI seeded free-electron laser in the extreme ultraviolet”, Nature Photonics 6, 699 (2012)
  31. S. Di Mitri, E. M. Allaria, P. Craievich, W. Fawley, L. Giannessi, A. Lutman, G. Penco, S. Spampinati, M. Trovo, “Transverse emittance preservation during bunch compression in the Fermi free electron laser”, Physical Review Special Topics - Accelerators and Beams 15, 020701 (2012)
  32. E. Allaria, A. Battistoni, F. Bencivenga, R. Borghes, C. Callegari, F. Capotondi, D. Castronovo, P. Cinquegrana, D. Cocco, M. Coreno, L. Giannessi, E. Pedersoli, G. Penco, E. Principi, L. Raimondi, R. Sergo, P. Sigalotti, C. Spezzani, C. Svetina, M. Trovò, M. Zangrando, “Tunability experiments at the FERMI@Elettra free-electron laser”, New Journal of Physics 14, 113009 (2012)
  33. E. Nichelatti and R.M. Monteverali, “Photoluminescence from a homogeneous volume source within an optical multilayer: analytical formulas”, J. Opt. Soc. Am. A 29, 3 (2012) 303-312.
  34. R.M. Monteverali, F. Bonfigli, F. Menchini and M.A. Vincenti, “Optical spectroscopy and microscopy of radiation-induced light-emitting point defects in lithium fluoride crystals and films”, Low Temperature Physics 38, 8 (2012) 779-785, DOI: 10.1063/1.4740241.
  35. R.M. Monteverali, F. Bonfigli, F. Menchini and M.A. Vincenti, “Optical spectroscopy and microscopy of radiation-induced light-emitting point defects in lithium fluoride crystals and films”, Fizika Nizkikh Temperatur 38, 8 (2012) 976-984.
  36. G. Baldacchini, P. Chiacchieretta, R.B. Pode, M.A. Vincenti, Q.-M. Wang, “Phase transitions in thermally annealed films of Alq<sub>3</sub>”, Low Temperature Physics 38, 8 (2012) 786-791, DOI: 10.1063/1.4740245
  37. G. Baldacchini, P. Chiacchieretta, R.B. Pode, M.A. Vincenti, Q.-M. Wang, “Phase transitions in thermally annealed films of Alq<sub>3</sub>”, Fizika Nizkikh Temperatur 38, 8 (2012) 985-992.
  38. G. Baldacchini, P. Chiacchieretta, R.B. Pode, M.A. Vincenti, Q.-M. Wang, “Phase transitions in thermally annealed films of Alq<sub>3</sub>”, Low Temperature Physics 38, 8 (2012) 786-791, DOI: 10.1063/1.4740245
  39. S. Heidari Bateni, F. Bonfigli, A. Cecilia, T. Baumbach, D. Pelliccia, F. Somma, M.A. Vincenti and R.M. Monteverali, “Optical characterization of lithium fluoride detectors for broadband X-ray imaging”, Nucl. Instr. Meth. A (2012), <http://dx.doi.org/10.1016/j.nima.2012.12.023>.
  40. D. Hampai, F. Bonfigli, S.B. Dabagov, R.M. Monteverali, G. Della Ventura, F. Bellatreccia and M. Magi, “LiF detectors-Polycapillary Systems as a New Approach for Advanced X-Ray Imaging”, Nucl. Instr. Meth. A, <http://dx.doi.org/10.1016/j.nima.2012.12.022>.
  41. M.R. Rajesh Menon, A. Mancini, C. Sudha Kartha, K.P. Vijayakumar, A. Santoni, “Band offset of the In<sub>2</sub>S<sub>3</sub>/ITO interface measured by X-Ray photoelectron spectroscopy”, Thin Solid Films 520 (2012) 5856-5859.
  42. E. Borsella, R. D’Amato, M. Falconieri, E. Trave, A. Panariti, I. Rivolta, “An outlook on the potential of Si nanocrystals as luminescent probes for bio-imaging”, Journal of Materials Research (2012), DOI: 10.1557/jmr.2012.295.
  43. P. Saccomandi, E. Schena, M.A. Caponero, F.M. Di Matteo, M. Martino, M. Pandolfi, S. Silvestri, “Theoretical Analysis and Experimental Evaluation of Laser-Induced Interstitial Thermo-therapy in Ex Vivo Porcine Pancreas”, IEEE Transactions on Biomedical Engineering, 59, 10 (2012) 2958-2964, doi: 10.1109/TBME.2012.2210895.
  44. L. Benussi, S. Bianco, M.A. Caponero, S. Colafranceschi, M. Ferrini, F. Felli, L. Passamonti, D. Pierluigi, A. Polimadei, A. Russo, G. Saviano, C. Vendittozzi, “A Novel Temperature Monitoring Sensor for Gas-Based Detectors in Large HEP Experiments”, Physics Procedia 37 (2012) 483-490, doi: 10.1016/j.phpro.2012.02.400
  45. A. Mostacci, M. Bellaveglia, E. Chiadroni, A. Cianchi, M. Ferrario, D. Filippetto, G. Gatti, C. Ronsivalle “Chromatic effects in quadrupole scan emittance measurements”, Physical Review Special Topics - Accelerators and Beams 15, 082802 (2012)
  46. V. Petrillo, A. Bacci, R. Ben Ali Zinati, I. Chaikovska, C. Curatolo, M. Ferrario, C. Maroli, C. Ronsivalle, A.R. Rossi, L. Serafini, P. Tomassini, C. Vaccarezza, A. Variola, “Photon flux and spectrum of X-rays Compton sources”, Nuclear Instruments and Methods in Physics Research A 693, 109-116 (2012)
  47. P. Antici, M. Migliorati, A. Mostacci, L. Palumbo, L. Picardi, C. Ronsivalle, “Sensitivity study in a compact accelerator for laser-generated protons”, Journal of Plasma Physics Volume: 78 Special Issue: SI Pages: 441-445 DOI: 10.1017/S0022377812000414 Part: Part 4 AUG (2012)
  48. P. Di Lazzaro, S. Bollanti, F. Flora, L. Mezi, D. Murra, A. Torre: “Mitigation of ion and particulate emission from laser-produced plasmas used for extreme ultraviolet lithography” Applied Surface Science (2012). Published online 16 April 2012. <http://dx.doi.org/10.1016/j.apsusc.2012.03.155>
  49. S. Bollanti, P. Di Lazzaro, F. Flora, L. Mezi, D. Murra, A. Torre: “New technique for aberration diagnostics and alignment of an extreme ultraviolet Schwarzschild objective” Nuclear Instruments and Methods in Physics Research A (2012). Published online <http://dx.doi.org/10.1016/j.nima.2012.12.00>
  50. P. Di Lazzaro, D. Murra, E. Nichelatti, A. Santoni, G. Baldacchini: “Superficial and Shroud-like coloration of linen by short laser pulses in the vacuum ultraviolet” Applied Optics 51, 8567-8578 (2012)
  51. C. Ronsivalle, M. Carpanese, R. Fantoni, L. Picardi, M. Balduzzi, M. T. Mancuso, C. Marino, M. Benassi, M. D’Andrea, L. Strigari, E. Cisbani, C. De Angelis, G. Esposito, S. Frullani, F. Ghio, V. Macellari, M.A. Tabocchini, “Perspectives of the use of a compact linear accelerator for proton therapy”, EAI Energia Ambiente e Innovazione 2/2012, p.78-86
  52. S. Bollanti, P. Di Lazzaro, F. Flora, L. Mezi, D. Murra, A. Torre, F. Bonfigli, R. Monteverali, M. Vincenti: “Is this artwork original or is it a copy? The answer by a new anti-counterfeiting tag”, in Energia, Ambiente, Innovazione, Special Issue II-2012 on “Knowledge, Diagnostics and Preservation of Cultural Heritage” 162-168 (2012). Available online at <http://www.afs.enea.it/project/webenea/EAI/Speciale-BENI.pdf>
  53. P. Di Lazzaro, D. Murra, A. Santoni, E. Nichelatti: “The conservation of the Shroud of Turin: optical studies” Energia, Ambiente, Innovazione, Special Issue II-2012 on “Knowledge, Diagnostics and



Preservation of Cultural Heritage”, 89-94 (2012). Available online at <http://www.afs.enea.it/project/webenea/EAI/Speciale-BENI.pdf>

54. A. Doria, G.P. Gallerano, E. Giovenale, G. Messina, I.P. Spassovsky, A.C. More, A. Petralia, “Phase-Sensitive Reflective Imaging in the Terahertz and mm-Wave Regions Applied to Art Conservation”, *Energia, Ambiente, Innovazione, Special Issue II-2012 on “Knowledge, Diagnostics and Preservation of Cultural Heritage”* 155-161 (2012) Available online at <http://www.afs.enea.it/project/webenea/EAI/Speciale-BENI.pdf>

### 6.3 CONFERENCE PROCEEDINGS

- Fantoni R., Caneve L., Colao F., Fiorani L., Palucci A. LIF measurements on medieval frescos by Giusto de' Menabuoi in the Padua Baptistery Ferrari A. (ed.), *Proceedings 5th International Congress on “Science and Technology for the Safeguard of Cultural Heritage on the Mediterranean Basin”, VALMAR, Rome, Italy (2012)* pp. 42-53
- Fantoni R., Ferri De Collibus M., Francucci M., Fornetti G., Guarneri M., Ricci R., Caneve L., Colao F., Fiorani L., Palucci A., Ortiz Calderon M. P. High resolution laser remote imaging: innovative tools for the preservation of painted surfaces. Ferrari A. (ed.), *Proceedings 5th International Congress on “Science and Technology for the Safeguard of Cultural Heritage on the Mediterranean Basin”, VALMAR, Rome, Italy (2012)* pp. 122-133
- Pittalis D., Iocola I., Fiorani L., Menicucci I., Palucci A., Lugliè A., Ghiglieri G., Iannetta M. Fluorescence spectroscopy techniques for water quality monitoring. Greppi G. F., Mura S. (eds.), *Biosensors and biotechnology for environmental monitoring, EDES, Cagliari, Italy (2012)* pp. 39-53
- R. Fantoni, M. Francucci, M. Ferri De Collibus, G. Fornetti, M. Guarneri, M. Nuvoli “U-AMLOR: an Underwater Amplitude-Modulated Laser Optical Radar for accurate 3D modeling and investigation of submerged real scenes” *Proceedings of the Conference DESE 2012 (Bucarest, Romania, 5 – 7 September 2012)*.
- R. Fantoni, M. Guarneri, G. Fornetti, M. Ferri De Collibus, M. Francucci, M. Nuvoli “Innovative 3D laser-color scanner application from non-invasive remote monitoring, for both accurate color and structural diagnosis, to virtual fruition in real exhibitions” *Proceedings of the Conference DESE 2012 (Bucarest, Romania, 5 – 7 September 2012)*.
- R. Chirico, S. Almaviva, S. Botti, L. Cantarini, F. Colao, L. Fiorani, M. Nuvoli, A. Palucci “Stand off detection of traces and explosives and precursors on fabrics by UV Raman spectroscopy” *Optics and Photonics for Counterterrorism, Crime Fighting, and Defence VIII, Proc. SPIE 8546, 85460W (October 30, 2012); doi: 10.1117/12.974518*.
- S. Almaviva, S. Botti, L. Cantarini, A. Palucci, A. Rufoloni, L. Landström, F.S. Romolo, “Trace detection of explosives and their precursors by surface enhanced Raman spectroscopy, *Optics and Photonics for Counterterrorism, Crime Fighting, and Defence VIII*, edited by Colin Lewis, Douglas Burgess, *Proc. SPIE 8546, 854602 (October 30, 2012); doi: 10.1117/12.970300*.
- L. Caneve, F. Colao, R. Fantoni, L. Fiorani “Scanning lidar fluorosensor for remote diagnostic of surfaces” *Nuclear Instruments & Methods In Physics Research A (2013)*, <http://dx.doi.org/10.1016/j.nima.2012.12.009i>.
- R. Fantoni, F. Colao, V. Spizzichino “Perspective of laser spectroscopic techniques in archaeometry: qualitative and quantitative information from LIF and LIBS” in “The Unknown Face of the Artwork” R. Radvan, S. Akyüz, and M. Simileanu Eds. *Istanbul Kültür University (Istanbul, 2012)* p. 17-26.
- S. Almaviva, S. Botti, L. Cantarini, A. Palucci, A. Rufoloni, L. Landström, F.S. Romolo, “Trace detection of explosives and their precursors by surface enhanced Raman spectroscopy”, *Optics and Photonics for Counterterrorism, Crime Fighting, and Defence VIII*, edited by Colin Lewis, Douglas Burgess, *Proc. SPIE 8546, 854602 (October 30, 2012); doi: 10.1117/12.970300*

- R. Chirico, S. Almaviva, S. Botti, L. Cantarini, F. Colao, L. Fiorani, M. Nuvoli, A. Palucci, “Stand off detection of traces and explosives and precursors on fabrics by UV Raman spectroscopy”, *Optics and Photonics for Counterterrorism, Crime Fighting, and Defence VIII, Proc. SPIE 8546, 85460W (October 30, 2012); doi: 10.1117/12.974518*.
- S. Almaviva, L. Caneve, F. Colao, R. Fantoni, G. Maddaluno “Vacuum laser-produced plasma for analytical application in fusion technologies” *Journal of Physics: Conference Series 406 (2012) 012014 doi:10.1088/1742-6596/406/1/012014*
- V. Spizzichino, L. Caneve, R. Fantoni F. De Nicola “Spectral database of Renaissance fresco pigments by LIBS, LIF and colorimetry” *Proceed. 3rd Balkan Symposium on Archaeometry, R. Radvan, S. Akyüz, M. Simileanu and V. Dragomir Eds., Bucharest Oct. 2012*.
- Dattoli, L. Giannessi, J. V. Rau, A. Petralia, M. Artioli, M. Quattromini, M. Del Franco, V. Surrenti, E. Di Palma and I. Spassovsky, “High Voltage Electron Gun for High Average Power FEL”, *agli atti della 19° International Conference on High-Power Particle G. Beams 30 settembre- 4 ottobre 2012, Karlsruhe (Germania)*, pp. 96-98.
- R.M. Montereali, S. Almaviva, E. Castagna, F. Bonfigli, M.A. Vincenti, “Lithium Fluoride X-ray Imaging Film Detectors for Condensed Matter Nuclear Measurements”, *Proceedings of 15th International Conference on Condensed Matter Nuclear Science (ICCF15), October 5-9, 2009, Rome, Italy, ed. ENEA (January 2012), ISBN: 978-88-8286-256-5 (<http://iccf15.frascati.enea.it/ICCF15-PROCEEDINGS.pdf>)*
- R.M. Montereali, “Novel Radiation Imaging Detectors based on Photoluminescence of Point Defects in Lithium Fluoride for Life Sciences”, *Proc. 4th International Conference on Luminescence and its Applications, ICLA2012, Hyderabad, India, February 7-10, 2012, ISBN-81-6717-806-5, p.13*.
- F. Somma, F. Bonfigli, S. Heidari Bateni, A. Cecilia, D. Pelliccia, M.A. Vincenti and R.M. Montereali, “Investigation of color centers distribution in X-ray irradiated LiF crystals by confocal fluorescence microscopy”, *Proc. 4th International Conference on Luminescence and its Applications, ICLA2012, Hyderabad, India, February 7-10, 2012, ISBN-81-6717-806-5, p.14*.
- F. Bonfigli, M.A. Vincenti and R.M. Montereali E. Nichelatti, S. Heidari Bateni, F. Somma, T. Baumbach, A. Cecilia, D. Pelliccia, “Confocal fluorescence microscopy for mapping of color center in X-ray irradiated lithium fluoride crystal and thin film detectors”, in *Fotonica 2012, 14° Convegno Nazionale delle Tecnologie Fotoniche, Firenze, 15-17 maggio 2012 – ISBN 9788887237146*.
- M.A. Vincenti, F. Bonfigli, G. Messina, R.M. Montereali A. Rufoloni E. Nichelatti, E. Di Bartolomeo, S. Licoccia, “Lithium fluoride thin films for imaging of radiation beams by colour centres stable formation”, in *Fotonica 2012, 14° Convegno Nazionale delle Tecnologie Fotoniche, Firenze, 15-17 maggio 2012 – ISBN 9788887237146*.
- A. Mostacci, A. Bacci, M. Bellaveglia, E. Chiadroni, A. Cianchi, G. Di Pirro, M. Ferrario, G. Gatti, C. Ronsivalle, A. R. Rossi, C. Vaccarezza, “Characterization of ps-spaced COMB beams at SPARC”, *Proceedings of IPAC2012, New Orleans, Louisiana, USA, p.1527-1529*
- C. Vaccarezza, O. Adriani, S. Albergo, D. Alesini, M. Anania, A. Bacci, R. Bedogni, M. Bellaveglia, C. Biscari, R. Boni, I. Boscolo, M. Boscolo, F. Broggi, P. Cardarelli, M. Castellano, L. Catani, E. Chiadroni, A. Cianchi, A. Clozza, C. Curatolo, C. De Martinis, G. Di Domenico, E. Di Pasquale, G. Di Pirro, A. Drago, A. Esposito, M. Ferrario, A. Gallo, M. Gambaccini, G. Gatti, A. Ghigo, G. Graziani, F. Marcellini, C. Maroli, M. Marziani, G. Mazzitelli, E. Pace, G. Passaleva, L. Pellegrino, V. Petrillo, R. Pompili, R. Ricci, R. Rossi, M. Serio, L. Serafini, F. Sgamma, B. Spataro, A. Stecchi, A. Stella, P. Tomassini, A. Tricomi, M. Veltri, S. Vescovi, F. Villa, C. Ronsivalle, P. Antici, M. Coppola, E. Iarocci, L. Lancia, A. Mostacci, M. Migliorati, V. Nardone, L. Palumbo, I. Chaickovska, O. Dadoun, F. Druon, P. Fichot, P. Georges, A. Mueller, A. Stocchi, A. Variola, F. Zomer, D. Angal-Kalinin, N. Bliss, J. Clarke, B. Fell, A. Goulden, J. Herbert, S. Jamison, B. Martlew, P. Mcintosh, R. Smith, S. Smith, “A European proposal for the Compton gamma-ray source of ELI-NP”, *Proceedings of IPAC2012, New*

- Orleans, Louisiana, USA, p.1086-1088
22. M. Ferrario, D. Alesini, M. Anania, A. Bacci, M. Bellaveglia, R. Boni, M. Castellano, E. Chiadroni, A. Cianchi, C. De Martinis, D. Di Giovenale, G. Di Pirro, U. Dosselli, A. Drago, A. Esposito, R. Faccini, R. Fedele, A. Gallo, M. Gambaccini, C. Gatti, G. Gatti, A. Ghigo, D. Giulietti, P. Londrillo, S. Lupi, A. Mostacci, E. Pace, L. Palumbo, G. Passaleva, L. Pellegrino, V. Petrillo, R. Pompili, A. R. Rossi, L. Serafini, B. Spataro, P. Tomassini, G. Turchetti, C. Vaccarezza, F. Villa, G. Dattoli, E. Di Palma, L. Giannessi, A. Petralia, M. Quattromini, C. Ronsivalle, I. Spassovsky, V. Surrenti, L. Gizzi, L. Labate, T. Levato, J.V. Rau "Recent results at the SPARC\_LAB facility", Proceedings of IPAC2012, New Orleans, Louisiana, USA, p.2758-2760
  23. E. Chiadroni, A. Bacci, M. Bellaveglia, M. Castellano, G. Di Pirro, M. Ferrario, G. Gatti, E. Pace, A. R. Rossi, C. Vaccarezza, P. Calvani, A. Nucara, D. Nicoletti, O. Limaj, S. Lupi, B. Marchetti, A. Cianchi, A. Mostacci, C. Ronsivalle, A. Perucchi, "The THz Radiation Source at the SPARC Facility", 6th Workshop on Infrared Spectroscopy and Microscopy with Accelerator-Based Sources, IOP Publishing, Journal of Physics: Conference Series 359 (2012) 012018
  24. E. Chiadroni, A. Bacci, M. Bellaveglia, P. Calvani, M. Castellano, A. Cianchi, G. Di Pirro, M. Ferrario, G. Gatti, O. Limaj, S. Lupi, B. Marchetti, A. Mostacci, D. Nicoletti, A. Nucara, E. Pace, C. Ronsivalle, A. R. Rossi, C. Vaccarezza, "The THz radiation source at SPARC", IX International Symposium on Radiation from Relativistic Electrons in Periodic Structures, IOP Publishing Journal of Physics: Conference Series 357 (2012) 012034
  25. G.P. Gallerano, A. Doria, E. Giovenale, G. Messina and I. Spassovsky, "The ENEA Compact Advanced THz Source: upgrade and new imaging capabilities", Proceedings 37th International Conference on Infrared, Millimeter and Terahertz Waves, IRMMW-THz2012, Wollongong, NSW, Australia, 2-7 October 2011, ISBN: 978-1-4673-1598-2, 13192186 (2012)
  26. Doria, G.P. Gallerano, E. Giovenale, G. Messina, A. Ramundo Orlando, I. Spassovsky, "Electromagnetic pulser for the investigation of cell membranes", Proceeding della "XIX Riunione Nazionale di Elettromagnetismo", Roma 10-14 Settembre 2012.
  27. P. Di Lazzaro, S. Bollanti, F. Flora, L. Mezi, D. Murra, A. Torre, F. Bonfigli, R.M. Montereali, M.A. Vincenti: "Extreme ultraviolet marking system for anti-counterfeiting tags with adjustable security level", Proc. SPIE of the XIX Int. Symposium on High-Power Laser Systems and Applications, edited by K. Allahverdi (2012)
  28. F. Flora, S. Bollanti, F. Bonfigli, P. Di Lazzaro, L. Mezi, R.M. Montereali, D. Murra, A. Torre, M.A. Vincenti, "A new anticounterfeiting technique based on lithium fluoride films coloration by EUV radiation", in Fotonica 2012, 14° Convegno Nazionale delle Tecnologie Fotoniche, Firenze, 15-17 maggio 2012 – ISBN 9788887237146.
  4. L. Fiorani, S. Babichenko, J. Bennes, R. Borelli, R. Chirico, A. Dolfi-Bouteyre, L. Hespel, T. Huet, V. Mitev, A. Palucci, M. Pistilli, A. Puiu, O. Rebane "Lidar detection of explosive precursors" 26th International Laser Radar Conference, ICLAS, Porto Heli, Greece (2012)
  5. L. Fiorani, W.R. Saleh, M. Burton, L. Hespel, T. Huet "Lidar detection of carbon dioxide in volcanic emissions" 26th International Laser Radar Conference, ICLAS, Porto Heli, Greece (2012)
  6. Chirico R., Almaviva S., Botti S., Cantarini L., Colao F., Fiorani L., Nuvoli M., Palucci A. "Stand-off detection of traces of explosives and precursors on fabrics by UV Raman spectroscopy" 2012 SECURITY+Defence, SPIE, Edinburgh, UK (2012)
  7. Fiorani L., Borelli R., Marullo S., Montes-Hugo M. "Biogeo-optical characterization of the St. Lawrence Estuary by laser-induced fluorescence and satellite radiometry" 3rd MERIS/(A)ATSR and OCLI-SLSTR (Sentinel-3) preparatory workshop, ESA, Frascati, Italy (2012)
  8. Lucente M., Salomè A., Limiti E., Ferri M., Fiorani L., Saleh W. R. Stallo C., Ruggieri M., Codispoti G. "PLATON: satellite remote sensing and telecommunication by using millimetre waves" 2012 IEEE Gold Remote Sensing Conference, IEEE, Rome, Italy (2012)
  9. E. Borsella, L. Caneve, R. D'Amato, C. Giancristofaro, F. Persia, L. Pilloni, A. Rinaldi "Development of nanocomposites for conservation of artistic stones" NanotechItaly2012, Venezia 21-23 Novembre 2012.
  10. L. De Dominicis, M. Francucci, M. Ferri de Collibus, G. Fornetti, M. Guarneri, M. Nuvoli, A. AL Obaidi, D. Mcstay "Developments in laser 3D measurement and imaging for Oil and Gas Industry Applications" Oral presentation at EOSAM 2012, 25-28 September 2012, Aberdeen (UK).
  11. L. De Dominicis, M. Francucci, M. Ferri de Collibus, G. Fornetti, M. Guarneri, M. Nuvoli "Presentazione delle attività ENEA nell'ambito del progetto BLUARCHEOSYS" Oral presentation at the final meeting of the BluArcheosys project, Frascati 16 Aprile 2012
  12. M. Francucci, L. De Dominicis, M. Ferri de Collibus, G. Fornetti, M. Guarneri, M. Nuvoli, R. Ricci, "Simulazione Monte Carlo di propagazione in acqua di fasci laser modulati: applicazione per imaging e comunicazioni ottiche" Fotonica 2012, 14° Convegno Nazionale delle Tecnologie Fotoniche (Florence, Italy, 15 – 17 May 2012), ISBN 9788887237146.
  13. M. Francucci, G. Fornetti, M. Ferri de Collibus, L. De Dominicis, M. Guarneri, M. Nuvoli "Fruizione conservativa: il laser scanner 3D a colorimetria remota (RGB-ITR)" Oral presentation for Workshop "Smart, sostenibile e sicuro: il futuro dei centri storici", Lu.Be.C. 2012 (Lucca Beni Culturali), 8th Edition, (Lucca, 18 – 20 October 2012).
  14. R. Fantoni, M. Guarneri, G. Fornetti, M. Ferri De Collibus, M. Francucci, M. Nuvoli "Innovative 3D laser-color scanner application from non-invasive remote monitoring, for both accurate color and structural diagnosis, to virtual fruition in real exhibitions". DESE 2012 (Bucarest, Romania, 5 – 7 September 2012). Invited lecture
  15. Laura Teodori, Barbara Perniconi, Alessandra Costa, Paola Aulino, Massimo Fini, Dario Coletti; "Directing the 3 D Patterning of skeletal muscle biongered constructs" ISAC International Congress, Leipzig, June 2012
  16. Laura Teodori, Vera Donnemberg, Anne Plant "Cytometry challenges and opportunities for regenerative medicine" ISAC International Congress, Leipzig, June 2012
  17. Dario Coletti, Barbara Perniconi, Zbigniew Darzynkiewicz, Dorota Halicka, Anna Giovanetti, Massimo Fini and Laura Teodori "Glioblastoma cells dna induced damage by X Rays exposure is modulated by static magnetic field" ISAC International Congress, Leipzig, June 2012
  18. Alessandra Costa, Barbara Perniconi, Paola Aulino, Paola Aprile, Laura Teodori et al. "Decellularized scaffolds from skeletal muscle as a tool for 3D cell culture and muscle repair" ISAC International Congress, Leipzig, June 2012
  19. Dario Coletti, Paola Aulino, Emanuele Berardi, Alessandra Costa, Laura Teodori, Sergio Adamo. "Strategies to enhance myogenesis following acute injury" ISAC International Congress, Leipzig,

#### 6.4 CONFERENCE LECTURES

1. V. Lasic: "Laser ablation in presence of liquid coverage: processes, applications and LIBS spectroscopy. 11th European Workshop on Laser Ablation, Gijón (Spain), June 19-22, 2012. Invited lecture.
2. Saleh W., Fiorani L., Burton M., Volcanic CO2 detection using 1.57 μm differential absorption lidar 14o Convegno Nazionale delle Tecnologie Fotoniche – Fotonica 2012, AICT-AEIT, Firenze, Italy (2012)
3. Trees C., Arnone R., Barale V., Besiktepe S., Chami M., Chekalyuk A., Churnside J., Coelho E., Concannon B., Dolin L., Feygels V., Fiorani L., Fry E., Gilbert G., Gray D., Hou W., Hu Y., Kopelevich O., Kopilevich Y., McBride W., McKee D., Muth J., Pennucci G., Roy G., Sanjuan Calzado V., Voss K., Walther T., Weidemann A., Zege E. "Lidar observation of optical and physical properties" (LOOPP) workshop 2012 Ocean Sciences Meeting, TOS-ASLO-AGU, Salt Lake City, USA (2012)

June 21012

20. L. Teodori, A. Costa, B. Pernigoni, P. Aprile, D. Coletti - Extracellular matrix in tissue engineering - India Asian Polymer Association International Congress in Advances in Health care system. Invited lecture
21. L. Teodori Indian-European Union Members States Conference: "Health: the main elements of a medium to long term strategic agenda for Indo-European research and innovation" Brussels 31 May 2012
22. P. Rossi, Mario Ferri De Collibus et al., "IVVS actuating system compatibility test to ITER gamma radiation conditions", Submitted to SOFT-2012 , - 27Th Symposium on fusion technologies, Liège (Belgium), 24 – 28 September 2012
23. Sabina Botti, S. Almaviva, L. Cantarini, A. Rufoloni, A. Palucci, A. Puiu, "Surface enhanced Raman spectroscopy of explosive molecules adsorbed on gold coated substrates", Fotonica 2012, 15-17 Maggio, Firenze. Invited lecture
24. S. Almaviva, S. Botti, L. Cantarini, A. Palucci, A. Rufoloni, L. Landström, F.S. Romolo, "Trace detection of explosives and their precursors by surface enhanced Raman spectroscopy", 2012 SPIE Security and Defence, 24-27 Settembre 2012, Edinburgo, UK.
25. S. Almaviva, S. Botti, L. Cantarini, R. Chirico, F. Colao, L. Fiorani, M. Nuvoli, A. Palucci, "Stand off detection of traces and explosives and precursors on fabrics by UV Raman spectroscopy", 2012 SPIE Security and Defence, 24-27 Settembre, 2012, Edinburgh, UK.
26. S. Almaviva, S. Botti, L. Cantarini, R. Fantoni, A. Palucci, A. Puiu, A. Rufoloni, "Surface Enhanced Raman Spectroscopy analysis of explosives compounds: study of detection capabilities as a function of laser energy and fluence", 11th ECONOS, 8-11 July 1012, Aberdeen, UK.
27. S. Botti, L. Fiorani S. Almaviva, R. Borelli, L. Cantarini, R. Chirico, F. Colao, M. Pistilli, A. Palucci, A. Puiu, "Development of a lidar/DIAL and a SERS sensor for the detection of improvised explosive devices", 43rd International Annual Conference of the Fraunhofer ICT, 26-29 June 2012, Edinburgh, UK
28. R.Fantoni, De Dominicis L., Ferri De Collibus M., Francucci M., Fornetti G., Guarneri M., Caneve L., Colao F., Fiorani L., Lazic V., Palucci A., Spizzichino V. "Remote and in-situ characterization of CH surfaces: How the use of robotic platforms can help". RICH "Robotics and Cultural Heritage, Venice 3-4-/12/2012. Invited lecture
29. R. Fantoni, F. Colao, V. Spizzichino "Perspective of laser spectroscopic techniques in archaeometry: qualitative and quantitative information from LIF and LIBS" 3rd Balkan Symposium on Archaeometry" Bucarest (Romania) 29-30/10/2012. Invited lecture
30. R. Fantoni, S. Almaviva, L. Caneve, F. Colao, G. Maddaluno "LIBS diagnostics inside nuclear fusion reactors: Development of CF-LIBS based techniques for deposited layers diagnostics on ITER like tiles" LIBS 2012 – 7th Int. Conf. Laser induced Breakdown Spectroscopy" . Luxor (Egitto) 29/09 – 4/10/2012. Invited lecture
31. S. Almaviva, L. Caneve, F. Colao, R. Fantoni, G. Maddaluno "Vacuum laser-produced plasma for analytical application in fusion technologies" 12th High-Tech Plasma Processes Conference (HTPP-12), Bologna June 2012.
32. V. Spizzichino, L. Caneve, R. Fantoni F. De Nicola "Spectral database of Renaissance fresco pigments by LIBS, LIF and colorimetry" 3rd Balkan Symposium on Archaeometry" Bucarest (Romania) 29-30/10/2012.
33. L. Caneve, F. Colao, F. De Nicola, C. Giancristofaro, F. Persia, G. Ricci, V. Spizzichino "LIBS and LIF for the characterization of artistic marbles and Renaissance frescoes" LIBS 2012 – 7th Int. Conf. Laser induced Breakdown Spectroscopy Luxor (Egitto) 29/09 – 4/10/2012.
34. S. Ratynskaia, M. De Angeli, S. Almaviva, G. Dilecce, C. Castaldo, F. Colao, L. Caneve "Energy distribution of prompt electrons emitted during laser ablation of targets". 39th European Physical Society Conference on Plasma Physics Stockholm, Sweden, 2-6 July 2012
35. A. Palucci "Il progetto Europeo BONAS". 14° Convegno Nazionale delle Tecnologie Fotoniche, Firenze, 15-17 maggio 2012. Invited lecture
36. A. Palucci "Raman Detection of Explosive" NATO Workshop on "Explosive and Chemical detection technologies". Bruxelles October 15th – 17th 2012. Invited lecture
37. M. Ferrario, D. Alesini, M. Anania, A. Bacci, M. Bellaveglia, R. Boni, M. Castellano, E. Chiadroni, A. Cianchi, C. De Martinis, D. Di Giovenale, G. Di Pirro, U. Dosselli, A. Drago, A. Esposito, R. Faccini, R. Fedele, A. Gallo, M. Gambaccini, C. Gatti, G. Gatti, A. Ghigo, D. Giulietti, P. Londrillo, S. Lupi, A. Mostacci, E. Pace, L. Palumbo, G. Passaleva, L. Pellegrino, V. Petrillo, R. Pompili, A. R. Rossi, L. Serafini, B. Spataro, P. Tomassini, G. Turchetti, C. Vaccarezza, F. Villa, G. Dattoli, E. Di Palma, L. Giannessi, A. Petralia, M. Quattromini, C. Ronsivalle, I. Spassovsky, V. Surrenti, L. Gizzi, L. Labate, T. Levato, J.V. Rau, "Recent Results at the SPARC LAB Facility", International Particles Accelerator Conference 2012
38. G. Dattoli, L. Giannessi , J. V. Rau , A. Petralia , M. Artioli , M. Quattromini ,M. Del Franco , V. Surrenti , E. Di Palma , I. Spassovsky, "High voltage electron gun for high average power FEL", 4th Euro-Asian Pulsed Power Conference and the 19th International Conference on High-Power Particle Beams., Karlsruhe, Germany; 09/2012
39. G. Dattoli, "FEL WAVE undulators", Channeling 2012, Alghero Settembre 2012
40. F. Ciocci, "Seeding and Self Seeding at New FEL sources", Trieste 10-11 December 2012.
41. Simone Spampinati, Enrico Allaria, Laura Badano, Silvano Bassanese, Davide Castronovo, Miltcho B. Danailov, Alexander Demidovich, Simone Di Mitri, Bruno Diviacco, William M. Fawley, Lars Froelish, Giuseppe Penco, Carlo Spezzani, Mauro Trovò, Giovanni DeNinno, Eugenio Ferrari, "Commissioning of the Fermi@Elettra laser heater", 2012 FEL Conference
42. Sandra Biedron, Luca Giannessi\*, Karen Horovitz, Stephen Milton, "Nonlinear harmonic selection in an FEL undulator system", 2012 FEL Conference
43. Nicolas Yann Joly, Giovanni De Ninno, Benoît Mahieu , Franco Ciocci, Luca Giannessi, Alberto Petralia, Marcello Quattromini, Giancarlo Gatti, Julietta V. Rau, Vittoria Petrillo , Wonkeun Chang, Philipp Hölzer, KaFai Mak, Philip Russell, Francesco Tani, John Colin Travers, Serge Bielawski, Marie- Emmanuelle Couprie, Marie Labat, Takanori Tanikawa, "Seeding of SPARC-FEL with a tunable fibre-based source", 2012 FEL Conference
44. M.D. Alaimo, M. Manfreda, V. Petrillo, M.A.C Potenza, D. Redoglio, L.Serafini,M. Artioli, F. Ciocci, A. Petralia, M. Quattromini, V. Surrenti, A. Torre, L. Giannessi J.V. Rau, M. Bellaveglia, E. Chiadroni, A. Cianchi, G. Di Pirro, G. Gatti, M. Ferrario, A. Mostacci, "Measurement of the transverse coherence of the SASE FEL radiation in the optical range using an heterodyne SPECKLE method", 2012 FEL Conference
45. L. Giannessi et al., "First lasing of FERMI FEL-2 (1° stage) and FERMI FEL-1", 2012 FEL Conference
46. G. Penco , E. Allaria, P. Craievich, G. De Ninno, S. Di Mitri, W. B. Fawley, E. Ferrari, L. Giannessi, C. Spezzani, M. Trovo`, S. Spampinati, "Recent results, time-sliced emittance and energy spread measurements at FERMI@ELETTRA", Proceedings of the 2012 FEL Conference
47. E. Allaria, S. Di Mitri, W. M. Fawley, E. Ferrari, L. Froehlich, G. Penco, Spezzani, M. Trovo, G. De Ninno, B. Mahieu, S. Spampinati, L. Giannessi, "Spectral characterization of the FERMI pulses in the presence of Electron-Beam Phase-Space modulations", Proceedings of the 2012 FEL Conference
48. M. Svandrlik, E. Allaria, L. Badano, S. Bassanese, F. Bencivenga, E. Busetto, C. Callegari, F. Capotondi, D. Castronovo, M. Coreno, P. Craievich, I. Cudin, G. D'Auria, M. Dal Forno, M.B. Danailov, R. De Monte, G. De Ninno, A.A. Demidovich, M. Di Fraia, S. Di Mitri, B. Diviacco, A. Fabris, R. Fabris, W.M. Fawley, M. Ferianis, E. Ferrari, L. Froehlich (L. Fröhlich), P. Furlan Radivo, G. Gaio, L. Giannessi, R. Gobessi, C. Grazioli, E. Karantzoulis, M. Kiskinova, M. Lonza, B. Mahieu, C. Masciovecchio, S. Noe (S. Noè), F. Parmigiani, G. Penco, E. Principi, F. Rossi, L. Rumiz, C. Scafuri,

- S. Spampinati, C. Spezzani, C. Svetina, M. Trovo (M. Trovò), A. Vascotto, M. Veronese, R. Visintini, M. Zaccaria, D. Zangrando, M. Zangrando, "Status of the FERMI@Elettra Project", International Particles Accelerator Conference 2012
49. Rosa Maria Montereali, "Novel Radiation Imaging Detectors based on Photoluminescence of Point Defects in Lithium Fluoride for Life Sciences", 4th International Conference on Luminescence and its Applications, ICLA2012, Hyderabad, India, February 7-10, 2012 (invited lecture).
  50. F. Somma, F. Bonfigli, S. Heidari Bateni, A. Cecilia, D. Pelliccia, M.A. Vincenti and R.M. Montereali, "Investigation of color centers distribution in X-ray irradiated LiF crystals by confocal fluorescence microscopy", 4th International Conference on Luminescence and its Applications, ICLA2012, Hyderabad, India, February 7-10, 2012.
  51. F. Bonfigli, A. Faenov, F. Flora, P. Gaudio, A. Lai, R.M. Montereali, T. Pikuz, L. Reale, M. Richetta, "Solid state lithium fluoride detectors for soft x-ray contact microscopy", Convegno Nazionale Sensori - Innovazione, attualità e prospettive, Roma 15 - 17 Febbraio 2012, P45.
  52. F. Bonfigli, M.A. Vincenti and R.M. Montereali E. Nichelatti, S. Heidari Bateni, F. Somma, T. Baumbach, A. Cecilia, D. Pelliccia, "Confocal fluorescence microscopy for mapping of color center in X-ray irradiated lithium fluoride crystal and thin film detectors", Fotonica 2012, 14° Convegno Nazionale delle Tecnologie Fotoniche, Firenze, 15-17 maggio 2012.
  53. M.A. Vincenti, F. Bonfigli, G. Messina, R.M. Montereali A. Rufoloni E. Nichelatti, E. Di Bartolomeo, S. Licoccia, "Lithium fluoride thin films for imaging of radiation beams by colour centres stable formation", Fotonica 2012, 14° Convegno Nazionale delle Tecnologie Fotoniche, Firenze, 15-17 maggio 2012.
  54. F. Bonfigli, A. Cecilia, S. Heidari Bateni, E. Nichelatti, D. Pelliccia, F. Somma, P. Vagovic, M.A. Vincenti, T. Baumbach and R.M. Montereali, "Broadband X-ray imaging by high resolution lithium fluoride detectors", 8th International Conference on Luminescent Detectors and Transformers of Ionizing radiation, LUMDETR 2012, Halle, Germany, September 10-14, 2012, O-Thu-09.
  55. R.M. Montereali, F. Bonfigli, I. Chiamenti, H.J. Kalinowski, F. Michelotti, "Colour-centre optical channel waveguides directly written in LiF crystals by femtosecond laser", XCVIII Congresso Nazionale Società Italiana di Fisica, Napoli, 17-21 Settembre 2012, p.10.
  56. F. Somma, F. Bonfigli, A. Cecilia, S. Heidari Bateni, E. Nichelatti, P. Vagovic, T. Baumbach, R.M. Montereali, "Studio di rivelatori di LiF per imaging a raggi X con fascio bianco", XCVIII Congresso Nazionale Società Italiana di Fisica, Napoli, 17-21 Settembre 2012, p.119.
  57. A.P. Voitovich, V.S. Kalinov, E.F. Martynovich, R.M. Montereali, L.P. Runets, A.P. Stupak, G. Baldacchini, "Color centers aggregation kinetics in lithium fluoride", Proc. of 16th International Workshop on Inorganic and Organic Electroluminescence, 2012 International Conference on the Science and Technology of Emissive Displays and Lighting, EL2012, 10-14 December 2012, Lam Woo International Conference Centre, Hong Kong, 2P-24.
  58. G. Baldacchini, P. Chiacchieretta, G. Dattoli, R.B. Pode, M.A. Vincenti, "Long time decay kinetics of photoluminescence from Alq3 films", Proc. of 16th International Workshop on Inorganic and Organic Electroluminescence, 2012 International Conference on the Science and Technology of Emissive Displays and Lighting, EL2012, 10-14 December 2012, Lam Woo International Conference Centre, HKBU, 5B7.
  59. R. D'Amato, M. Falconieri, G. Terranova, E. Borsella, "Synthesis of nanoparticles by laser pyrolysis, 19th International Symposium on Analytical and Applied Pyrolysis", Linz (Austria), 21-25 Maggio 2012.
  60. M. Falconieri, E. Trave, R. D'Amato, E. Borsella, "Study of defect-related light emission in oxidized Silicon nanocrystals", E-MRS 2012 Fall Meeting, Simposio L: Defect-induced effects in nanomaterials, Varsavia (Polonia), 17-21 Settembre 2012.
  61. Rosaria D'Amato, "Synthesis of nanoparticles by laser pyrolysis: from ceramic nanocomposites to nanofluids", Nanoforum 2012, VIII edizione, Micro, nano and advanced technologies: where research meets business, Università di Roma Sapienza, Roma, 24-26 Settembre 2012. Invited lecture
  62. E. Borsella, L. Caneve, R. D'Amato, C. Giancristofaro, F. Persia, L. Pilloni, A. Rinaldi, "Development of nanocomposites for conservation of artistic stones", NanotechItaly2012, International Conference, Promoting responsible innovation, Venezia, 21-23 novembre 2012.
  63. L. Benussi, S. Bianco, M.A. Caponero, S. Colafranceschi, M. Ferrini, F. Felli, L. Passamonti, D. Pierluigi, A. Polimadei, A. Russo, G. Saviano, C. Vendittozzi, "Use of fiber optic technology for Relative Humidity monitoring in RPC detectors", 11th Workshop on Resistive Plate Chambers and Related Detectors (RCP2012), Rome, Italy, 5-10 Feb. 2012
  64. P. Corvaglia, D. Cardone, M.A. Caponero, G. Maddaluno, "Innovative Devices for Structural Control and Monitoring of Civil Infrastructures", EACS 2012 - 5th European Conference on Structural Control, Paper No. 165, Genoa, Italy, 18-20 Jun. 2012.
  65. A. Coricciati, P. Corvaglia, A. Largo, M.A. Caponero, "Smart composite device for structural health monitoring", CIMTEC 2012 - 4th International Conference Smart Materials Structures Systems, Paper No. G3-L16, Montecatini Terme, Italy, 10-15 Jun. 2012.
  66. P. Corvaglia, D. Cardone, M.A. Caponero, G. Maddaluno, "Innovative Devices for Structural Control and Monitoring of Civil Infrastructures", EACS 2012 - 5th European Conference on Structural Control, Paper No. 165, Genoa, Italy, 18-20 Jun. 2012.
  67. A. Coricciati, P. Corvaglia, A. Largo, M.A. Caponero, "Smart composite device for structural health monitoring, CIMTEC 2012" - 4th International Conference Smart Materials Structures Systems, Paper No. G3-L16, Montecatini Terme, Italy, 10-15 Jun. 2012.
  68. S. Paolini, "Indagini storiche e macrosismica nel Lazio", La pericolosità sismica nella regione Lazio, Regione Lazio, Roma, 15 marzo 2012.
  69. D. Rinaldis, G. Martini, "Analisi della sismicità regionale per la Nuova Zonazione Sismica e definizione degli accelerogrammi di riferimento per gli studi di MS", La pericolosità sismica nella regione Lazio, Regione Lazio, Roma, 15 marzo 2012.
  70. S. Paolini, "Il terremoto di Rieti del 1898 - Storia e macrosismica", Archivio di Stato di Rieti, 20 aprile 2012 - XIV Settimana della cultura.
  71. D. Rinaldis, G. Martini, V. Verrubbi, Cerreto di Spoleto (Umbria-Italy): "Topographic amplification at the ENEA local array stations", XV World Conference on Earthquake Engineering Lisbon, Portugal, 24th- 28th September 2012.
  72. F. Bozzano, C. Esposito, S. Martino, A. Prestininzi, G. Scarascia Mugnozza, G. Martini, D. Rinaldis, "A spectrum-compatibility method for deriving earthquake-induced displacements of unstable slopes", XV World Conference on Earthquake Engineering Lisbon, Portugal, 24th- 28th September 2012.
  73. F. Bozzano, S. Martino, A. C. Giacomi, L. Lenti, G. Martini & M. P. Santisi D'Avila, "Numerical modeling of nonlinear dynamic shear strains in heterogeneous soils by 1D-3C finite difference SWAP", XV World Conference on Earthquake Engineering Lisbon, Portugal, 24th- 28th September 2012.
  74. D. Rinaldis, G. Martini, V. Verrubbi, "Topographic amplification at the ENEA local array stations. - A spectrum-compatibility method for deriving earthquake-induced displacements of unstable slopes", XV World Conference on Earthquake Engineering Lisbon, Portugal, 24th- 28th September 2012.
  75. G.P. Gallerano, "Electric vs. Electromagnetic pulses: an introduction to the next speakers", 3rd International THz-Bio Workshop, Seoul University, 06-08 February 2011 (invited lecture)
  76. G.P. Gallerano, A. Doria, E. Giovenale, G. Messina, I. Spassovsky, A. Ramundo Orlando, M.R. Scarfi, S. Romeo, O.Zeni, "Electric vs. Electromagnetic ultrashort pulses: search for a unifying view", II Convegno Nazionale su "Interazione fra Campi Elettromagnetici e Biosistemi" Bologna, 27 - 29 June

2012

77. G.P. Gallerano, A. Doria, E. Giovenale, G. Messina, I. Spassovsky, A. Ramundo-Orlando, K. Cosentino, F. Mattia, S. Romeo, M.R. Scarfi, O. Zeni "Ultrashort Electric vs. Radiation Pulses: Search for a Unifying View" *Bioelectrics* 2012, 9th International Bioelectrics Symposium, Kumamoto – Japan, September 5-8, 2012. Invited lecture
78. F. Flora, S. Bollanti, F. Bonfigli, P. Di Lazzaro, L. Mezi, R.M. Montereali, D. Murra, A. Torre, M.A. Vincenti: "A new anticounterfeiting technique based on lithium fluoride films coloration by EUV radiation", contributo a FOTONICA 2012, 14° Convegno Nazionale delle Tecnologie Fotoniche, Firenze 15-17 maggio 2012
79. L. Mezi, S. Bollanti, P. Di Lazzaro, F. Flora, D. Murra, A. Torre: "EUV and XUV sources at ENEA-Frascati Laboratories for photonic applications", contributo a FOTONICA 2012, 14° Convegno Nazionale delle Tecnologie Fotoniche, Firenze 15-17 maggio 2012
80. P. Di Lazzaro, "Ipotesi scientifiche sulla formazione dell'immagine sulla Sindone", Lezione presso l'Ateneo Pontificio Regina Apostolorum, 18 Aprile 2012. Invited lecture
81. P. Di Lazzaro: "Could a burst of radiation create a Shroud-like coloration? Summary of 5-years experiments at ENEA Frascati", 1st International Congress on the Holy Shroud, Valencia, Spain 28 Aprile 2012. Invited lecture
82. R. Balvetti, M.L. Bargellini, M. Battaglia, G. Casadei, A. Filippini, E. Pancotti, L. Puccia, C. 6.5M. Traballese, S. Brunelli, F. Paradisi, A. Grandinetti, E. Di Stanislao, R. Rosellini "The Cybernetic can improve the quality of life: An Intelligent Limb Prosthesis", Bio-and Medical Informatics and Cybernetics: BMIC 2012 Orlando, Florida, USA
83. Balvetti R., Bargellini M.L., Battaglia M., Botticelli A., Bozanceff G., Brunetti G., Casadei G., Chiapparelli A., Filippini A., Grandinetti A., Guidoni A., Pancotti E., Puccia L., Rubini L., Tripodo A., Zampetti C., Traballese M., Brunelli S., Paradisi F., Delussu A.S., Di Stanislao E., Rosellini R. "Il ripristino della dinamica del passo con l'uso di una protesi intelligente: coincidenza tra intenzionalità e propriocezione del movimento", Congresso Società Italiana di Fisica, XCVIII Congresso Nazionale (Napoli, 17 - 21 Settembre, 2012).
84. R. Fedele, F. Tanjia, C. Ronsivalle, S. De Nicola, D. Jovanovic, "Transverse charge particle beam dynamics in the presence of space charge effects", XCVIII Congresso Nazionale Napoli, 17-21/09/2012
85. C. Ronsivalle, "Generation of high phase space density beams", WORKSHOP May 14-16 2012 Milano, Italy - "European Proposal for ELI-NP Gamma Beam System: the Machine and the Experiments"
86. G.P. Gallerano, A. Doria, E. Giovenale, I. Spassovsky, "High power THz sources and applications at ENEA-Frascati" Int. Symposium on Frontiers in THz Technology FTT2012, Nara – Japan, November 26-30, 2012. Invited lecture

## 6.5 TECHNICAL REPORTS

1. Colao F., Caneve L., Fiorani L., Fantoni R., Dell'Erba R., Fassina V. "Detailed report on "LIF measurements of frescos by Giusto De' Menabuoi in the Padua baptistry" - Technical Reports of the Italian National Agency for New Technologies, Energy and Sustainable Economic Development (ISSN\* 0393-3016), Rome, Italy (2012)
2. Colao F., Caneve L., Fiorani L., Palucci A., Fantoni R., Ortiz P., Gómez M. A., Vázquez M. A. "Report on "LIF measurements in Seville. Part 1: Virgen del Buen Aire chapel" Technical Reports of the Italian National Agency for New Technologies, Energy and Sustainable Economic Development (ISSN\* 0393-3016), Rome, Italy (2012)
3. Colao F., Caneve L., Fiorani L., Palucci A., Fantoni R., Ortiz P., Gómez M. A., Vázquez M. A. Report

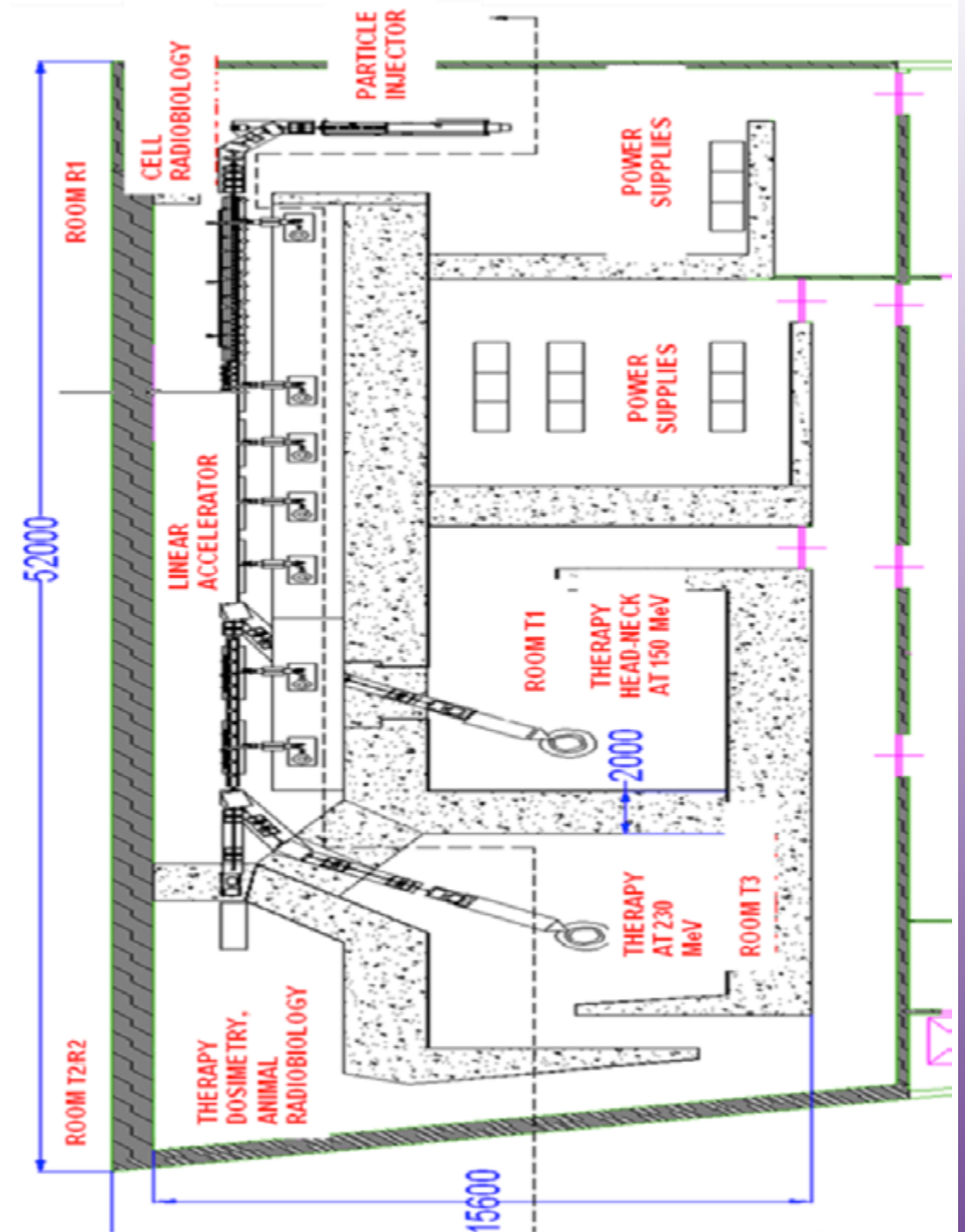
- on "LIF measurements in Seville. Part 2: Santa Ana church" Technical Reports of the Italian National Agency for New Technologies, Energy and Sustainable Economic Development (ISSN\* 0393-3016), Rome, Italy (2012)
4. F. Artuso & D. Cataldi, "Misure di clorofilla a e b in acqua di mare con metodo HPLC presso il laboratorio di chimica analitica ambientale di Frascati", RT/2012/3/ENEA.
5. L. Caneve, F. Colao, F. Arci: "Studio di marmi e consolidanti di interesse artistico mediante fluorescenza indotta da laser". ENEA Report RT/2011/13/ENEA, ISSN/0393-3016.
6. M. Francucci, L. De Dominicis, M. Ferri de Collibus, G. Fornetti, M. Guarneri, M. Nuvoli "Determination of the range error in the incoherent amplitude-modulated laser optical radars". Rapporto tecnico ENEA, RT/2012/17/ENEA, ISSN/0393-3016 (2012), 1 – 48.
7. R.M. Montereali, F. Bonfigli, D. Brogioli, A. Santoni, M.A. Vincenti, E. Nichelatti, "Optical technologies, thin films and interfaces for organic photonics", *Rivista ENEA Energia, Ambiente e Innovazione*, EAI 3/2012, p. 114-121.
8. E. Nichelatti, R.M. Montereali, M.A. Vincenti, F. Di Pompeo, E. Segreto, N. Canci, F. Cavanna, Optical "Characterization of Organic Light-Emitting Thin Films in the Ultraviolet and Visible Spectral Ranges", ENEA Technical Report RT/2010/31/ENEA, arXiv:1203.4098v1 [physics.ins-det] (2012).
9. F. Biccari, C. Malerba, M. Valentini, C. Azanza, M. Müller, E. Esposito, R. Chierchia, P. Mangiapane, E. Salza, G. Arabito, A. Santoni, L. Mannarino, M. Capizzi, P. Scardi, A. Mittiga, "Ottimizzazione dei processi di realizzazione di dispositivi fotovoltaici in film sottili di Cu<sub>2</sub>ZnSnS<sub>4</sub>", *Ricerca di Sistema Elettrico*, Report RdS/2012/213.
10. F. Persia, R. D'amato, F. Padella, L. Pilloni, A. Rinaldi, A. Tati, "Performance of Nanomaterials for the Conservation of Artistic Stones", *Rivista ENEA Energia, Ambiente e Innovazione, Speciale EAI Vol. II/2012 - Knowledge, Diagnostics and Preservation of Cultural Heritage* (2012).
11. S. Paolini, G. Martini, B. Carpani, M. Forni, G. Bongiovanni, P. Clemente, D. Rinaldis, V. Verrubbi, "The May 2012 seismic sequence in Pianura Padana Emiliana: hazard, historical seismicity and preliminary analysis of accelerometric records", *Rivista ENEA Energia Ambiente e Innovazione, Focus on The Pianura Padana Emiliana Earthquake* (2012).
12. E. Candigliotta, F. Immordino, G. Martini, C. Vaccaro, "Sand liquefaction phenomena induced by the May 2012 Emilia Romagna Earthquake: geomorphological features and relations with the territory and building stability", *Rivista ENEA Energia Ambiente e Innovazione, Focus on The Pianura Padana Emiliana Earthquake* (2012).
13. G. Bongiovanni, G. Buffarini, P. Clemente, A. Paciello, D. Rinaldis, V. Verrubbi, G. Martini, A. Zini, S. Martino, "Seismic Preservation of the Cerreto di Spoleto Historical Centre", *Rivista ENEA Energia Ambiente e Innovazione, Speciale EAI Vol. II/2012 - Knowledge, Diagnostics and Preservation of Cultural Heritage* (2012).
14. C. Puglisi, L. Falconi, A. Screpanti, V. Verrubbi, G. Martini, S. Paolini, "The Geomorphological Hazard of Machu Picchu Citadel and Aguas Calientes Village", *Speciale EAI Vol. II/2012 - Knowledge, Diagnostics and Preservation of Cultural Heritage* (2012)
15. S. Paolini, F. Poggi, "Il terremoto di Rieti del 1898 Raccolta, digitalizzazione e fruizione on line dei documenti d'archivio" Archivio di Stato di Rieti - <http://www.asrieti.it/PUBBLICAZIONI/terremoto/index.htm>
16. L. Mezi e F. Flora: "La sorgente "DPP" di radiazione nell'estremo ultravioletto a scarica elettrica in gas rarefatto: principi fisici, caratterizzazione ed ottimizzazione", RT/2012/15/ENEA ISSN/0393-3016
17. S. Bollanti, D. De Meis, P. Di Lazzaro, A. Fastelli, F. Flora, G.P. Gallerano, L. Mezi, D. Murra, A. Torre, D. Vicca: "Calcolo analitico della posizione del sole per l'allineamento di impianti solari ed altre applicazioni", RT/2012/24/ENEA ISSN/0393-3016.
18. P. Di Lazzaro, D. Murra, B. Schwartz: "Perception of patterns after digital processing of low-contrast

images, the case of the Shroud of Turin“ RT/2012/12/ENEA (2012).

[http://opac.bologna.enea.it:8991/RT/2012/2012\\_12\\_ENEA.pdf](http://opac.bologna.enea.it:8991/RT/2012/2012_12_ENEA.pdf)

19. P. Di Lazzaro, D. Murra, E. Nichelatti, A. Santoni, G. Baldacchini “Shroud-like coloration of linen by nanosecond laser pulses in the vacuum ultraviolet” RT/2012/16/ENEA (2012).

[http://opac.bologna.enea.it:8991/RT/2012/2012\\_16\\_ENEA.pdf](http://opac.bologna.enea.it:8991/RT/2012/2012_16_ENEA.pdf)



**EXTERNAL COVER :** picture of the current TOP- IMPLART realization with the bending magnet to perform radiobiology on cell at 7 MeV (with magnetic focalisation structures).

**INTERNAL COVER :** TOP-IMPLART complete design.